CHAPTER ONE

1. INTRODUCTION AND LITERATURE REVIEW

Inositol hexaphosphate (IP_6) or phytate is ubiquitous in nature and comprises the bulk of eukaryotic cell inositol phosphate content. Phytic acid or phytate is the primary storage form of phosphorus in plant seeds (Fig. 1.1, Brinch-Pedersen *et al*., 2002; Vats and Banerjee, 2004) and is associated with fibre in many foods, such as soy- and cereal based products (Haros *et al*., 2005). In forage, one-third of the phosphorus (P) is present as digestible inorganic P with two-thirds as organic P in the form of phytin®, which is a mixture of calcium-magnesium salts of inositolhexaphosphoric acid known as phytic acid (Vats and Banerjee, 2004).

Since IP_6 is a common compound in nature some microorganisms are expected to have the ability to degrade it and utilize the hydrolyzed phosphorus. This is true for certain bacteria (Kerovuo and Tynkkynen, 2000) and many fungi (Sandberg and Andlid, 2002) which are known to synthesize phytases. Phytase is present in very low levels in the gastrointestinal tract of some monogastric animals. As a result, the phytate ingested by these animals is excreted into the environment (Fig. 1.1) causing eutrophication (Vats and Banerjee, 2002). Furthermore, monogastric animals such as pigs and poultry suffer from anti-nutritional problems associated with the limited or non-digestibility of phytate (Ashyma and Satyanarayana, 2001). To enhance plant phosphorus utilization and to circumvent the deleterious effect of phytic acid in animal nutrition, phytases from microbial origin have been fed to monogastric animals (Mroz *et al*., 1994) and is considered of significant value in upgrading the nutritional quality of phytate-rich feeds (Palacios *et al*., 2005).

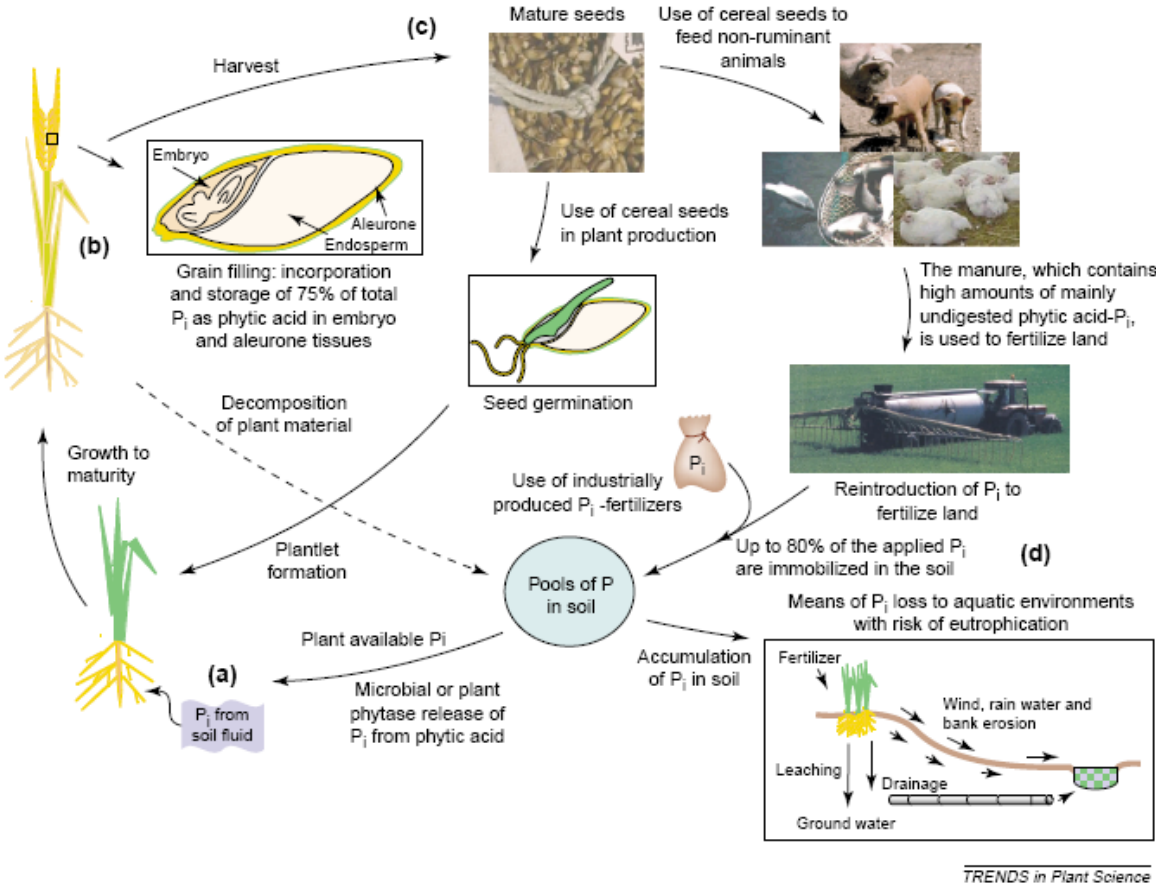

Fig. 1.1. Phytic acid phosphate cycles in natural and agricultural ecosystems. (a) Inorganic phosphate (P_i) is absorbed by plant roots from the soil fluid and translocated by the xylem and the phloem to all parts of the plant. Only a limited amount of the soil P_i is available to the plant because the mobility of P_i is low and it has high affinity for organic and inorganic compounds, and for soil particles. (b) Phytic acid is the major phosphate storage compound in seeds. (c) In agricultural systems, seeds are used either for plant production or as feed for livestock production. In particular, feeding of non-ruminant animals causes the excretion of large amounts of undigested phytic acid, because the digestive system of these animals lacks phytases. (d) Up to 80 % of phosphorus supplied via fertilizers becomes fixed in the soil (Brinch-Pedersen *et al*., 2002).

1.1. Phytate

Phytate consists of an inositol, which is a hexa-hydroxycyclohexane in a chair configuration (Fig. 1.2) with six phosphate ester bonds (Haros *et al*., 2005). The phosphate groups confer a high negative charge to this molecule and therefore a strong chelating ability, that reduces the dietary bioavailability of amino acids and minerals such as Ca^{2+}, Zn^{2+} and Fe^{2+} (Haros *et al*., 2005).

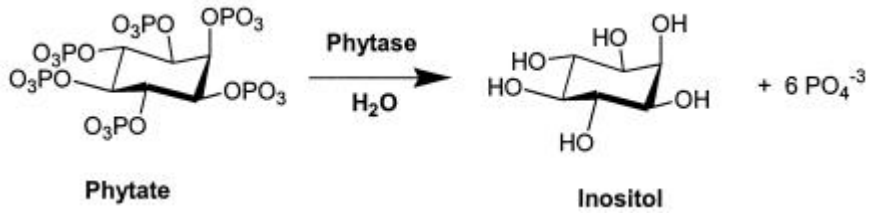

Fig. 1.2. Phytate chair-configuration and its conversion by phytase (Haros *et al*., 2005).

Phytic acid is the primary phosphate storage compound in seeds, and typically approximately 70 % of the phosphate reserves are sequestered into phytic acid. In small-grain cereals, approximately 90 % of the seed phytic acid is in the aleurone, and the remaining 10 % in the scutellum. In contrast, in maize, 90 % is found in the scutellum and 10 % in the aleurone. In dicotyledons and cotyledons, phytic acid is deposited in the endosperm. Almost all the phytic acid is present as phytin, a mixed salt (usually with K^+, Ca^{2+}, Mg^{2+} or Zn^{2+}) that is deposited as globoid crystals in single-membrane vesicles together with protein. Phytic acid deposition is restricted to cells which remain alive through the quiescent phase of seed development, but it is also found in vegetative tissues and in pollen (Loewus and Murthy, 2000).

Phytic acid is synthesized from *myo*-inositol via a series of phosphorylation steps (Fig. 1.3). There is only limited information available about the intracellular location of the intermediates in phytic acid biosynthesis. In the developing castor bean endosperm, phytin particles is detected in single-membrane vesicles in the cytosol or associated with

the endoplasmic reticulum (ER) and protein storage vesicles. It is hypothesized that phytic acid biosynthesis takes place in the cytoplasm or in the ER, after which the phytin particles are transported in vesicles to the protein bodies. In the slime mould *Dictyostelium*, analyses of lysates indicated a cytosolic route for the biosynthesis of phytic acid. Other studies have shown that the stepwise phosphorylation of the secondary messenger *myo*-inositol-1, 4, 5-trisphosphate to phytic acid can occur in the nucleus (Loewus and Murthy, 2000).

1.2. Antinutritional effects of phytate

Phytic acid has a strong antinutritive effect (Pallauf and Rimbach, 1996) and this effect is based on the unusual molecular structure of phytic acid. At complete dissociation, the six phosphate groups of phytic acid carry a total of twelve negative charges. Therefore, phytic acid has a strong binding capacity and it effectively binds different mono-, di-, and trivalent cations and their mixtures, forming insoluble complexes (Reddy *et al*., 1989). It forms fairly stable chelates with almost all multivalent cations which are insoluble at pH 6 to 7, although pH, type and concentration of cations have a tremendous influence on their solubility characteristics (Reddy *et al*., 1989). The formation of insoluble phytate-mineral complexes in the intestinal tract prevents mineral absorption. This reduces the bioavailability of essential minerals (Davies, 1982). Zinc appears to be the trace element of which its bioavailability is most influenced by phytic acid. Rimbach and Pallauf (1992) indicated that graduated phytic acid supplementations had a negative influence on apparent Zn^{2+} absorption and life-weight gain of growing rats.

Phytic acid interacts with proteins over a wide pH range, forming phytate-protein complexes due to electrostatic interactions. At a low acidic pH, phytic acid has a strong negative charge due to total dissociation of the phosphate groups while at pH 6 to 7, a ternary phytic acid-mineral-protein complex is formed which dissociates at high Na^{+} concentrations. Under these conditions a negative influence of phytic acid on the solubility of proteins can be expected, because of the ionic binding between the basic phosphate groups of phytic acid and protonized amino acid (lysyl, histidyl and arginyl) residues (Urbano *et al*., 2000; Fretzdorff *et al*., 1995).

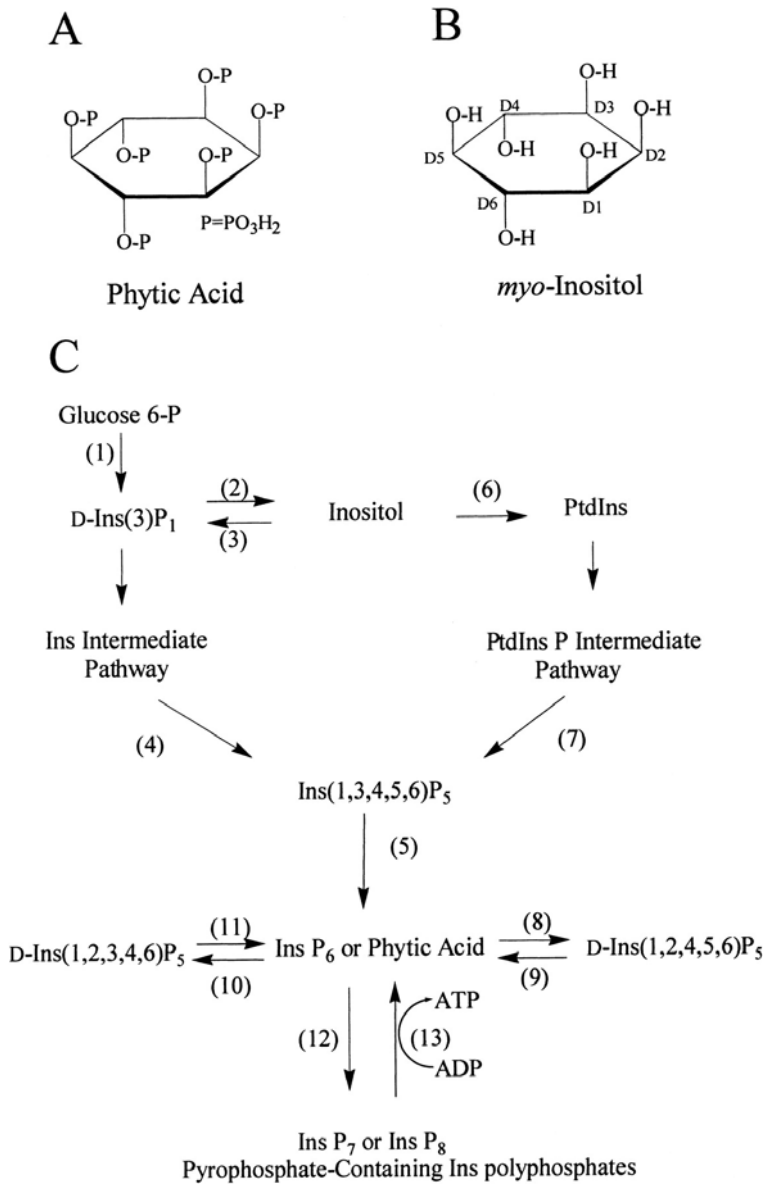

Fig.1.3. Biosynthetic pathways of phytic acid (*myo*-inositol-1, 2, 3, 4, 5, 6-hexa*kis*phosphate or $InsP_6$) in the eukaryotic cell: (A) Structure of phytic acid. (B) Structure of Inositol. The numbering of the carbon atoms follows the "D-Convention" (Loewus and Murthy, 2000). (C) Biochemical pathways: (1), D-Ins(3)-P_1 (or L-Ins[1]-P_1) synthase; (2), D-Ins 3-phosphatase (or L-Ins 1-phosphatase); (3), D-Ins 3-kinase (or L-Ins 1-kinase); (4), Ins P- or polyP kinases; (5), Ins (1,3,4,5,6) P_5 2-kinase or phytic acid-ADP phosphotransferase; (6), PtdIns synthase; (7), PtdIns and PtdIns P kinases, followed by PtdIns P-specific phospholipase C, and Ins P kinases; (8), D-Ins(1,2,3,4,5,6) P_6 3-phosphatase; (9), D-Ins(1,2,4,5,6) P_5 3-kinase; (10), D-Ins(1,2,3,4,5,6) P_6 5-phosphatase; (11), D-Ins(1,2,3,4,6) P_5 5-kinase; (12), pyrophosphate-forming Ins P_6 kinases; (13), pyrophosphate-containing Ins PolyP-ADP phosphotransferases (Loewus and Murthy, 2000).

Under acidic conditions phytic acid is likely to bind tightly to plant proteins, since the isoelectric point of plant proteins is generally around a pH of 4 to 5. In the intermediate pH range (6.0 to 8.0) both phytic acid and plant proteins have a net negative charge. However, under these conditions complex formation occurs between phytic acid and proteins. Possible mechanisms include direct binding of phytic acid to protonated α-NH_2 terminal groups and α-NH_2 groups of lysine residues, and a multivalent cation-mediated interaction (Kerovuo and Tynkkynen, 2000). By binding to plant proteins, phytic acid decreases their solubility and digestibility, therefore also reducing their nutritive value. In addition to complexing with minerals and proteins, phytic acid interacts with enzymes such as trypsin, pepsin, α-amylase and galactosidase, resulting in a decrease in the activity of these important digestive enzymes (Kerovuo and Tynkkynen, 2000).

1.3. Phytases

Phosphatases constitute a diverse group of enzymes that catalyze the hydrolysis of phosphomonoester bonds of a variety of phosphate esters. Phytases are a subgroup of phosphatases which catalyzes the partial or complete hydrolytic removal of orthophosphate from phytate (Vohra and Satyanarayana, 2003). The complete hydrolysis of phytate (Fig. 1.1.) results in the production of one molecule of inositol and six molecules of inorganic phosphate (Shamsuddin, 2002).

1.3.1. Classes of phytases

Three structurally distinct classes of enzymes have been described as phytases. The three classes include histidine acid phosphatases (HAPs), β-propeller phytases (βPP) and purple acid phosphatases (PAP) (Mullaney and Ullah, 2003). Non-specific acid phosphatases constitute another subgroup of phosphatases, which have a high hydrolysis rate for monophosphorylated compounds, but a low level of activity against phytate (Palacios *et al*., 2005). Most studies have focused on histidine acid phosphatases which have a high specific activity for phytic acid.

1.3.1.1. Histidine acid phosphatase (HAP)

All members of this class share both a common active site motif, RHGXRXP, and a two-step mechanism that hydrolyzes phosphomonoesters (Mullaney and Ullah, 2003). All phytases that belong to the family of HAPs do not need any co-factor for optimal activity (Konietzny and Greiner, 2004). However, not all HAPs are catalytically active as phytases. Recent research has established a vital role for the enzyme's substrate specificity site (SSS) (Konietzny and Greiner, 2004).

Wyss *et al*. (1999a) compared the catalytic properties of several fungal phytases and proposed two classes of HAP phytases. One class has a broad substrate specificity but lower specific activity for phytic acid and the second class has a narrow substrate specificity but a high specific activity for phytate. No significant variation in the catalytic centers of these fungal phytases has been found. However, when the amino acid residues comprising the SSS are examined, a pattern of low specific activity for phytase and a neutral amino acid occupying the residue analogous at K300 in *Aspergillus niger* NRRL 3135 phytase (phyA) is evident (Mullaney *et al*., 2002). When the three-dimensional model of the phyA molecule was examined, the six amino acids in its substrate specificity site, K91, K94, E228, D262, K300 and K301, were found to encircle the cavity containing the HAP active center (Mullaney *et al*., 2002). They appear to have a role as a gate-keeper for any substrate's access to the HAP active site. Thus far, phyA (HAP) has been isolated from filamentous fungi, bacteria, yeast and plants (Wyss *et al*., 1999a). Because of the proven afficacy of phyA as an animal feed additive, several of these phyA phytases are now being marketed.

A second phytase (phyB) has been isolated from *A. niger* NRRL 3135 (Ullah and Cummins, 1987). Its catalytic properties are distinct from those of *A. niger* NRRL 3135 phyA. In fact, it first appeared not as a phytase but as an *A. niger* acid phosphatase having an optimum pH of 2.5 (Wyss *et al*., 1999a). When it was isolated and tested for phytase activity, the activity assay was conducted at pH 5.0, the optimum pH for A. niger NRRL 3135 phyA. However, the pH optimum for phyB is lower, pH 2.5, and only minimal activity was observed at pH 5.0. This lack of activity at pH 5.0 for phyB can

now be understood by examining its SSS. Kostrewa *et al*. (1999) identified the SSS of phyB which is different from the SSS of phyA. It is composed of two amino acids at D75 and E272. This means that the phyB SSS is more electrostatically neutral and therefore can accommodate a broader substrate spectrum than *A. niger* phyA. It also means that at pH 2.5 the SSS of *A. niger* T213 phyB is uncharged and will accept negatively charged phytate as a substrate. However, at pH 5.0, it is negatively charged and would repel a negatively charged substrate (Kostrewa *et al*., 1999).

Another difference between *A. niger* phyA and phyB is that the active form of phyA is a monomer, whereas the active form of phyB is a tetramer (Wyss *et al*., 1999b). This tetrameric structure initially provides phyB with thermostability, but it also explains why it is incapable of proper refolding after it has been denatured by heating.

1.3.1.2. β-Propeller phytase (βPP)

βPP (EC 3.1.3.8) is a recently discovered class of enzymes with a novel mechanism for hydrolyzing its substrate. BPPs have been isolated and their genes cloned from *Bacillus subtilis* (phyC) (Kerovuo *et al*., 1998) and *Bacillus amyloliquefaciens* (TS-Phy) (Kim *et al*., 1998). A three-dimensional model of its molecule displays a basic form similar to a propeller with six blades (Ha *et al*., 2000). The dependence on binding Ca^{2+} for thermostability and catalytic activity distinguishes phyC from other subclasses of phytases. BPP has two phosphate binding sites (Shin *et al.,* 2001). The hydrolysis of its substrate occurs at the cleavage site and the adjacent affinity site, which increases the binding affinity for substrates like phytic acid that feature neighbouring phosphate groups. The calcium ions facilitate the binding by creating a favourable electrostatic environment (Shin *et al*., 2001).

1.3.1.3. Purple acid phosphatase (PAP)

Another phytase, GmPhy (EC 3.1.3.2), has recently been isolated from the cotyledons of germinating soybeans (Hegeman and Grabau, 2001). GmPhy has the active site seguence motif of a purple acid phosphatase (PAP) which is DXG..GDXXY.GNH(E, D)..VXXH..GHXH. This class of metalloenzyme has been widely studied. Both its

three-dimentional structure and a proposed mechanism of catalysis are known. Studies of genomic databases have revealed PAP-like sequences in plants, mammals, fungi and bacteria. The estimated size of purified GmPhy, 70-72 kDa, suggests a molecular mass similar to other plant PAPs. However, GmPhy is the only known PAP reported to have significant phytase activity. An *A. niger* NRRL 3135 PAP (Apase6) has previously been reported and displays only a minimum ability to utilize phytate as a substrate (Ha *et al*., 2000). The lower catalytic activity of GmPhy than that of *A. niger* NRRL 3135 phyA may be necessary during germination in soybeans because the germination process require a steady breakdown of phytate over a period of several days (Mullaney and Ullah, 2003).

1.3.2. Biochemical properties of the phytase system

Phytase, phyB is a tetramer with two types of protein folding. The first type, adopted by *E. coli* and *A. niger*, has an alpha domain and a conserved alpha/beta domain with two helices on each side of the seven-stranded sheet (Lim *et al*., 2000 and Kostrewa *et al*., 1997). The active site is in an indentation between these domains. The indentation is closed off at the back by an N-terminal lid. Basic amino acids at the active site help bind the negatively charged 3-phosphorus group on phytate. This enzyme contains a catalytic histidine in the conserved Arg-His-Gly motif and it is thought this histidine (59) makes the nucleophilic attack on the phosphorus group, resulting in a phospho-histidine intermediate and an aspartate (339) provides the proton for the leaving alcohol Fig. 1.4 (Kostrewa *et al*., 1997). These structures closely resemble the overall fold of other histidine acid phosphatases (Lim *et al*., 2000). The other type is the calcium-dependent phytase from *Bacillus amyloliquefaciens*, which adopts a β-propeller conformation with six-stranded blades (Ha *et al*., 2000). The enzyme reaction appears to act through a direct attack of the metal-bridging water molecule on the phosphorus atom of phytate and the subsequent stabilization of the pentavalent transition state by the bound calcium ions (Ha *et al*., 2000).

1.3.3. Enzymatic properties of Phytases

1.3.3.1. Biophysical characteristics

Most phytases characterized are monomeric enzymes from fungi (Dvorakova *et al*., 1997), and bacteria such as *E. coli, Klebsiella terrigena* (Greiner *et al*., 1993; Greiner *et al*., 1997), and *B. subtilis* (natto) (Shimizu, 1992). However, some plant and animal phytases appear to be comprised of multiple subunits. A phytase accumulating in maize seedlings during germination is a dimeric enzyme consisting of two 38 kDa subunits (Laboure *et al*., 1993). Purified rat intestinal phytase exhibited two protein bands in SDS-PAGE with estimated molecular masses of 70 and 90 kDa (Yang *et al*., 1991). However, since only the 90 kDa subunit is induced by phytic acid, it is likely that these protein bands represent two different enzymes (alkaline phosphatase and phytase, respectively). An inositol hexakisphosphate dephosphorylating enzyme from the protozoan *Paramecium* has been proposed to have a hexameric structure (Freund *et al*., 1992).

Known phytase has an estimated molecular mass of 35-700 kDa, depending upon the sources of origin. An unusual large molecule (700 kDa), together with an exceedingly small peptide (10-13 kDa) were found in *Klebsiella aerogenes* (Liu *et al*., 1998). The two distinct molecular forms of phytases exhibited difference in physiochemical properties such as the Michaelis constant (Km), optimal pH, and thermo stability (Liu *et al*., 1998 and Tambe *et al*., 1994). Bacterial phytases are generally smaller than their fungal counterparts. The predicted size of fungal phytases is around 50 kDa and the experimental size is between 65 and 70 kDa, indicating heavy glycosylation. *A. niger* NRRL 3135 native phytase is 27 % glycosylated. It contains a substantial proportion of N-linked mannose chains and galactose (Kerovuo and Tynkkynen, 2000).

a.

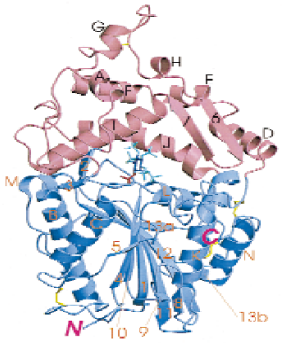

b.

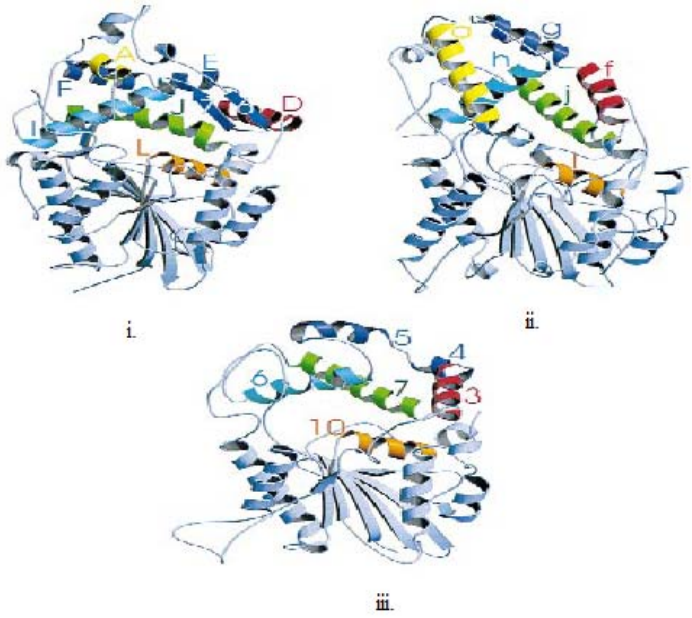

Fig. 1.4. The three-dimensional structure of *E. coli* phytase. (a) A prominent central cavity divides the protein into an α-domain (red) and an α/β-domain (blue). The α/β-domain contains a twisted seven-stranded β-sheet of mixed topology with two α-helices on each side of the β-sheet. The α-domain is predominantly made up of α-helices but also contains a β-hairpin structure (strands 6 and 7) that forms part of the rim of the binding pocket. The four disulfide bonds are shown in yellow. The N- and C-termini are labelled as N and C, respectively. Helices are labelled with capital letters, while β-strands are labelled with numerals. A stick model of phytate is shown with its 3-phosphate (red) in the active site. (b) A comparison of the structures of (i) *E. coli* phytase (ii) *A. niger* phytase and (iii) rat prostatic acid phosphatase. The α/β domain, which consists of the main β-sheet and surrounding α-helices, are well conserved among the three structures. A comparison of the α-domains of the phytases from *E. coli* and *A. niger* and the rat prostatic acid phosphatase shows a number of structurally homologous helices, which are topologically identical and have been colored the same in all three structures. Helices were labeled using capital letters for *E. coli* phytase, small letters for *A. niger* phytase, and numerals for rat prostatic acid phosphatase.

Wyss *et al*. (1999b) reported that glycosylation of recombinant phytases are highly variable. Whereas glycosylation was moderate in *A. niger*, it was excessive and highly variable in *Hansenula polymorpha* and *Saccharomyces cerevisiae*. Surprisingly, glycosylation differed not only between the different expression systems used but also between different batches of a phytase produced in the same expression system (Wyss *et al*., 1999a). Analysis of the glycosylation pattern of *A. niger* phytase showed that the heterogeneity was due to incomplete glycosylation of two out of ten potential N-glycosylation sites.

In general, glycosylation may have several effects on the properties of an enzyme. Firstly, it may influence the catalytic properties or have an impact on the stability of the enzyme. Secondly, it may influence the pI of the protein. Thirdly, by consuming metabolic energy it may lower the level of expression of the protein. Surprisingly, different extents of glycosylation had no effect on the catalytic properties, thermostability or refolding properties of *A. niger* phytase (Wyss *et al*., 1999a).

The importance of glycosylation for the structure and function of phytase is further brought into question by the fact that only two potential N-glycolysation sites are conserved in fungal phytases (Pasamontes *et al*., 1997). Han and Lei (1999) studied the role of glycosylation in the functional expression of *A. niger* phytase (*phyA*) in *Pichia pastoris*. Their results indicated an identical capacity of phytic acid hydrolysis and slightly improved thermostability in glycosylated enzyme produced in *P. pastoris* compared to the same enzyme over expressed in *A. niger*. Deglycosylation of the phytase resulted in 34 % reduction in thermostability. Suppression of glycosylation by tunicamycin during expression resulted in a significant reduction of phytase production indicating that glycosylation is vital for the biosynthesis of recombinant PhyA in *P. pastoris*. However, tunicamycin might also impair the production by other means since there was no accumulation of intracellular phytase protein, the impairment did not appear to occur at the level of translocation of the phytase.

Wyss *et al*. (1999a) suggested that glycosylation has no or only a minor effect on the pI of the fungal phytases tested. The only exceptions were the phytases expressed in *H. polymorpha*, in which a pronounced shifts to acidic pI values were observed. All the fungal, bacterial, and plant phytases hitherto investigated have acidic pI values, with the exception of *A. fumigatus* phytase, which has a basic pI. Bacterial phytases seem to be less acidic than fungal phytases; their pI is generally above 6, whereas fungal enzymes have pI values below 5.5. *A. fumigatus*, *Emericella nidulans*, *A. terrus*, and *Myceliophthora thermophila* phytases have a tendency to undergo proteolytic degradation when expressed in *A. niger* and stored as concentrated culture supernatants at 4º C (Wyss *et al*., 1999a). The activity of phytase from *B. subtilis* is unaffected by proteases such as trypsin, papain and elastase (Kerovuo and Tynkkynen, 2000), indicating a stronger protease resistance than that of fungal phytases.

1.3.3.2. Temperature and pH stabilities and Optima

The pH optimum of phytases varies from 2.2 to 8. Most microbial phytases, especially those of fungal origin, have a pH optimum between 4.5 and 5.6. In contrast to most fungal phytases, *A. fumigatus* phytase has a broad pH optimum, at least 80 % of the maximal activity is observed at pH values between 4.0 and 7.3. Some bacterial phytases, especially those from *Bacillus*, have a pH optimum at 6.5 to 7.5. The pH optima of plant seed phytases range from 4.0 to 7.5, most having an optimum between 4.0 and 5.6. Two alkaline plant phytases having a pH optimum at about 8.0 have been described in legume seed (Scott, 1991) and lily pollen (Hara *et al*., 1985). *A. niger* NRRL 3135 and *Citrobacter freundii* phytases differ from other phytases in having two pH optima.

The temperature optima of phytases vary from 45 to 77º C. Wyss *et al*., (1998) studied the thermostability of three acid phosphatases of fungal origin (*A. fumigatus* and *A. niger* phytase, and *A. niger* pH 2.5 optimum acid phophatase) by circular dichroism (CD) spectroscopy and fluorescence, and by measuring the enzymatic activity. They concluded that *A. niger* phytase was not thermostable, neither did it have the capacity to refold after heat denaturation. At temperatures between 50 and 55º C it underwent an irreversible conformational change that resulted in 70-80 % loss of enzyme activity. The

A. fumigatus phytase was not thermostable, but had the remarkable property of being able to refold completely into native-like, fully active conformation after 20 min heat denaturation at 90^{o} C. Compared to two phytases, *A. niger* pH 2.5 acid phosphatase had a higher intrinsic thermostability. At temperatures up to 80^{o} C, only minor changes in CD spectral characteristics and only slight, but irreversible enzyme inactivation were observed. However, exposure to 90^{o} C resulted in an irreversible conformational change and complete loss of activity.

Bacillus spp. strain DS11 phytase (Kim *et al*., 1998) had a temperature optimum at 70 ^{o}C, which is higher than the temperature optimum of phytases in general. It was also very thermostable: 100 % residual activity after 10 min incubation at 70^{o} C (in the presence of $CaCl_2$). The enzyme stability of *Bacillus spp*. strain DS11 phytase was drastically reduced above 50^{o} C in the absence of $CaCl_2$, whereas it was rather stable up to 90^{o} C in the presence of $CaCl_2$. After incubation at 90^{o} C for 10 min, the residual enzyme activity was approximately 50 % of the initial activity. This indicates that the Ca^{2+} ion has a strong protecting effect on the enzyme against thermal denaturation.

1.4. Microbial sources of phytases

Microbial phytase activity is most frequently detected in fungi, particularly in *Aspergillus spp.* Phytase has also been detected in various bacteria and in some yeasts. Over 2000 microorganisms screened for phytase production have been isolated from soil (Kerovuo and Tynkkynen, 2000).

1.4.1. Bacterial phytases

The enzyme activity of bacterial phytases is estimated at 200 to 388 U.ml^{-1} (Quan *et al*., 2001). Several bacteria (wild or genetically modified) such as *Lactobacillus amylovorus, E. coli, Bacillus subtilis, B. amyloliquefaciens, Klebsiella spp*., etc., have been employed for phytase synthesis (Pandey *et al*., 2001). Sunitha *et al.* (1999) optimized the medium for recombinant phytase production by *E. coli* BL21 using response surface methodology. A 2^3 central composite experimental design was used to study the combined effects of the medium components, tryptone, yeast extract and NaCl. The

optimized medium with glucose showed the highest phytase activity. A genetically modified *B. subtilis* KHU-10 also produced extracellular phytase which constituted over 90 % of the total protein. The yield was 100-fold higher than the wild type *B. amyloliquefaciens* DS11 (Kim *et al*., 1999). Kim *et al*. (1998), Shimizu (1992) and Griener *et al*. (1993) studied bacterial strains, *Bacillus spp* and *E.coli* isolated from soil near the roots of leguminous plants. These bacteria produced high levels of an extracellular phytase under optimized conditions in a maltose, peptone and beef extract medium. The phytases of *E. coli* have been reported to be periplasmic enzymes (Greiner *et al*., 1993) and phytase activity in *Selenomonas ruminantium, Bacillus spp.* and *Mitsuokella multiacidus* was found to be associated with the outer membrane (D' Silva *et al*., 2000). Sreeramulu *et al*. (1996) evaluated 19 strains of lactic acid-producing bacteria of the genera *Lactobacillus* and *Streptococcus* for the production of extra-cellular phytases. The majority exhibited enzyme activity in the fermentation medium but *Lactobacillus amylovorus* B 4552 produced the highest amount of phytase, ranging from 125 to 146 U/ml (Yoon *et al*., 1996) in phytase screening medium (PSM), pH of 5.5 after 3 days of cultivation at 37º C using glucose and inorganic phosphate.

Phytases are also found in enteric bacteria such as *Pseudomonas spp.*, *Bacillus spp., Raoultella spp., E. coli, Citribacter braakii, Enterobacter*; anaerobic rumen bacteria, *Selenomonas ruminantium, Prevetella spp.* and *Megasphaera elsdenii* (Konietzny and Greiner, 2004). Although many gut microorganisms have the ability to produce phytase, little activity is available since these microbes do not secrete the enzyme and the pH of the intestine is not favourable for this enzyme (Garrett *et al*., 2004). Some bacterial phytases, especially those of the genera *Bacillus* and *Enterobacter*, exhibit pH optima in the range from 6.0 to 8.0 (Shimizu, 1992). Therefore, they would be more beneficial as feed additives for poultry as their pH optimum is close to the physiological pH of the poultry crop.

1.4.2. Mold phytases

Generally, the phytases produced by fungi are extracellular and the activity is estimated at 600 $U.ml^{-1}$ (Kim *et al*., 1999). Ahmad *et al*. (2000) and Ebune *et al*. (1995) used maize

starch-based and canola meal medium for the production of phytase in Submerged Fermentation (SmF) and Solid State Fermentation (SSF) using *Aspergillus spp*. Optimum substrate moisture was 64 %. Age of the inoculum had a profound effect on enzyme synthesis by the culture. Using a strain of *A. carbonarius* on canola meal (Alasheh and Duvnjak, 1995) found 53-60 % moisture as the optimum (Alasheh and Duvnjak, 1994). Extracellular phytase produced by *Aspergillus spp*. 5990 in maize starch-based liquid medium showed a fivefold higher activity at pH 5.5 and 40º C for 10 days when compared with cultures of *A. ficuum* NRRL 3135. The phytase had a higher optimum temperature for its activity than the commercial enzyme, Natuphos, from *A. ficuum* NRRL 3135 (Kim *et al*., 1999).

1.4.3. Yeast phytases

Yeast phytase activities are estimated at 20-1070 $U.ml^{-1}$ (Quan *et al*., 2001). Phytase production using yeast cultures has generally been carried out in SmF systems. The strains used included *Schwanniomyces castellii, S. occidentalis, Hansenula polymorph, Arxula adeninivorans, Rhodotorula gracilis,* etc. (Pandey *et al*., 2001). In a continuous culture using a strain of *S. castellii*, phytase production increased with pH and dilution rate. It decreased when phytic acid or phosphate content increased (Pandey *et al*., 2001). Mayer *et al*. (1999) developed an efficient process for the low-cost production of phytases using *Hansenula polymorpha*. Glucose or glucose syrups were used as main carbon sources during fermentation. Compared with the process using glycerol, glucose led to a reduction of more than 80 % in the raw material costs. In addition, exceptionally high concentrations of active enzyme (up to 13.5 $g.l^{-1}$) were obtained in the medium, with phytase representing over 97 % of the total accumulated protein (Pandey *et al*., 2001).

1.5. Regulation of phytase synthesis

Phytase regulation was studied in bacteria by Konietzny and Greiner (2004) and Zamudio *et al*. (2002). They found that phytase was an inducible enzyme and its expression was subjected to a complex regulation. In exponential growing bacteria, *E. coli* and *Raoultella terrigena,* phytase formation was turned off, but it started as soon as the cultures entered the stationary phase under anaerobic conditions in non-limiting media.

Due to either nutrients or an energy depletion known to occur during the stationary phase, it was suggested that the synthesis of the enzymes started as soon as the growth rate began to fall and it could be the time when the enzyme was induced. Among the nutrient limitations tested, only carbon starvation was able to provoke an immediate synthesis of the *R. terrigena* phytase, whereas in *E. coli*, phytase synthesis was triggered when bacteria starved for inorganic phosphate while carbon, nitrogen, and sulfur limitation were ineffective. A tight regulatory inhibition of phytase formation by inorganic phosphate levels was generally observed in all microbial phytase producers, including molds, yeast and bacteria, with the exception of *R. terrigena* and the rumen bacteria (Konietzny and Greiner, 2004). It is not known, however, what components in the complex media account for the reduced repression.

The activation of a set of genes in *E. coli* that allow a better utilization of the nutrients present in low concentration or the utilization of other substances that belong to the same class of nutrient was shown to be the primary response due to the limitation of a specific nutrients (Konietzny and Greiner, 2004). These nutrient-specific systems include the cyclic AMP (cAMP) and its receptor the catabolite activator protein (CAP) for the use of alternative carbon sources, the NtrB/NtrC/σ^{54} regulon that is induced under nitrogen limitation and the PhoB/PhoR regulon that is induced under phosphorus limitation (Konietzny and Greiner, 2004). However, if the nutrients are exhausted from the environment, the cells enter into stationary phase. As already mentioned, phytase formation in *E. coli* is induced in non-limiting media as soon as the cultures enter into the stationary phase. The expression of the phytase-encoding gene *appA* was shown to be dependent on the *rpoS*-encoded sigma factor σ^s which have been identified as a central regulator for many stationary-phase-responsive genes. Many promoters regulate σ^s – dependent genes and only one of them is controlled by σ^s. Thus, not all genes identified as σ^s -controlled are entirely dependent on σ^s for expression. In minimal medium, starvation for phosphate but not for glucose or ammonia resulted in a strong stimulation of *rpoS* expression followed by an increase in phytase activity. In addition, phytase expression depends on the nature of the carbon source used for growth. Glucose, which is known to cause catabolite repression, has been widely used to improve phytase

production. The cAMP-CAP complex, rather than the carbon source itself, is directly involved in this regulation as was shown in *E. coli*. Synthesis of the phytases in both *E. coli* and *R. terrigena* have been reported to be negatively regulated by cAMP (Zamudio *et al*., 2002), which is suggested to be involved in the amphibolic metabolism of glucose and galactose as well as directly or indirectly in controlling the expression of an important stationary growth regulator (Konietzny and Greiner, 2004). Greiner *et al*. (1997) reported that in *Raoultella spp.* phytate is needed to induce phytase production. The formation of phytase in *Pseudomonas spp*. and *Raoultella aerogenes* was found to be induced in the presence of myo-inositol as the sole carbon source.

1.6. Biotechnological applications of phytases

1.6.1. Phytases and the animal feed industry

Phytases have an immense potential in biotechnological applications, particularly for the reduction of phytate content in feed and food (Vohra and Satyanarayana, 2003). Depending on the feed application, a phytase in which there is a commercial interest should fulfill a series of quality criteria. Enzymes used as feed additives should be effective in releasing phytate phosphate in the digestive tract, stable to resist inactivation by heat from feed processing and storage, and cheap to produce (Konietzny and Greiner, 2004). Ruminants digest phytate through the action of phytases, produced by microbial flora in the rumen. The anaerobic gut fungi and bacteria present in the microflora of ruminants are responsible for the primary colonization of plant material within the rumen. The inorganic phosphate hydrolyzed from phytate by phytases is utilized by both the microflora and the ruminant host. The situation is different with monogastric animals. Monogastrics, such as pigs, poultry and fish are unable to metabolize phytic acid, since they lack gastrointestinal phytase. Therefore, inorganic phosphate is added to their feed to meet their phosphate requirements. This increases costs and contributes to phosphate pollution problems. The supplementation of animal feed with phytase enables the assimilation of phosphate in the feed ingredients and diminishes the amount of phosphate in the manure and subsequent environmental pollution. The effect of feeding phytase to animals and impact on pollution has been quantitatively determined (Vohra and Satyanarayana, 2003). If phytase were used in the feed of all of the monogastric animals

reared in the U.S., it would release phosphorus with a value of 168 million U.S dollars and would preclude 8.23 x 10^4 tonnes of phosphate from entering the environment per annum. The use of phytase as a feed additive has been approved in 22 countries. The FDA (The Food and Drug Administration) has awarded phytase preparation a GRAS (Generally Regarded As Safe) status (Wodzinski, and Ullah, 1996).

Finase® phytase added to corn-soybean pig diet converted approximately one-third of the unavailable phosphate to an available form (Cromwell *et al*., 1993). In a similar way, experiments with Allzyme® Phytase and Natuphos phytase additions to pig and chicken diets indicated that phytase improved the bioavailability of phytate phosphorus for pigs and broiler chickens (O'Quinn *et al*., 1997). Several experiments with pigs and chickens confirmed the possibility of replacing inorganic phosphate supplementation by the use of microbial phytase in phytate-rich diets for monogastric animals. In Holland, *A. niger* phytase has been successfully introduced as a feed supplement, leading to a 30 to 40 % reduction in phosphate pollution. This represents a nation-wide saving that is greater than the reduction obtained by phosphate-free detergent products (Cromwell *et al*., 1993).

The use of phytase as a feed enzyme sets certain demands on the properties of the enzyme. Particularly, the enzyme should withstand high temperatures which are commonly used to pellet poultry and pig feeds (Kim *et al*., 1999). Thermostability is an important aspect since feed pelleting is commonly performed at temperatures between 65 and 95º C. Although phytase inclusion using an after-spray apparatus for pelleted diets and/or chemical coating of phytase may help bypass or overcome the heat destruction of the enzyme, thermostable phytases will no doubt be better candidates for feed supplements (Vohra and Satyanarayana, 2003). Naturally-occuring phytases having the required level of thermostability for application in animal feeding have not been found in nature so far, therefore thermostability of phytases is still a major challenge for animal feed applications (Vohra and Satyanarayana, 2003).

The ability of a phytase to hydrolyze phytate in the digestive tract is determined by its enzymatic properties (Konietzny and Greiner, 2004). As the stomach is the main

functional site of supplemental phytase, an enzyme with an acidic pH optimum and a high resistance to pepsin is desirable. Most of the described microbial phytases have optimum pH range of 4.0 to 5.5.

Finally, a phytase will not be competitive if it cannot be produced in high yield and purity by a relatively inexpensive system. Recently, economically competitive expression and/or secretion systems for microorganisms have been developed (Miksch *et al*., 2002).

Reduction of phytase level or increase in phytase activity in the plant seed itself are alternative strategies for improving nutrient management in animal production. Increased phytase activity in the plant seed by heterologous expression of a fungal phytase was already achieved and it was shown that only limited amounts of transgenic seeds are required in compound feeds to ensure proper degradation of phytate (Brinch-Pedersen *et al*., 2000). Recently, swine were generated with a gene from *E. coli* for the production of a phytase in the saliva. It was shown that provision of salivary phytase activity enables essentially complete digestion of dietary phytate (Konietzny and Greiner, 2004), largely relieving the requirement for phosphate output supplementation, and reduces feacal phosphate output by up-to 75 %. This reduction even exceeds the 40 % reduction for pigs fed expensive phytase supplements (Konietzny and Greiner, 2004).

Since it is evident that the inability of plants to utilize phosphate from soil phytate is associated with a lack of extracellular phytase activity, an opportunity exists for using gene-technology to improve the ability of plants to utilize phytate phosphate. Extracellular secretion of a phytase from *Aspergillus niger* by plant roots was shown to enable the plants to obtain phosphate from soil phytate (Norris *et al*., 1998). A more effective utilization of phosphate from soil and fertilizer sources would be particularly beneficial to agriculture throughout the world.

1.6.2. Phytases and human health

A diet rich in cereal fibers, legumes and soy protein results in an increased uptake of phytate. Vegetarians, elderly people consuming unbalanced food with high amounts of

cereals, people in underdeveloped countries who eat unleavened bread and babies eating soy-based infant formulas take in large amounts of phytate (Kerovuo *et al*., 2000).

Undigested phytate in the small intestine negatively affects the absorption of zinc, calcium, magnesium and iron. It also reduces the digestability of dietary proteins and inhibits digestive enzymes. Using Finase® phytase, Kerovuo *et al*., (2000) reported the preparation of a phytate-free soy protein isolate with increased solubility at low pH (pH 3) compared to the control soy protein isolate. Anno *et al*. (1985) eliminated phytate from soybean milk using wheat phytase. Additions of *A. niger* phytase to flour containing wheat bran increased iron absorption in humans (Sandberg *et al*., 1996).

However, more studies should be performed before accepting phytase as a food additive. The food industry may also be interested in using phytases on the one hand to improve mineral bio-availability by reducing phytate content of a given food, on the other hand to produce functional foods.

Phytic acid and inositol intermediates have been implicated in blood glucose response, lowering of cholesterol and triglycerides (Konietzny and Greiner, 2004), renal stone formation, in the treatment of Parkinson's diseases, Alzheimer's disease, multiple sclerosis and certain types of cancer (Vats and Banerjee, 2004; Shamsuddin, 2002).

1.6.3. Pulp and Paper Industry

The removal of plant phytic acid might be important in the pulp and paper industry. A thermostable phytase could have potential as a novel biological agent to degrade phytic acid during pulp and paper processing. The enzymatic degradation of phytic acid would not produce carcinogenic and highly toxic by-products. Therefore, application of phytases in the pulp and paper process could be environmentally friendly and would assist in the development of cleaner technologies (Liu *et al*., 1998).

1.7. Yeasts

Yeasts are fungi which reproduce by budding or fission. Yeasts can be classified into two phylogenic groups i.e. ascomycetous or basidiomycetous yeasts. The yeasts differ from other fungi in that they produce their sexual spores without the use of fruiting bodies (Kurtzman and Fell, 1998).

Yeasts are associated to aquatic and terrestrial habitats. Yeasts, which are living primarily in fresh and estuarine waters, are difficult to characterize as specific yeast habitats, given that their microbiology is highly affected by the surrounding terrestrial fauna and flora, soil, run-off, or effluents of human sources. Terrestrial yeasts are abundantly found in plants, animals and soil (Kurtzman and Fell, 2000).

Yeasts are used in many industrial processes, such as the production of alcoholic beverages, biomass (baker's, food and fodder yeasts) and various metabolic products. Most of the primary and secondary metabolites are synthesized through the introduction of recombinant DNA into yeasts. These include enzymes, vitamins, capsular polysaccharides, carotenoids, polyhydric alcohols, lipids, ethanol and carbon dioxide (Kurtzman and Fell, 2000). Some of these products are produced commercially while others are potentially valuable in biotechnology.

Yeasts are producers of the four leading fermentation products in terms of tons/year worldwide. These are beer, wine, single cell protein, fodder and bakers yeast. A fifth product is citric acid which is made by yeast and molds (Kurtzman and Fell, 2000).

1.7.1. Identification of yeasts

Classification and identification of yeasts is based on the methods for both filamentous fungi and bacteria. Yeasts are fungi and their classification into families is based mainly on the morphology of vegetative cells and spores, if formed. Species are classified and identified by using physiological tests, similar to those used in bacterial identification (Campbell and Duffus, 1988).

1.7.1.1. Conventional identification

The criteria and tests for identification of yeasts involve the observation of culture characteristics, which include colour, shape and texture of the colonies. This is followed by observation of sexual structures, which include shape and size of the sexual spores. The mode of conidia formation and the characteristics of pseudohyphae or true hyphae is also used as valuable information in the identification of yeasts (Yarrow, 2000).

Physiological properties primarily serve to describe and identify yeast species and to a lesser extent, genera (Yarrow, 2000). The tests mostly used include fermentation of and growth on various carbon sources, growth on different nitrogen sources, vitamin requirements for growth and growth at various maximum temperatures and the ability to grow on media with a high sugar or sodium chloride content (Barnett *et al*., 2000; Yarrow, 2000).

1.7.1.2. Molecular tools

Recently, considerable developments in the identification and classification of yeasts have come with the introduction of molecular techniques. These include pulsed-field gel electrophoresis (PFGE, karyotyping), restriction enzyme analysis (RFLP) and PCR-based techniques, for example, ribotyping, Randomly Amplified Polymorphic DNA (RAPD) analysis (Andrighetto *et al*., 2000) and sequencing of ribosomal RNAs (Cappa and Cocconcelli, 2001).

The introduction of DNA studies provides a parameter for estimating evolutionary distances among taxa. Different methods resolve different taxonomic levels. The two features of the nuclear genome that were thought to be useful in recognition of species, involved accurate determination of the mean molar percentage guanine plus cytosine (mol % G + C) of the presumed homogenous nuclear DNA. However, the mean mol % G + C does not reflect differences in base sequences. It is mainly exclusionary and therefore different species may have more or less coincidental G + C values (Kurtzman, 1998).

In the last decade, microbial identification has undergone a revolutionary change by the introduction of PCR-based methodologies. These techniques were first used for bacterial identification but have since been adapted for yeasts. One of the most successful methods for yeast species identification is polymerase chain reaction- restriction fragment length polymorphism (PCR-RFLP) analysis of the 5.8S rRNA gene and the two flanking internal transcribed sequences (ITS) (Andrighetto *et al*., 2000). This technique consists of direct PCR amplification using conserved oligonucleotide primers against the 26S and 18S rRNA genes, followed by endonuclease restriction analysis of the amplified product. Because ribosomal regions evolve in a concerted fashion they have low intraspecific polymorphism and high interspecific variability. Consequently, PCR-RFLP analysis of the 5.8S-ITS region is an excellent tool for yeast identification. Restriction enzymes are a family of over 205 separate bacteria-derived enzymes that recognize specific sequences of typically 4 to 8 base pair regions of DNA and then cleave the phosphodiester bonds between the nucleotides. The resulting fragments are usually separated according to molecular size using gel electrophoresis. In order to estimate for the fragment size, molecular markers are used. The observed differences result from base substitutions, additions, deletions or sequence rearrangement within restriction enzyme recognition sequences or sites (Merz, 1990). PCR-RFLP is the most suited technique for studies at the intraspecific or among closely related taxa.

Phylogenetic analysis of closely related species is possible from the use of the region spanning the two intergenic transcribed spacers (ITS1 and ITS2) and the 5.8S ribosomal subunit. The ITS1 region separates the conserved 18S and the 5.8S rRNA genes and the ITS2 region is found between 5.8S and 28S rRNA genes. The ITS1 and ITS2 have been shown to play a role in primary rRNA processing (Musters *et al*., 1990).

1.8. Aim and objectives

In the literature, the importance of phytase enzymes and some of their considerable potential in commercial and environmental applications were discussed. Phytase research has centered on the discovery of novel phytase enzymes which could improve phosphate bioavailability in animal feed. These phytases should have appropriate pH and

temperature profiles for effective functioning in the digestive tract of monogastric animals. Previously, 23 phytase producing yeasts were isolated from soil in the Limpopo Province. The enzyme activities of these yeast isolates will be determined and the best three producers will be further characterized taxonomically and enzymatically.

To achieve the aim, the following objectives were set:

a) Determine the phytase activities of the 23 yeast isolates;
b) Identification of the best three phytase producing yeasts using standard identification methods;
c) Determine the genetic relatedness of the yeasts using molecular techniques;
d) Determine growth conditions to optimally produce phytase by these yeasts and
e) Characterize crude phytase enzymes.

CHAPTER TWO

2. MATERIAL AND METHODS

2.1. Yeast isolates

Previously, 23 yeast isolates were isolated from various soil samples in the Limpopo Province, South Africa. The yeast isolates and their origin are indicated in Table 2.1. All yeast isolates were kept on YM slants (10.0 $g.l^{-1}$ glucose, 5.0 $g.l^{-1}$ peptone, 3.0 $g.l^{-1}$ yeast extract, 3.0 $g.l^{-1}$ malt extract and 15.0 $g.l^{-1}$ agar) at 25º C. The yeast isolates were sub-cultured on YM slants every 4 months.

Table 2.1. The origin of the yeasts isolated in the Limpopo Province

Yeast isolates	Origin	Yeast isolates	Origin	Yeast isolates	Origin
LD 4	Lunds Farm	LD 19	Lunds Farm	HBD 9	Houtbosdorp
LD 5.1	Lunds Farm	POL 14.1	Polokwane	HBD 11	Houtbosdorp
LD 5.2	Lunds Farm	POL 14.2	Polokwane	HBD 17	Houtbosdorp
LD 7	Lunds Farm	POL 16.1	Polokwane	HBD 18	Houtbosdorp
LD 9	Lunds Farm	POL 16.2	Polokwane	HBD 19	Houtbosdorp
LD 10	Lunds Farm	HBD 1	Houtbosdorp	HBD 20.1	Houtbosdorp
LD 13	Lunds Farm	HBD 6.2	Houtbosdorp	HBD 20.2	Houtbosdorp
LD 15	Lunds Farm	HBD 6.3	Houtbosdorp		

2.2. Screening for high phytase producing yeast isolates

The methods described by Vats and Banerjee (2002), Quan *et al*. (2001) and Harland and Harland (1980) were followed to determine the enzyme activities. All isolates were grown on a synthetic medium, PSM agar (5.0 $g.l^{-1}$ calcium phytate, 15.0 $g.l^{-1}$ glucose, 5.0 $g.l^{-1}$ NH_4NO_3, 0.5 $g.l^{-1}$ $MgSO_4.\ 7H_2O$, 0.5 $g.l^{-1}$ KCl, 0.01 $g.l^{-1}$ $FeSO_4.\ 7H_2O$, 0.01 $g.l^{-1}$ $MnSO_4.\ H_2O$, 15.0 $g.l^{-1}$ agar) and the pH was adjusted to 5.5 before autoclaving at 121º C for 15 min. These plates were inoculated with the yeast isolates and incubated at 30º C

for 3 days. Two loopfuls of each culture from the PSM plates were inoculated into 50 ml PSM broth (same ingredients as PSM agar without the inclusion of agar and calcium phytate) in 500 ml Erlenmeyer flasks in triplicate. All the flasks were incubated for 3 days at 30º C in an orbital shaker (200 rpm). Samples were centrifuged at 10 000 rpm for 10 min and the supernatant was used for phytase analysis. Phytase activity was estimated colorimetrically by monitoring the release of inorganic phosphorus from phytic acid. Ten milliliters of a 0.2 M sodium acetate buffer pH 5.15, 0.4 ml of 0.1 M $MgSO_4$, 5 ml of water, 4.4 ml of 6,82 mM sodium phytate, and 0.2 ml of the supernatant were mixed (total volume 20 ml) and incubated for 30 min at 37º C. The reaction was stopped by adding 1ml 10 % trichloroacetic acid. One milliliter of this reaction mixture was used to analyze the release of inorganic phosphate. One enzyme unit (U) was defined as the amount of the enzyme liberating 1 nmol of inorganic phosphate in 1 min. A colour reaction was developed by adding 2 ml of water and 5 ml of Taussky-Schoor reagent. The contents were mixed and the absorbance was read immediately at 660 nm. The Taussky-Schoor reagent was prepared by placing 10 g of ammonium molybdate (NH_4Mo) in a 100 ml volumetric flask and dilute it to volume with 10 N H_2SO_4. Ten milliliters of H_2SO_4-NH_4Mo solution was placed into a separate 100 ml volumetric flask and diluted with 70 ml of distilled water. To this solution, 5 g of ferrous sulfate (heptahydrate) was added and the solution was diluted to the desired volume with distilled water.

2.3. Identification of yeast isolates

The best three phytase producers were characterized using standardized conventional methods described by Yarrow (2000).

2.3.1. Morphological characteristics

2.3.1.1. Cell and colony morphology

The yeast isolates were grown on 5 % malt extract agar and were incubated for 3 to 5 days at 25º C. Colonies were studied using a stereomicroscope and the cells using a light microscope (Yarrow, 2000).

2.3.1.2. Dalmau plate technique

This test was performed in order to note the presence or absence of pseudomycelium or true hyphae or single cells. The yeast isolates were inoculated on corn meal agar (17 $g.l^{-1}$), sterilized cover slides were placed on top of the inoculated cultures, and the plates were incubated for 7 to 10 days at 25º C. The presence and absence of mycelium were noted using a light microscope (Yarrow, 2000).

2.3.1.3. Sexual spores

In order to visualize the presence of the sexual spores, cultures were grown on four different media i.e. Gorodkowa agar (1 $g.l^{-1}$ glucose, 10 $g.l^{-1}$ peptone, 5 $g.l^{-1}$ sodium chloride and 20 $g.l^{-1}$ agar), McClary's acetate agar (1 $g.l^{-1}$ glucose, 1.8 $g.l^{-1}$ potassium chloride, 2.5 $g.l^{-1}$ yeast extract, 8.2 $g.l^{-1}$ sodium acetate trihydrate and 15 $g.l^{-1}$ agar), malt extract agar (50 $g.l^{-1}$ malt extract agar) and 1/10 YM agar (1 $g.l^{-1}$ glucose, 0.3 $g.l^{-1}$ malt extract, 0.3 $g.l^{-1}$ yeast extract, 0.5 $g.l^{-1}$ peptone and 15 $g.l^{-1}$ agar) medium. The media were inoculated with the yeast isolates and incubated at 25º C for 24 h, after which the slants were placed at 15º C for another six weeks. The presence of sexual spores were examined at least once every 5 days (Yarrow, 2000).

2.3.2. Biochemical characteristics

2.3.2.1. DBB test

This test was performed in order to differentiate between ascomycetous and basidiomycetous yeasts. The yeast isolates were inoculated on Sabourads agar plates (40 $g.l^{-1}$ Sabourads glucose agar and 5.0 $g.l^{-1}$ yeast extract) and were incubated at 25º C for 3 weeks. The DBB salt reagent was prepared by adding 46 mg DBB salt in a chilled Tris buffer (0.25 M), pH 7.0. This reagent was poured onto the colonies and the colour change was noted. A pink colour is indicative of basidiomycetous yeasts and a yellow or no colour change indicative of ascomycetous yeasts (Yarrow, 2000).

2.3.2.2. Fermentation

The yeast isolates were tested on 14 sugars (glucose, D-galactose, and maltose, sucrose, α-trehalose, melibiose, lactose, cellobiose, melezitose, raffinose, inulin, starch and D-

xylose) for their fermentation ability. The Durham test tube technique was employed. Each test tube contained 20 $g.l^{-1}$ sugar and 5 $g.l^{-1}$ yeast extract. The inoculated tubes were incubated at 25º C for 3-14 days. The results were noted after 3, 5, 7, and 14 days (Yarrow, 2000).

2.3.2.3. Carbon assimilation

The yeast isolates were tested on 46 carbon sources (D-glucose, D-galactose, D-mannitol, glucosamine, ribose, xylose and, D and L-lactate, glucuronate, gluconate, glucarate, glucitol, galactonate, galacturonic acid, arabinose, raffinose, mannose, α,α trehalose, methyl α-glucoside, cellobiose, salicin, melibiose, lactose, meso erythritol, ribitol, sucrose, methanol, L-sorbose, L-arabinitol, rhamnose, L-arabinose, dulcitol, myo-inositol, glucono-lactone, 2-keto-D-gluconnate and 5-keto-D- gluconate, succinate, ethanol, propane 1,2 diol, butane 2,3 diol, glycerol, sol. starch, inulin, melezitose, quinic acid, xylitol and citrate) for their carbon assimilation ability. Each tube contained 5 ml consisting of carbon equivalent to 5 $g.l^{-1}$ glucose (11 $g.l^{-1}$ in the case of raffinose) and 6.7 $g.l^{-1}$ yeast nitrogen base. For acids and salts, the pH was adjusted to 5.6 with NaOH. The inoculated tubes were incubated at 25º C for 21 days. The results were noted after 4, 7, 14, and 21 days (Yarrow, 2000).

2.3.2.4. Nitrogen assimilation

The auxanographic method was employed. Petri dishes containing Bacto yeast carbon base (11.7 $g.l^{-1}$), agar (15 $g.l^{-1}$) and the yeast isolates were prepared. The following compounds were placed on the agar plates as sole source of nitrogen: cadaverine, sodium nitrite, potassium nitrate, ethylamine, lysine, imidazole, creatine, glucosamine, D-tryptophan and creatinine. The plates were incubated at 25º C for 3 days. The appearance of zones around the nitrogen sources was indicative of a positive result. Ammonium sulphate was used as a positive control (Yarrow, 2000).

2.3.2.5. Splitting of arbutin

Aliquots of arbutin medium (5 $g.l^{-1}$ arbutin, 5 $g.l^{-1}$ yeast extract and 20 $g.l^{-1}$ agar) were distributed (approximately 5 ml) to test tubes and sterilized. After sterilization, 2-3 drops

of ferric ammonium citrate (10 $g.l^{-1}$ ferric ammonium citrate) were added to the tubes, mixed properly and slanted. The slants were inoculated with yeast isolates and incubated at 25º C for 2-7 days. A dark brown to black colour was indicative of a positive reaction (Yarrow, 2000).

2.3.2.6. Growth on 50 % glucose yeast extract agar

Slants containing 50 % glucose yeast extract medium (5 $g.l^{-1}$ yeast extract, 500 $g.l^{-1}$ glucose and 30 $g.l^{-1}$ agar) were inoculated with the yeast isolates. The slants were incubated at 25º C for up to three weeks. Growth was indicative of a positive result (Yarrow, 2000).

2.3.2.7. Growth in 10 % NaCl

Test tubes containing 4.5 ml of a 10 % NaCl and 5 % glucose solution were prepared and sterilized. After sterilization 0.5 ml of a 6.7 $g.l^{-1}$ YNB solution was added to the test tubes. The tubes were inoculated with fresh yeast cultures and were incubated at 25º C for three weeks. Results were noted every 7 days (Yarrow, 2000).

2.3.2.8. Formation of extracellular, amyloid material

One or two drops of Lugol's iodine solution (1.0 g iodine and 2.0 g potassium iodide were added into 300 ml H_2O) was added to the 3 weeks old glucose assimilation test tubes. A blue, purple, or green reaction was an indication of a positive reaction (Yarrow, 2000).

2.3.2.9. Urease test

A urease agar medium consisting of 1.0 $g.l^{-1}$ peptone, 1.0 $g.l^{-1}$ glucose, 5.0 $g.l^{-1}$ sodium chloride, 2.0 $g.l^{-1}$ potassium dihydrogen phosphate and 0.012 $g.l^{-1}$ phenol red were distributed into test tubes containing 4.5 ml aliquots and sterilized. Immediately after sterilization, 0.5 ml of a 20 % filter sterilized urea solution was added to the test tubes and mixed well after which the tubes were slanted. The slants were inoculated with the yeast isolates and incubated at 25º C for up to 5 days. A basidiomycetous yeast was used as a control and a pinkish colour was indicative of a positive reaction (Yarrow, 2000).

2.3.2.10. Cycloheximide resistance (0.1 % and 0.01 %)

Yeast isolates were tested on 0.01 % or 0.1 % cycloheximide solution. Yeast isolates were inoculated in a 5 ml solution containing 4.5 ml dH_2O and 0.5 ml of the appropriate cycloheximide concentration to the YNB solution (6.7 % yeast nitrogen base and 10 % glucose) and the test tubes were incubated at 25º C for 3 weeks. Results were noted every 7 days for 21 days (Yarrow, 2000).

2.3.2.11. Maximum growth temperature

The yeast isolates were inoculated on YM slants (10 $g.l^{-1}$ glucose, 5 $g.l^{-1}$ peptone, 3 $g.l^{-1}$ malt extract and 3 $g.l^{-1}$ yeast extract) and incubated at the following temperatures for 7 days: 30º C, 35º C, 37º C, 40º C, and 45º C. A positive result was noted when growth appeared on the slants (Yarrow, 2000).

2.3.2.12. Acetic acid production

The yeast cultures were inoculated on Custer's chalk medium (50 $g.l^{-1}$ glucose, 5.0 $g.l^{-1}$ calcium carbonate, 5.0 $g.l^{-1}$ yeast extract and 20 $g.l^{-1}$ agar) and the plates were incubated at 25º C for up to 2 weeks. Clearing zones around the colonies indicated that acetic acid has been produced and noted as a positive result (Yarrow, 2000).

2.3.2.13. Tolerance of 1 % acetic acid

Acetic acid plates (100 $g.l^{-1}$ glucose, 10 $g.l^{-1}$ tryptone, 10 $g.l^{-1}$ yeast extract and 20 $g.l^{-1}$ agar) were inoculated with the yeast isolates and were incubated at 25º C for 3 to 6 days. Growth on the plates indicated a positive result (Yarrow, 2000).

2.3.3. Molecular characterization

2.3.3.1. DNA extraction for PCR

The test yeasts *Candida guilliermondii* HBD6.2*, Candida diddensiae* LD9*, Candida famata* LD7, and the reference strains obtained from the yeast culture collection (University of the Free State) *Debaryomyces hansenii* Y0219, *Debaryomyces hansenii* Y0610, *Candida diddensiae* Y0774, *Pichia guilliermondii* Y0209, *Pichia guilliermondii* Y0053, *Pichia guilliermondii* Y0054 were grown on YM broth for 3 days and used for

PCR-RFLP analysis. Total DNA was isolated using the method of Rose *et al*. (1990). Fifty milligrams of cells were collected by centrifugation at 12 000 rpm for 5 min. Two hundred microliters of lysis buffer, 200 µl of phenol/chloroform and 0.3 g glass beads were added to the cells and vortexed for 2 min. The mixture was incubated for 5 min at room temperature followed by vortexing for 2 min. Two hundred microliters of TE_1 (pH 8.0) buffer were added to the mixture, followed by vortexing for 5 sec. The upper phase containing DNA was collected by centrifuging at 12 000 rpm for 5 min. Two volumes of ice cold 100 % ethanol were added to precipitate DNA. The solution was mixed gently and incubated for 24 hrs at -20º C. The DNA was collected by centrifuging at 12 000 rpm for 20 min. For the degradation of RNA, 3 µl RNAse (10 $mg.ml^{-1}$) was added and the mixture was incubated at 37º C for 15 min. After incubation, equal volume of chloroform: isopropanol was added to the homogenate, it was then mixed gently and centrifuged for 5 min. The upper phase was collected into a fresh eppendorf tube where 2 volumes of ethanol were added, mixed gently and incubated for overnight at -20º C. The homogenate was centrifuged for 20 min at 12 000 rpm and the pellet was washed twice with 70 % ethanol. The pellet was vacuum dried and dissolved in 50 µl TE_1 buffer. The quality of DNA was checked on 1 % agarose gel electrophoresis in 1x TAE buffer and the bands were visualized with ethidium bromide. DNA concentration was determined in relation to the concentrations of λDNA/*Hind* III molecular weight marker.

2.3.3.2. PCR-RFLP

Thirty seven micrograms of DNA were amplified in a 50 µl reaction volume containing 2U of ex*Taq* enzyme (TaKaRa), 250 µM dNTP mix (TaKaRa), 1x ex*Taq* buffer (TaKaRa) and 0.75 µM primer each. The primers used are NS1 (5′ GTAGTCATATGCTTGTCTC 3′) and ITS2 (5′ GCTGCGTTCTTCATCGATGC 3′) as described by (Vasdinyei and Deák, 2003). Amplification was carried out in a GeneAmp, PCR System 9700 machine (Applied Biosystem). The PCR program consisted of the following steps: an initial denaturation at 94º C for 2 min, 35 cycles of denaturation at 94º C for 1 min, annealing at 55º C for 1 min and extension at 72º C for 1 min, and a final extension at 72º C for 7 min.

Restriction endonucleases: *Alu*I, *Cfo*I, *Dra*I, *Hae*III, *Hpa*II, *Rsa*I and *Taq*I (Sigma Aldrich) were used to digest the PCR products. The 20 µl digestion mixture contained 8µl PCR products, 8 µl of sdH_2O, 15 U restriction enzyme, 5 $\mu g.\mu l^{-1}$ BSA and 1x buffer that was supplied with the enzyme. The mixture was incubated at 37º C for 3 hrs except the mixture digested with *Taq*I which was incubated for 24 hrs. The digests were run on 2 % agarose gel in 1x TAE buffer at a constant voltage of 70 V. After electrophoresis the gel was stained with 4 % ethidium bromide (10 $mg.ml^{-1}$) and visualised under UV light (Vasdinyei and Deák, 2003).

2.3.3.3. Data analysis

The gel fingerprints were scored for the presence (1) and absence of a band (0). The binary matrix was thus generated. The similarity matrix was generated with the DICE coefficient using the NTSYS (pc) program (Version 2.02i, Rohlf, 1998). The genetic distance between the taxa measured with Nei and Li (1979) distance coefficient (also known as DICE coefficient) was used to generate a UPGMA (unweighted pair group method using arithmetic averages) phylogenetic tree with a bootstrap of 100 replications using the Treecon program (Treecon, version 1.3b, Van der Peer and De Wachter, 1994). The genetic similarity between the isolates and their respective reference strains was assessed from the similarity matrix and the phylogenetic tree.

2.4. Effect of temperature and pH on enzyme activity

The yeast isolates were grown on PSM broth at various temperatures and pH levels. One thousand microliters of the supernatant were withdrawn at 5 hrs intervals and the growth (wet $weight.ml^{-1}$) was determined. The enzyme activity of the supernatant corresponding to each temperatures and pH combinations were recorded. A temperature range of 25-45ºC and a pH range of 4-6 were employed (Casey and Walsh, 2004). The pH was adjusted using concentrated HCl and 1 M NaOH. Growth curves and enzyme activity profiles were constructed.

2.5. Protein isolation and analysis of crude enzymes

After all the isolates were grown as described in Section 2.2 and supernatant fluid proteins were concentrated by precipitating with ammonium sulphate (Zhang *et al*., 2004). The concentrates were dialysed to remove the salt. The following agents were added to the crude protein concentrate: sterilized sodium azide (0.02 $g.l^{-1}$), 10 mM DTT and 17-174 $\mu g.ml^{-1}$ of 10 $mg.ml^{-1}$ PMSF (Phenyl methanesulfonyl fluoride) and the proteins were stored at 4º C. These crude protein extracts were used to determine the optimal pH and temperature of the crude phytase. The stability of the crude phytase extract was also determined as prescribed by Casey and Walsh (2004). Assays were set up and incubated as in (Section 2.4.) at a temperature range of 30-80º C and a pH range of 2-8.

2.6. Determination of protein concentration

Protein concentration was determined using a Bio-Rad protein assay kit according to the manufacturer's procedure.

2.6.1. Protein molecular weight markers

Pre-prepared Sigma molecular weight standard recombinant mixture with a range from 15 to 150 kDa was used.

2.6.2. SDS-PAGE analysis

The glass plates were assembled according to the manufacturer's instructions. In an Erlenmeyer flask, 10 ml of 12 % denaturing polyacrylamide was prepared. For the resolving gel, using the values given in Table 2.2, the components were mixed in the order shown. Since polymerization begins as soon as TEMED is added, the mixture was swirled gently and immediately poured. Using a Pasteur pipette, the acrylamide solution was overlaid with 1 ml of water to prevent oxygen from diffusing into the gel and inhibiting polymerization. The gel was placed in a vertical position and left to polymerize at room temperature for about 30 min. After polymerization, the overlay was poured-off and the top of the gel was washed with sdH_2O to remove any unpolymerized acrylamide. To prepare the stacking gel, the components were mixed in the order given

in Table 2.3. Immediately after the addition of TEMED, the mixture was mixed by gently swirling and poured. A clean comb was immediately inserted into the stacking gel solution, being careful to avoid trapping air bubbles. The gel was left to set as described before. Twenty microliters of concentrated supernatant (Section 2.6.) were taken and mixed with equal volumes of 2x Laemmeli buffer and boiled for 5 min to denature the proteins. The protein marker was also denatured in the same manner.

After polymerization, the comb was removed carefully and the wells were washed immediately with sdH_2O to remove any unpolymerized acrylamide. The gel was then mount in an electrophoresis apparatus. SDS-PAGE running buffer was added to the top and bottom reservoirs to cover the gel. Up to 20 µl of each of the samples were loaded into the wells with a Hamilton needle. The gel was run for 2 hrs at 60 V and 250 Amps. After electrophoresis the gel was stained with Coomassie stain (0.5 g Coomassie Blue R-250, 250 ml methanol and water to 500 ml) overnight on a shaker and destained with 50 % methanol for 4 to 6 hrs on a shaker.

Table 2.2. Solutions for preparing resolving gels for Tris-glycine SDS-PAGE gel electrophoresis

Solution components	**Component volumes (ml) per gel**					
12 %	5	10	15	20	25	30
Water	1.6	3.3	4.9	6.6	8.2	9.9
30 % Acrylamide	2.0	4.0	6.0	8.0	10.0	12.0
1.5 M Tris (pH 8.8)	1.3	2.5	3.8	5.0	6.3	7.5
10 % SDS	0.05	0.1	0.15	0.2	0.25	0.3
10 % Ammonium persulphate	0.05	0.1	0.15	0.2	0.25	0.3
TEMED	0.002	0.004	0.006	0.008	0.01	0.012

Table 2.3. Solution for preparing 5 % stacking gels for Tris-glycine SDS-PAGE gel electrophoresis

Solution components	**Component volumes (ml) per gel mold volume**					
5 %	1	2	3	4	5	6
Water	0.68	1.4	2.1	2.7	3.4	4.1
30 % Acrylamide mix	0.17	0.33	0.5	0.67	0.83	1.0
1.5 M Tri (pH 8.8)	0.13	0.25	0.38	0.5	0.67	0.75
10 % SDS	0.01	0.02	0.03	0.04	0.05	0.06
10 % Ammonium persulphate	0.01	0.02	0.03	0.04	0.05	0.06
TEMED	0.001	0.002	0.003	0.004	0.005	0.006

CHAPTER THREE

3. RESULTS

3.1. Phytase activity of the yeast isolates

The enzyme activities of 23 yeast isolates were determined and recorded in Table 3.1. The phytase activity reflects activity determined after 3 days of incubation of the yeasts. Three isolates, i.e., HBD6.2, LD9 and LD7 produced the highest phytase activities and were chosen for subsequent examination.

Table 3.1. Enzyme activities of the 23 yeast isolated soil samples in Limpopo Province

Yeast isolates	**Enzyme activity (Uml^{-1})**	**Yeast isolates**	**Enzyme activity (Uml^{-1})**
LD4	5.44	POL16.2	148.02
LD5.1	16.96	HBD1	27.11
LD5.2	4.27	HBD6.2	676.02*
LD7	440.94*	HBD6.3	125.15
LD9	630.21*	HBD9	7.60
LD10	34.50	HBD11	36.26
LD13	7.78	HBD17	10.12
LD15	23.57	HBD18	59.06
LD19	211.71	HBD19	188.89
POL14.1	122.81	HBD20.1	51.46
POL14.2	25.15	HBD20.2	98.88
POL16.1	53.67		

* indicates the yeast isolates with the highest enzyme activities.

Figures 3.1, 3.2 and 3.3 illustrate the production of phytase activity of the yeast isolates HBD6.2, LD9 and LD7 on phytase screening agar plates respectively. A clearing zone around the yeast colony represents phytase activity.

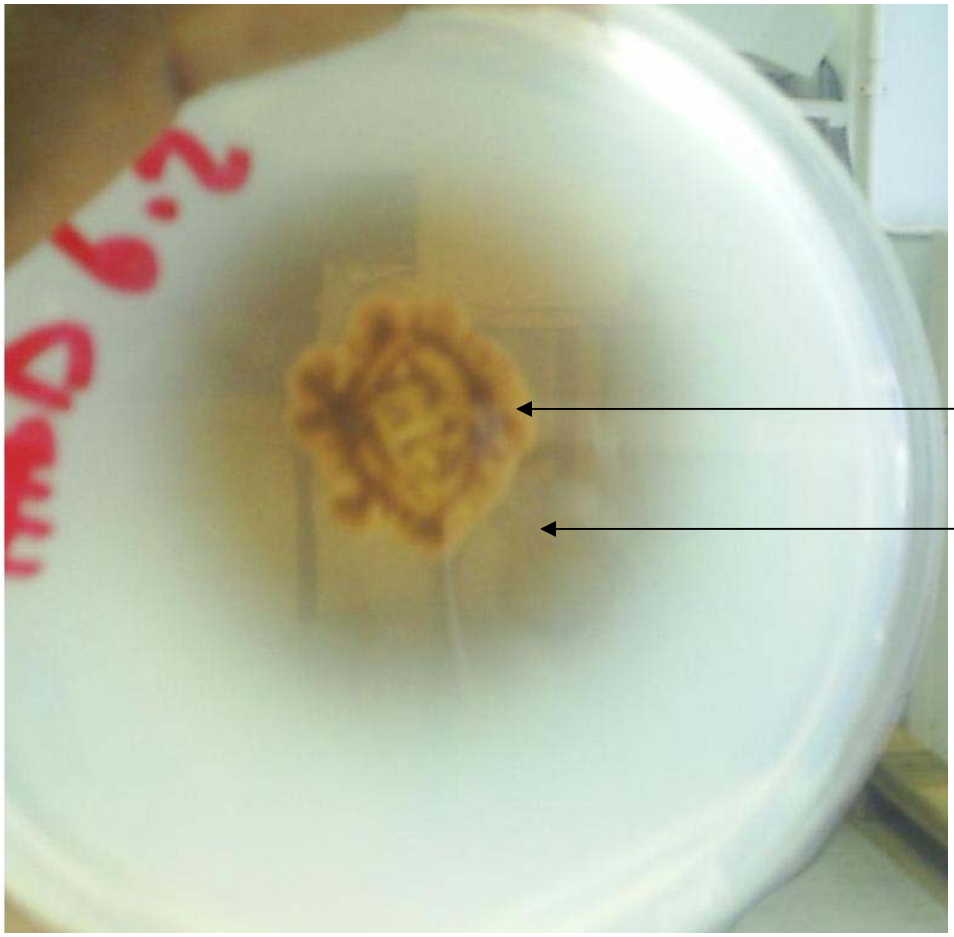

Fig. 3.1. Detection of extracellular phytase activity, produced by HBD6.2, when grown on phytase screening media.

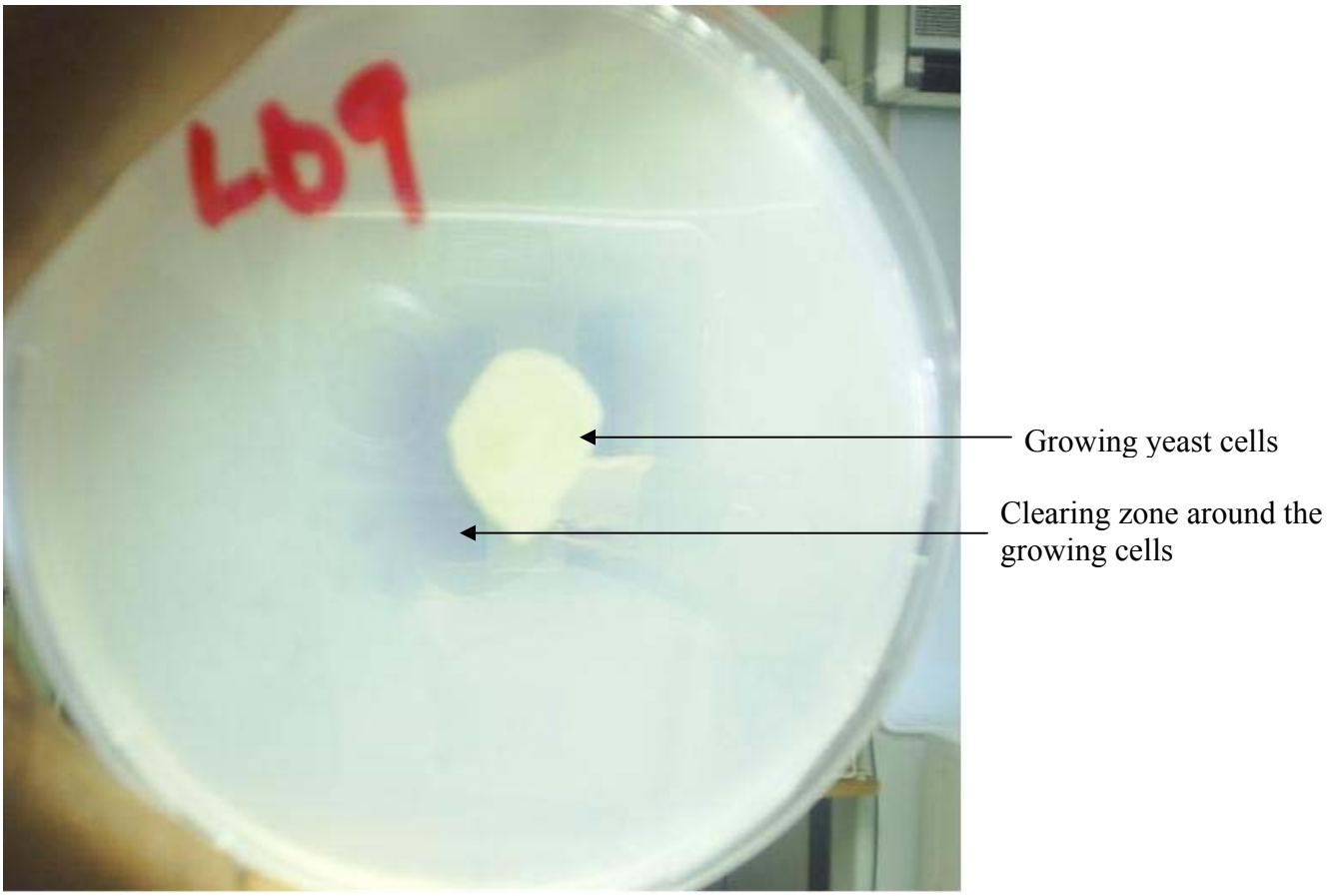

Fig. 3.2. Detection of extracellular phytase activity, produced by LD9, when grown on phytase screening media.

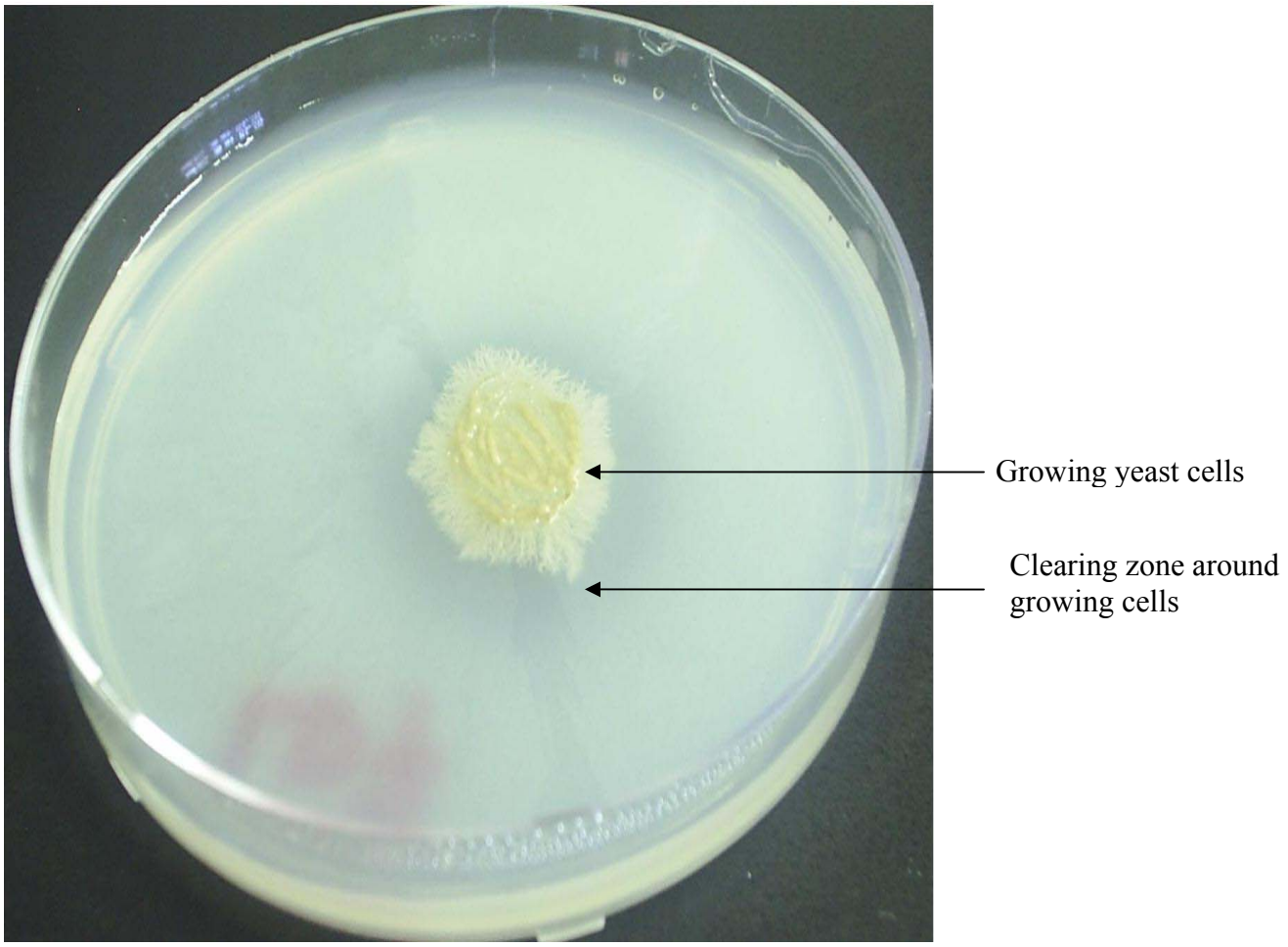

Fig. 3.3. Detection of extracellular phytase activity, produced by LD7, when grown on phytase screening media.

3.2. Identification of HBD6.2, LD9 and LD7

3.2.1. HBD6.2

Identified as: *Candida guilliermondii*

Colony morphology on YM agar: cream white to light brown in colour, round in shape, raised with a smooth margin.

Colony texture: Smooth

Morphology on Dalmau plates: Simple pseudohyphae with branches

Cell morphology: Round to oval cells which reproduce through multilateral budding

Formation of sexual spores: None

Biochemical characteristics:

Table 3.2. Fermentation results for HBD6.2

Sugar	**Result**	**Sugar**	**Result**
Cellobiose	_	Melezitose	_
Galactose	_	Raffinose	_
Glucose	D	Starch	_
Inulin	_	Sucrose	_
Lactose	_	Trehalose	_
Maltose	_	Xylose	_
Melebiose	_		

Keywords: (D) Delayed fermentation, (-) No fermentation occurred.

Table 3.3. Maximum growth temperature results for HBD6.2

Temperature (º C)	**Result**
30	+
35	+
37	+
40	-
45	-

Keywords: (-) No growth, (+) Growth occurred.

Table 3.4. Carbon assimilation results for HBD6.2

Carbon Source	**Result**	**Carbon Source**	**Result**	**Carbon Source**	**Result**
Butane 2,3 diol	D	Glucarate	D	Propane 1,2 diol	_
Cellobiose	+	Glucuronate	_	Quinic acid	D
Citrate	+	Glycerol	+	Raffinose	_
D-arabinose	_	Inulin	+	Ribitol	D
D-galactose	D	Lactose	_	Ribose	D
D-glucitol	+	L-arabinitol	+	Rhamnose	_
D-gluconate	_	L-arabinose	_	Salicin	+
D-glucono-1,5 lactose	+	Maltose	+	Sol. starch	D
D-glucosamine	_	Melebiose	+	Sorbose	+
DL-lactate	D	Melezitose	+	Succinate	D
D-mannitol	+	Meso-erythritol	+	Sucrose	+
Dulcitol	_	Methanol	_	Xylitol	D
Ethanol	+	Methyln α-D glucoside	+	Xylose	D
Glucose	+	Myo-inositol	D	α, α Trehalose	+

Keywords: (D) Delayed growth, (-) No growth occurred, (+) Growth occurred.

Table 3.5. Nitrogen assimilation test results for HBD6.2

Nitrogen source	Result	Nitrogen source	Result
Cadaverine	_	Imidazole	_
Creatine	_	Lysine	+
Ethylamine	+	Potassium nitrate	_
Glucosamine	_	Sodium nitrite	_

Keywords: (-) No growth, (+) growth occurred.

Table 3.6. Results from various other tests performed for HBD6.2

Test	Result	Test	Result
Acetic acid production	_	Resistance to 0.1% cyclohexamide	+
DBB test	_	Resistance to 0.01% cyclohexamide	+
Formation of extracellular amyloid material	_	Splitting of arbutin	+
Growth on 50% glucose	+	Tolerance of 1% acetic acid	_
Growth on 60% glucose	D	Urease test	+
Growth on 10% NaCl	+		

Keywords: (D) Delayed growth, (-) No growth, (+) Growth occurred.

Identification of HBD6.2 was not conclusive. It was identified up to species level, because most of the characteristics were similar when compared to *Candida guilliermondii*. However, the following differences were observed: assimilation on lactose, erythritol, myo-inositol, ethylamine and cadaverine as well as differences with the urease test.

3.2.2. LD9

I**dentified as:** *Candida diddensiae*

Colony morphology on YM agar: cream white in colour, round in shape, raised with a smooth margin.

Colony texture: Smooth

Morphology in Dalmau plates: Pseudohyphae with branches

Cell morphology: Round to oval cells which reproduce through multilateral budding

Formation of sexual spores: None

Biochemical characteristics:

Table 3.7. Fermentation results for LD9

Sugar	**Result**	**Sugar**	**Result**
Cellobiose	_	Melezitose	_
Galactose	_	Raffinose	+
Glucose	+	Starch	_
Inulin	_	Sucrose	+
Lactose	_	Trehalose	_
Maltose	+	Xylose	_
Melebiose	_		

Keywords: (+) fermentation occured, (-) No fermentation occurred.

Table 3.8. Maximum growth temperature test results for LD9

Temperature (º C)	**Result**
30	+
35	+
37	+
40	+
45	-

Keywords: (-) No growth, (+) Growth occurred.

Table 3.9. Carbon assimilation test results for LD9

Carbon Source	**Result**	**Carbon Source**	**Result**	**Carbon Source**	**Result**
Butane 2,3 diol	_	Glucarate	D	Propane 1,2 diol	_
Cellobiose	+	Glucuronate	_	Quinic acid	D
Citrate	_	Glycerol	_	Raffinose	_
D-arabinose	_	Inulin	_	Ribitol	D
D-galactose	D	Lactose	_	Ribose	+
D-glucitol	D	L-arabinitol	+	Rhamnose	_
D-gluconate	_	L-arabinose	_	Salicin	+
D-glucono-1,5 lactose	+	Maltose	+	Sol. starch	D
D-glucosamine	_	Melebiose	_	Sorbose	D
DL-lactate	D	Melezitose	D	Succinate	D
D-mannitol	D	Meso-erythritol	D	Sucrose	+
Dulcitol	D	Methanol	_	Xylitol	D
Ethanol	+	Methyln α-D glucoside	D	Xylose	+
Glucose	+	Myo-inositol	+	α, α Trehalose	+

Keywords: (D) Delayed growth, (-) No growth occurred, (+) Growth occurred.

Table 3.10. Nitrogen assimilation results for LD9

Nitrogen source	Result	Nitrogen source	Result
Cadaverine	+	Imidazole	_
Creatine	_	Lysine	+
Ethylamine	_	Potassium nitrate	_
Glucosamine	_	Sodium nitrite	+

Keywords: (-) No growth, (+) growth occurred.

Table 3.11. Results from various other tests performed for LD9

Test	Result	Test	Result
Acetic acid production	_	Resistance to 0.1% cyclohexamide	D
DBB test	_	Resistance to 0.01% cyclohexamide	+
Formation of extracellular amyloid material	_	Splitting of arbutin	+
Growth on 50% glucose	+	Tolerance of 1% acetic acid	_
Growth on 60% glucose	D	Urease test	+
Growth on 10% NaCl	+		

Keywords: (D) Delayed growth, (-) No growth, (+) Growth occurred.

Identification of LD9 was not conclusive. However, it was identified up to species level because most of the characteristics were similar when compared to *Candida diddensiae.* The following differences were observed: fermentation of galactose, growth on D-arabinose, L-arabinose, growth on sodium nitrite and resistance to 0.1 and 0.01 % cyclohexamide.

3.2.3. LD7

Identified as: *Candida famata*

Colony morphology on YM agar: cream white to pink in colour, oval in shape, raised with smooth margin.

Colony texture: Smooth

Morphology in Dalmau plates: simple pseudohyphae

Cell morphology: cylindrical to oval cells which reproduce through multilateral budding

Formation of sexual spores: None

Biochemical characteristics:

Table 3.12. Fermentation results for LD7

Sugar	**Result**	**Sugar**	**Result**
Cellobiose	_	Melezitose	_
Galactose	_	Raffinose	_
Glucose	+	Starch	_
Inulin	_	Sucrose	_
Lactose	_	Trehalose	_
Maltose	_	Xylose	_
Melebiose	_		

Keywords: (+) Fermentation occured, (-) No fermentation occurred.

Table 3.13. Maximum growth temperature results for LD7

Temperature (º C)	**Result**
30	+
35	+
37	+
40	+
45	D

Keywords: (D) Delayed growth, (+) Growth occurred.

Table 3.14. Carbon assimilation results LD7

Carbon Source	**Result**	**Carbon Source**	**Result**	**Carbon Source**	**Result**
Butane 2,3 diol	+	Glucarate	_	Propane 1,2 diol	_
Cellobiose	_	Glucuronate	_	Quinic acid	D
Citrate	+	Glycerol	+	Raffinose	+
D-arabinose	_	Inulin	+	Ribitol	D
D-galactose	D	Lactose	_	Ribose	D
D-glucitol	+	L-arabinitol	+	Rhamnose	+
D-gluconate	_	L-arabinose	_	Salicin	_
D-glucono-1,5 lactose	D	Maltose	_	Sol. starch	+
D-glucosamine	_	Melebiose	_	Sorbose	+
DL-lactate	D	Melezitose	+	Succinate	+
D-mannitol	+	Meso-erythritol	+	Sucrose	_
Dulcitol	+	Methanol	_	Xylitol	D
Ethanol	+	Methyl α-D glucoside	+	Xylose	D
Glucose	+	Myo-inositol	_	α, α Trehalose	+

Keywords: (D) Delayed growth, (-) No growth occurred, (+) Growth occurred.

Table 3.15. Nitrogen assimilation results for LD7

Nitrogen source	Result	Nitrogen source	Result
Cadaverine	_	Imidazole	_
Creatine	_	Lysine	+
Ethylamine	_	Potassium nitrate	_
Glucosamine	_	Sodium nitrite	_

Keywords: (-) No growth, (+) growth occurred.

Table 3.16. Results from various tests performed for LD7

Test	Result	Test	Result
Acetic acid production	_	Resistance to 0.1% cyclohexamide	_
DBB test	_	Resistance to 0.01% cyclohexamide	_
Formation of extracellular amyloid material	_	Splitting of arbutin	+
Growth on 50% glucose	+	Tolerance of 1% acetic acid	_
Growth on 60% glucose	D	Urease test	+
Growth on 10% NaCl	+		

Keywords: (D) Delayed growth, (-) No growth, (+) Growth occurred.

This yeast isolate could not be identified to species level. However, it was identified as belonging to *Candida* with the closest yeast being *Candida famata* with differences in the urease test and the assimilation of Butane 2, 3 diol, sucrose and maltose. However, morphologically it differed from *Candida famata* in producing cream white to pinkish colonies. It is therefore doubtful if LD7 is related to *C. famata.*

3.3. Molecular characterization

The PCR-RFLP technique was used to confirm the identification of the isolated yeasts performed with the taxanomical method. The evaluation was done in comparison with the reference strains listed in Table 3.17.

Table 3.17. Identified yeast isolates with their reference strains

Yeast Isolates	**Reference Strains**
Candida guilliermondii HBD6.2	*Pichia guilliermondii* (teleomorph of *Candida guilliermondii*) Y0209, *Pichia guilliermondii* Y0053 and *Pichia guilliermondii* Y0054
Candida diddensiae LD9	*Candida diddensiae* Y0774
Candida famata LD7	*Debaryomyces hansenii* (teleomorph of *Candida famata*) Y0219 and *Debaryomyces hansenii* Y0610

(Y) Yeast collection, University of the Free Sate.

3.3.1. DNA profiles

All the yeast strains produced similar bands with molecular weight of 23130 bp (Fig. 3.4). The average concentration of the DNA samples was 240 µg based on the concentration of the λDNA /*Hind* III marker.

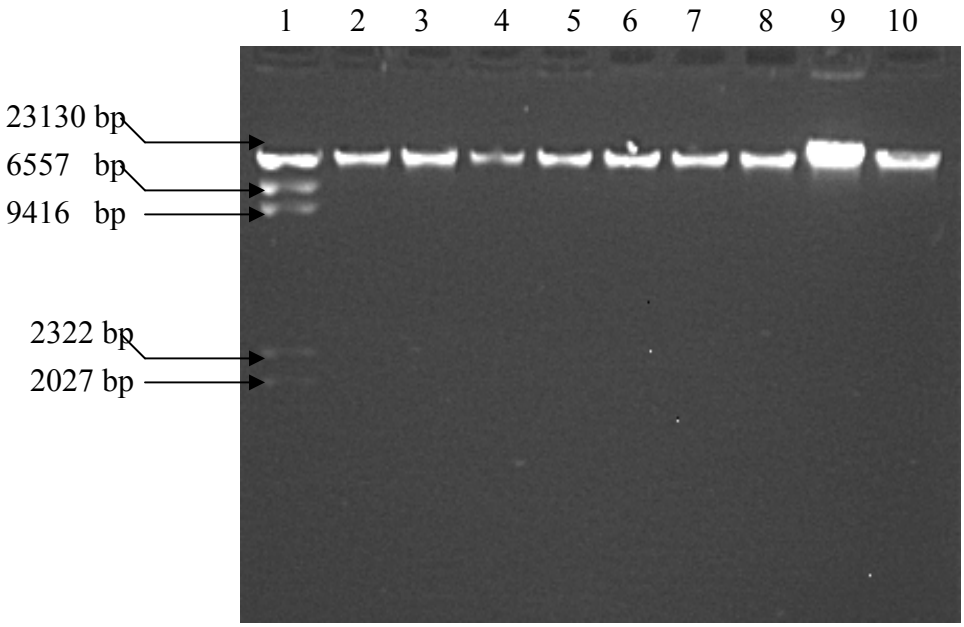

Fig. 3.4. DNA of three isolates with their reference strains. Lane 1: λDNA /*Hind* III MW Marker, 2: *Candida famata* LD7, 3: *Debaryomyces hansenii* Y0219, 4: *D. hansenii* Y0610, 5: *C. diddensiae* LD9, 6: *C. diddensiae* Y0774, 7: *C. guilliermondii* HBD6.2, 8: *Pichia guilliermondii* Y0209, 9: *P. guilliermondii* Y0053, 10: *P. guilliermondii* Y0054.

3.3.2. PCR amplification

Amplification with primers NS1 and ITS2 produced bands of similar size for all the yeast strains tested (Fig. 3.5). The size of the amplicon was approximately 2100 bp.

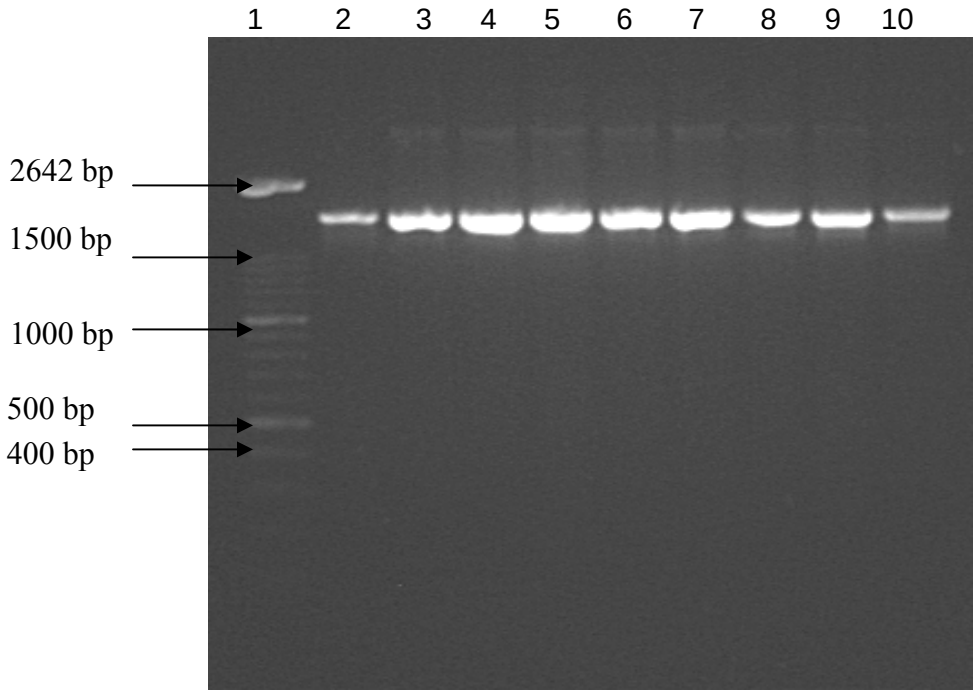

Fig. 3.5. PCR results of the nine yeast organisms following amplification with primers NS1 and ITS2. Lane 1: 100 bp DNA MW Marker, 2: *Candida famata* LD7, 3: *Debaryomyces hansenii* Y0219, 4: *D. hansenii* Y0610, 5: *C. diddensiae* LD9, 6: *C. diddensiae* Y0774, 7: *C. guilliermondii* HBD6.2, 8: *Pichia guilliermondii* Y0209, 9: *P. guilliermondii* Y0053, 10: *P. guilliermondii* Y0054.

3.3.3. Digestion of ampilcons with *Alu*I enzyme

Restriction digestion of PCR-RFLP products with *Alu*I produced nine markers (Fig. 3.6). *Candida famata* LD7, lane 2 has approximately 800 bp and 400 bp polymorphic bands that make it different from its reference strains, *D. hansenii* Y0219, lane 3 and *D. hansenii* Y0610, lane 4. *D. hansenii* Y0219, lane 3 and *D. hansenii* Y0610, lane 4 have a similar banding pattern with *C. diddensiae* LD9, lane 5; *C. diddensiae* Y0774, lane 6 and *C. guilliermondii* HBD6.2, lane 7. The reference strains, *P. guilliermondii* Y0209, lane 8, *P. guilliermondii* Y0053, lane 9 and *P. guilliermondii* Y0054, lane 10 have approximately 300 bp polymorphic band which which is absent in *C. guilliermondii* HBD6.2, lane 7.

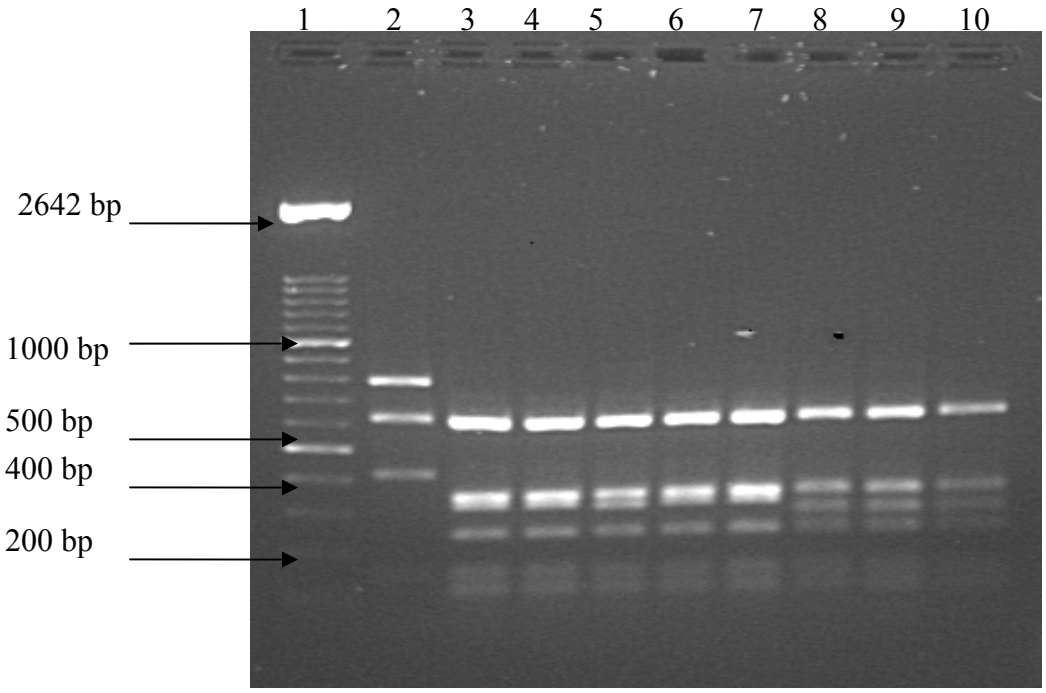

Fig. 3.6. Restriction digestion of PCR-RFLP products of yeast strains with *Alu*I enzyme. Lane 1: 100 bp DNA MW Marker, 2: *Candida famata* LD7, 3: *Debaryomyces hansenii* Y0219, 4: *D. hansenii* Y0610, 5: *C. diddensiae* LD9, 6: *C. diddensiae* Y0774, 7: *C. guilliermondii* HBD6.2, 8: *Pichia guilliermondii* Y0209, 9: *P. guilliermondii* Y0053, 10: *P. guilliermondii* Y0054.

3.3.4. Digestion of amplicons with *Cfo*I enzyme

Restriction digestion of PCR-RFLP products of yeast strains with *Cfo*I enzyme produced eight markers (Fig. 3.7). *Candida famata* LD7, lane 2 produced approximately 350 bp, 250 bp and 150 bp polymorphic bands that makes it to be different to its reference strains *D. hansenii* Y0219, lane 3 and *D. hansenii* Y0610, lane 4. *D. hansenii* Y0219, lane 3 and *D. hansenii* Y0610, lane 4 have the same banding pattern with *C. diddensiae* LD9, lane 5; *C. diddensiae* Y0774, lane 6; *C. guilliermondii* HBD6.2, lane 7 and *C. guilliermondii* Y0209, lane 8 respectively. *C. guilliermondii* HBD6.2, lane 7 produced bands that are different to its two reference strains *P. guilliermondii* Y0053, lane 9 and *P. guilliermondii* Y0054, lane 10. *P. guilliermondii* Y0053, lane 9 and *P. guilliermondii* Y0054, lane 10 have approximately 180 bp polymorphic band.

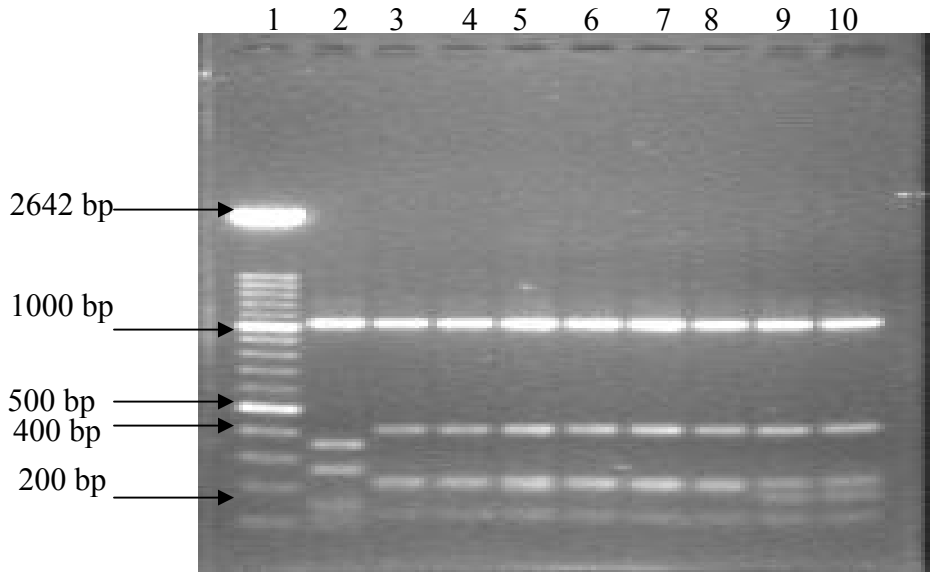

Fig. 3.7. Restriction digestion of PCR-RFLP products of yeast strains with *Cfo*I enzyme. Lane 1: 100 bp DNA MW Marker, 2: *Candida famata* LD7, 3: *Debaryomyces hansenii* Y0219, 4: *D. hansenii* Y0610, 5: *C. diddensiae* LD9, 6: *C. diddensiae* Y0774, 7: *C. guilliermondii* HBD6.2, 8: *Pichia guilliermondii* Y0209, 9: *P. guilliermondii* Y0053, 10: *P. guilliermondii* Y0054.

3.3.5. Digestion of amplicons with *Dra*I enzyme

Restriction digestion of PCR-RFLP products of yeast strains with *Dra*I enzyme produced six markers (Fig. 3.8). *Candida famata* LD7, lane 2 has approximately 2300 bp, 1500 bp and 500 bp bands that are different from its reference strains *D. hansenii* Y0219, lane 3 and *D. hansenii* Y0610, lane 4. *D. hansenii* Y0219, lane 3 and *D. hansenii* Y0610, lane 4 have the same banding pattern with *C. diddensiae* LD9, lane 5; *C. diddensiae* Y0774, lane 6; *C. guilliermondii* HBD6.2, lane 7; *P. guilliermondii* Y0053, lane 9 and *P. guilliermondii* Y0054, lane 10. *P. guilliermondii* Y0209, lane 8 also has approximately 2300 bp polymorphic band.

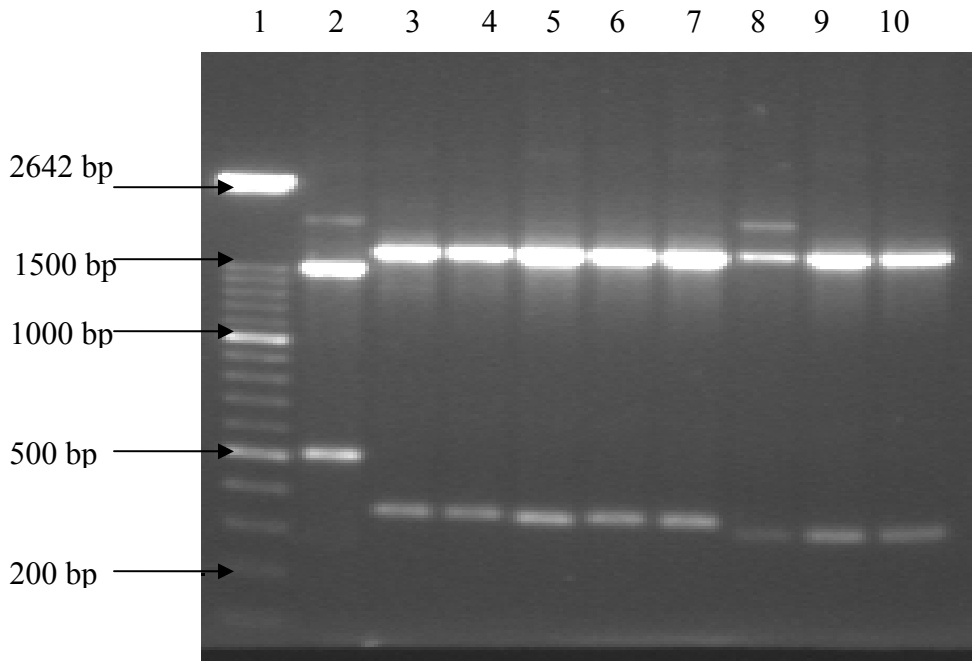

Fig. 3.8. Restriction digestion of PCR-RFLP products of yeast strains with *Dra*I enzymes. Lane 1: 100 bp DNA MW Marker, 2: *Candida famata* LD7, 3: *Debaryomyces hansenii* Y0219, 4: *D. hansenii* Y0610, 5: *C. diddensiae* LD9, 6: *C. diddensiae* Y0774, 7: *C. guilliermondii* HBD6.2, 8: *Pichia guilliermondii* Y0209, 9: *P. guilliermondii* Y0053, 10: *P. guilliermondii* Y0054.

3.3.6. Digestion of amplicons with *Hae*III enzyme

Restriction digestion of PCR-RFLP products of yeast strains with *Hae*III enzyme produced five markers (Fig. 3.9). *Candida famata* LD7, lane 2 has different banding pattern to its reference strains *D. hansenii* Y0219, lane 3 and *D. hansenii* Y0610, lane 4. *D. hansenii* Y0219, lane 3 and *D. hansenii* Y0610, lane 4 have the same banding pattern with *C. diddensiae* Y0774, lane 6 and *C. guilliermondii* HBD6.2, lane 7. *C. diddensiae* LD9, lane 5 has around 400 bp polymorphic band which makes it different compared to its reference strain, *C. diddensiae* Y0774, lane 6. *C. guilliermondii* HBD6.2, lane 7 has slightly different banding pattern *P. guilliermondii* Y0209, lane 8; *P. guilliermondii* Y0053, lane 9 and *P. guilliermondii* Y0054, lane 10 respectively.

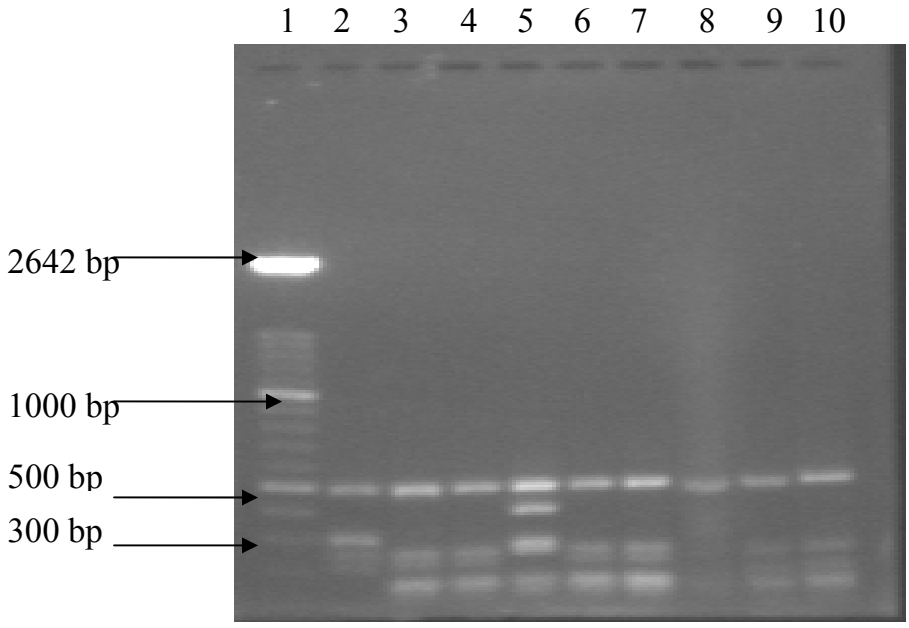

Fig. 3.9. Restriction digestion of PCR-RFLP products of yeast strains with *Hae*III enzyme. Lane 1: 100 bp DNA MW Marker, 2: *Candida famata* LD7, 3: *Debaryomyces hansenii* Y0219, 4: *D. hansenii* Y0610, 5: *C. diddensiae* LD9, 6: *C. diddensiae* Y0774, 7: *C. guilliermondii* HBD6.2, 8: *Pichia guilliermondii* Y0209, 9: *P. guilliermondii* Y0053, 10: *P. guilliermondii* Y0054.

3.3.7. Digestion of amplicons with *Hpa*II enzyme

Restriction digestion of PCR-RFLP products of yeast strains with HpaII enzyme produced 10 markers (Fig. 3.10). *Candida famata* LD7 has approximately 650 bp, 280 bp, 220 bp, 120 bp and 100 bp polymorphic bands which makes it different to its reference strains *D. hansenii* Y0219, lane 3 and *D. hansenii* Y0610, lane 4. *D. hansenii* Y0219, lane 3 and *D. hansenii* Y0610, lane 4 have the same banding pattern with *C. diddensiae* Y0774, lane 6 and *C. guilliermondii* HBD6.2, lane 7. *C. diddensiae* LD9, lane 5 has approximately 800 and 150 bp polymorphic bands which make it different from its reference strain *C. diddensiae* Y0774, lane 6. The reference strains *P. guilliermondii* Y0209, lane 8; *P. guilliermondii* Y0053, lane 9 and *P. guilliermondii* Y0054, lane 10 have a polymorphic band of approximately 350 bp which is absent in the test strain *C. guilliermondii* HBD6.2, lane 7.

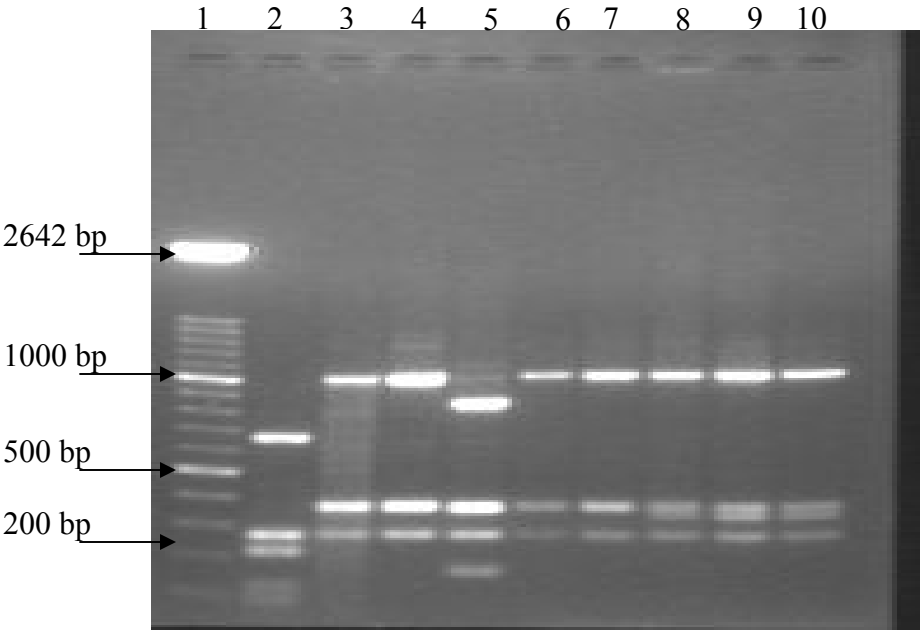

Fig. 3.10. Restriction digestion of PCR-RFLP products of yeast strains with *Hpa*II enzyme. Lane 1: 100 bp DNA MW Marker, 2: *Candida famata* LD7, 3: *Debaryomyces hansenii* Y0219, 4: *D. hansenii* Y0610, 5: *C. diddensiae* LD9, 6: *C. diddensiae* Y0774, 7: *C. guilliermondii* HBD6.2, 8: *Pichia guilliermondii* Y0209, 9: *P. guilliermondii* Y0053, 10: *P. guilliermondii* Y0054.

3.3.8. Digestion of amplicons with *Rsa*I enzyme

Restriction digestion of PCR-RFLP products of yeast strains with *Rsa*I enzyme produced five markers (Fig. 3.11). All the yeasts have a similar banding pattern of equal sizes. They produced approximately 900 bp, 400 bp, 190 bp and 110 bp monomorphic bands.

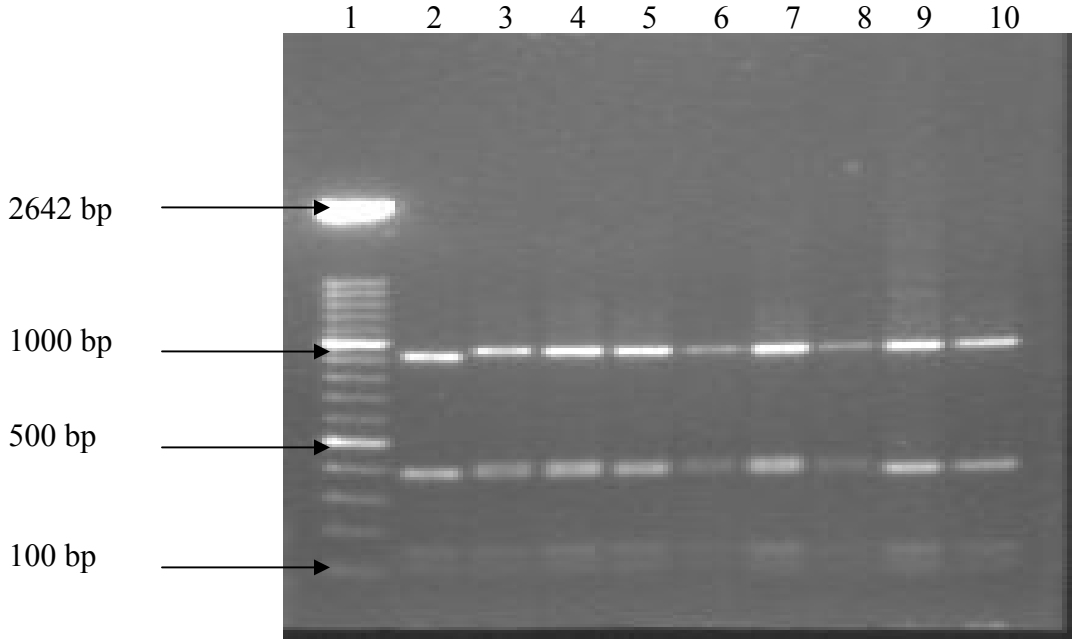

Fig. 3.11. Restriction digestion of PCR-RFLP products of yeast strains with *Rsa*I enzyme. Lane 1: 100 bp DNA MW Marker, 2: *Candida famata* LD7, 3: *Debaryomyces hansenii* Y0219, 4: *D. hansenii* Y0610, 5: *C. diddensiae* LD9, 6: *C. diddensiae* Y0774, 7: *C. guilliermondii* HBD6.2, 8: *Pichia guilliermondii* Y0209, 9: *P. guilliermondii* Y0053, 10: *P. guilliermondii* Y0054.

3.3.9. Digestion of amplicons with *Taq*I enzyme

Restriction digestion of PCR-RFLP products of yeast strains with *Taq*I enzyme produced 15 markers (Fig. 3.12). *Candida famata* LD7, lane 2 has a band of size 900 bp which is absent in the reference strains *D. hansenii* Y0219, lane 3 and *D. hansenii* Y0610, lane 4, on the other hand the reference strains have bands of 250 bp, 400 bp, 500 bp, and 600 bp that are absent in the test strain *Candida famata* LD7, lane 2. *D. hansenii* Y0219, lane 3 and *D. hansenii* Y0610, lane 4 have the same banding pattern with *C. guilliermondii* HBD 6.2, lane 7. *C. diddensiae* LD9, lane 5 has approximately 2100 and 2300 bp polymorphic bands that are absent in the reference strain *C. diddensiae* Y0774, lane 6. *C. guilliermondii* HBD6.2, lane 7 has 2100 bp and 2300 bp polymorphic bands which are absent in its reference strains *P. guilliermondii* Y0209, lane 8; *P. guilliermondii* Y0053, lane 9 and *P. guilliermondii* Y0054, lane 10.

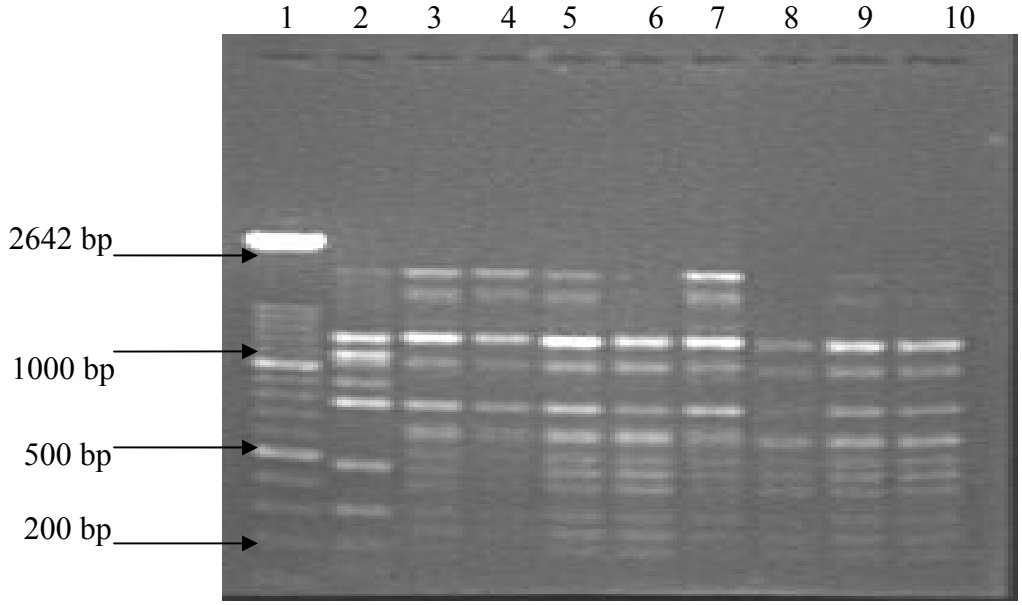

Fig. 3.12. Restriction digestion of PCR-RFLP products of yeast strains with *Taq*I enzyme. Lane 1: 100 bp DNA MW Marker, 2: *Candida famata* LD7, 3: *Debaryomyces hansenii* Y0219, 4: *D. hansenii* Y0610, 5: *C. diddensiae* LD9, 6: *C. diddensiae* Y0774, 7: *C. guilliermondii* HBD6.2, 8: *Pichia guilliermondii* Y0209, 9: *P. guilliermondii* Y0053, 10: *P. guilliermondii* Y0054.

3.3.10. Digestion of amplicons with *Hae*III and *Dra*I enzyme

Restriction digestion of PCR-RFLP (Fig. 3.13) products of yeast strains with *Hae*III and *Dra*I enzymes gave rise to six markers with *Candida famata* LD7, lane 2 having approximately 600 bp and 300 bp polymorphic bands that are different from its reference strains *D. hansenii* Y0219, lane 3 and *D. hansenii* Y0610, lane 4. *D. hansenii* Y0219, lane 3 and *D. hansenii* Y0610, lane 4 have the same banding pattern with *C. diddensiae* Y0774, lane 6 and *C. guilliermondii* HBD6.2, lane 7. C. *diddensiae* LD9, lane 5 has approximately 1000 and 800 bp polymorphic bands that are absent in its reference strain *C. diddensiae* Y0774, lane 6. *C. guilliermondii* HBD6.2, lane 7 gave rise to different bands from its reference strains *P. guilliermondii* Y0209, lane 8; *P. guilliermondii* Y0053, lane 9 and *P. guilliermondii* Y0054, lane 10. Each one of them has banding pattern different from each other.

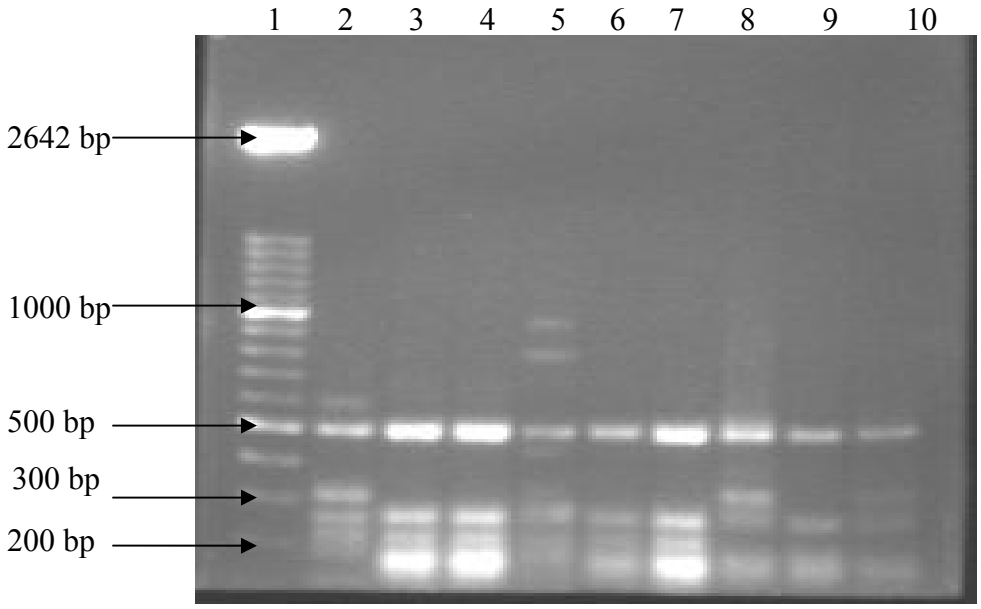

Fig. 3.13. Restriction digestion of PCR-RFLP products of yeast strains with *Hae*III and *Dra*I enzyme. Lane 1: 100 bp DNA MW Marker, 2: *Candida famata* LD7, 3: *Debaryomyces hansenii* Y0219, 4: *D. hansenii* Y0610, 5: *C. diddensiae* LD9, 6: *C. diddensiae* Y0774, 7: *C. guilliermondii* HBD6.2, 8: *Pichia guilliermondii* Y0209, 9: *P. guilliermondii* Y0053, 10: *P. guilliermondii* Y0054.

3.3.11. Digestion of amplicons with *Cfo*I and *Msp*I enzyme

Restriction digestion of PCR-RFLP products of yeast strains with *Cfo*I and *Msp*I enzymes produced seven markers (Fig. 3.14). *Candida famata* LD7, lane 2 has approximately 700 bp and 280 bp polymorphic bands which makes it to have a different banding pattern from its reference strains *D. hansenii* Y0219, lane 3 and *D. hansenii* Y0610, lane 4. *D. hansenii* Y0219, lane 3 and *D. hansenii* Y0610, lane 4 have the same banding pattern with *C. diddensiae* LD9, lane 5 and *C. diddensiae* Y0774, lane 6. *P. guilliermondii* Y0209, lane 8 and *P. guilliermondii* Y0053, lane 9 have approximately 180 bp polymorphic band which is absent in *C. guilliermondii* HBD6.2, lane 7. No bands were observed in lane 10.

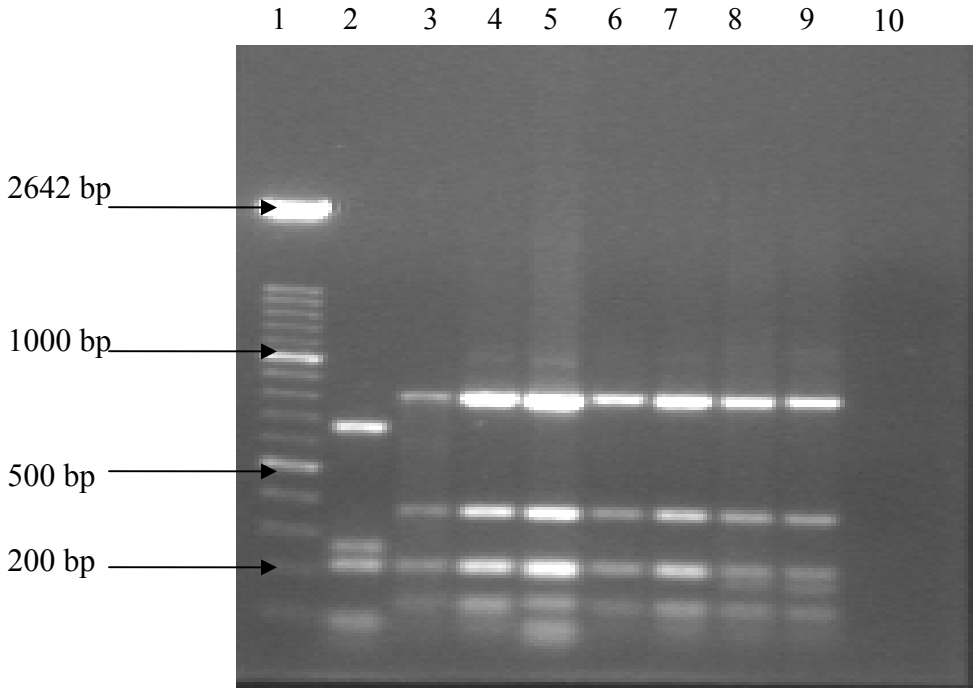

Fig. 3.14. Restriction digestion of PCR-RFLP products of yeast strains with *Cfo*I and *Msp*I enzymes. Lane 1: 100 bp DNA MW Marker, 2: *Candida famata* LD7, 3: *Debaryomyces hansenii* Y0219, 4: *D. hansenii* Y0610, 5: *C. diddensiae* LD9, 6: *C. diddensiae* Y0774, 7: *C. guilliermondii* HBD6.2, 8: *Pichia guilliermondii* Y0209, 9: *P. guilliermondii* Y0053.

3.3.12. Digestion of amplicons with *Rsa*I and *Cfo*I enzyme

Restriction digestion of PCR-RFLP products of yeast strains with *Rsa*I and *Cfo*I enzymes produced six markers (Fig. 3.15). *Candida famata* LD7, lane 2 can be distinguished from its reference strains *D. hansenii* Y0209, lane 3 and *D. hansenii* Y0610, lane 4 by the absence of approximately 300 bp and 220 bp bands. *D. hansenii* Y0209, lane 3 and *D. hansenii* Y0610, lane 4 have the banding pattern similar to those of *C. diddensiae* LD9, lane 5; *C. diddensiae* Y0774, lane 6 and *C. guilliermondii* HBD6.2, lane 7. *C. guilliermondii* HBD6.2, lane 7 has approximately 220 bp band which is absent in its reference strains *P. guilliermondii* Y0209, lane 8; *P. guilliermondii* Y0053, lane 9 and *P. guilliermondii* Y0054, lane 10.

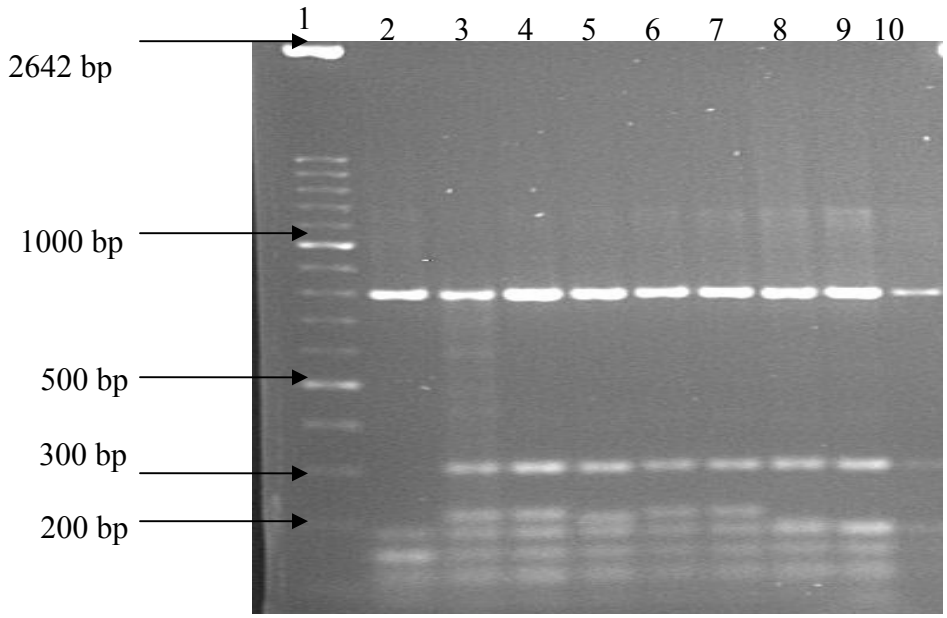

Fig. 3.15. Restriction digestion of PCR-RFLP products of yeast strains with *Rsa*I and *Cfo*I enzymes. Lane 1: 100 bp DNA MW Marker, 2: *Candida famata* LD7, 3: *Debaryomyces hansenii* Y0219, 4: *D. hansenii* Y0610, 5: *C. diddensiae* LD9, 6: *C. diddensiae* Y0774, 7: *C. guilliermondii* HBD6.2, 8: *Pichia guilliermondii* Y0209, 9: *P. guilliermondii* Y0053, 10: *P. guilliermondii* Y0054.

3.3.13. Digestion of amplicons with *Rsa*I and *Msp*I enzyme

Restriction digestion of PCR-RFLP products of yeast strains with *Rsa*I and *Msp*I enzymes produced nine markers (Fig. 3.16). *Candida famata* LD7, lane 2 has approximately 650, 230 and 50 bp polymorphic bands that makes it to have a different banding pattern from its reference strains *D. hansenii* Y0209, lane 3 and *D. hansenii* Y0610, lane 4. *D. hansenii* Y0209, lane 3 and *D. hansenii* Y0610, lane 4 show similar banding pattern with *C. diddensiae* Y0774, lane 6 and *C. guilliermondii* HBD6.2, lane 7. *C. diddensiae* LD9 lane 5 has an approximately 850 bp polymorphic bands. *C. guilliermondii* HBD6.2, lane 7 has approximately 380 bp band, and its reference strains *P. guilliermondii* Y0209, lane 8; *P. guilliermondii* Y0053, lane 9 and *P. guilliermondii* Y0054, lane 10 have approximately 350 bp band.

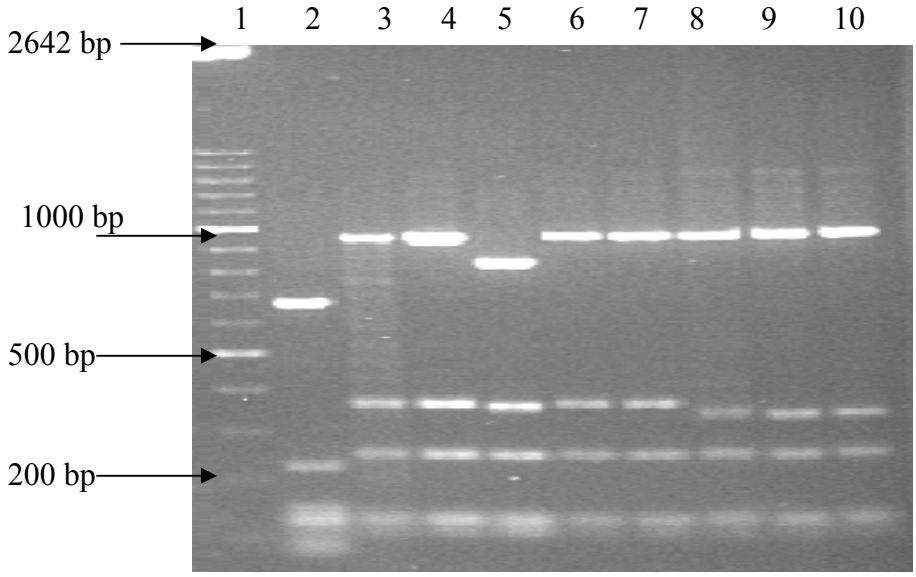

Fig. 3.16. Restriction digestion of PCR-RFLP products of yeast strains with *Rsa*I and *Msp*I enzymes. Lane 1: 100 bp DNA MW Marker, 2: *Candida famata* LD7, 3: *Debaryomyces hansenii* Y0219, 4: *D. hansenii* Y0610, 5: *C. diddensiae* LD9, 6: *C. diddensiae* Y0774, 7: *C. guilliermondii* HBD6.2, 8: *Pichia guilliermondii* Y0209, 9: *P. guilliermondii* Y0053, 10: *P. guilliermondii* Y0054.

3.3.14. The analysis with the DICE coefficient

According to the analysis with the DICE coefficient (Table 3.18) *Candida famata* LD7 was 53 % and 49 % genetically similar to its reference strains *D. hansenii* Y0219 and *D. hansenii* Y0610 respectively. It was also found to be 53 % genetically similar to *C. guilliermondii* HBD6.2 and *C. diddensiae* Y0774 and 52 % similar to *C. diddensiae* LD9.

The yeast *C. diddensiae* LD9 was found to be 89 % genetically similar to its reference strain *C. diddensiae* Y0774 and *C. guilliermondii* HBD6.2, but it showed a higher similarity to *D. hansenii* Y0219 at 91 %.

C. guilliermondii HBD6.2 showed a higher similarity of 85 %, 90 % and 86 % to its reference strains *P. guilliermondii* Y0209, *P. guilliermondii* Y0053 and *P. guilliermondii* Y0054 respectively. It also showed a higher similarity to *C. diddensiae* Y0774 at 100%. It was also found to be 98 % genetically similar to *D. hansenii* Y0219 and 95 % genetically similar to *D. hansenii* Y0610.

The analysis with the DICE coefficient indicated that the yeasts belonging to the same species, i.e., *P. guilliermondii* Y0209, *P. guilliermondii* Y0053 and *P. guilliermondii* Y0054 and the two strains *D. hansenii* Y0219 and *D. hansenii* Y0610 were genetically similar. However, *D. hansenii* Y0219 also had genetic similarity of 98 to *C. diddensiae* LD9 and *P. guilliermondii* Y0053.

Table 3.18. Genetic similarity indices of nine yeast strains based on the DICE coefficient

	LD7	Y0219	Y0610	LD9	Y0774	HBD6.2	Y0209	Y0053	**Y0054**
C. famata LD7	1.0								
D. hansenii Y0219	0.53	1.0							
D. hansenii Y0610	0.49	0.98	1.0						
C. diddensiae LD9	0.52	0.91	0.87	1.0					
C. diddensiae Y0774	0.53	0.98	0.94	0.89	1.0				
C. guilliermondii HBD6.2	0.53	0.98	0.95	0.89	1.0	1.0			
P. guilliermondii Y0209	0.51	0.87	0.86	0.80	0.86	0.85	1.0		
P. guilliermondii Y0053	0.48	0.91	0.88	0.84	0.91	0.90	0.95	1.0	
***P. guilliermondii* Y0054**	**0.45**	**0.88**	**0.85**	**0.81**	**0.88**	**0.86**	**0.93**	**0.99**	**1.0**

3.3.15. The analysis with the UPGMA dendrogram

The PCR-RFLP technique was used to confirm the identification of the three unknown yeast isolates HBD6.2, LD9 and LD7 that were identified as *Candida guilliermondii*, *C. diddensiae* and *C. famata* respectively, using conventional taxonomic classification method. The identified yeasts were paired with their respective reference strains (Table 3.17) for molecular classification. Eleven restriction digestion profiles used generated 84 markers. According to UPGMA analysis, the nine strains formed two subclusters separated by a bootstrap value of 100. The yeast isolate *C. guilliermondii* HBD6.2 clustered tightly with *C. diddensiae* Y0774 on the dendrogram at a bootstrap value of 90 (Fig. 3.17) and they were found to be 100 % genetically similar according to the analysis with the DICE coefficient (Table 3.18). Based on the analysis of the dendrogram, the test strain *C. guilliermondii* HBD6.2 relatively did not show any close genetic relationship with its reference strains, *P. guilliermondii* Y0209, *P. guilliermondii* Y0053 and *P. guilliermondii* Y0054, where they shared a similarity of 85 %, 90 % and 86 %, respectively according to the analysis with the DICE coefficient.

The yeast strains *P. guilliermondii* Y0053 clustered tightly with *P. guilliermondii* Y0054 at a bootstrap value of 97 and they were noted to be 99 % genetically similar. *P. guilliermondii* Y0209 formed a close pair with *P. guilliermondii* Y0053 and *P. guilliermondii* Y0054 strains and were separated by a bootstrap value of 97. This was the expected outcome since these strains belonged to the same species of yeasts. *P. guilliermondii* Y0290 showed a similarity of 95 % and 93 % to *P. guilliermondii* Y0053 and *P. guilliermondii* Y0054 respectively.

C. diddensiae LD9 did not cluster with its reference strain *C. diddensiae* Y0774, they were both within the same subcluster supported by a bootstrap value of 65. *C. diddensiae* LD9 showed a similarity of 89 % to its reference strain *C. diddensiae* Y0774, indicating genetic relatedness. *C. diddensiae* LD9 also showed a higher genetic similarity of 91 %, 89 % and 87 % to *D. hansenii* Y0219, *C. guilliermondii* HBD6.2 and *D. hansenii* Y0610, respectively.

The yeast isolate *Candida famata* LD7 appeared to be distantly related to all the other yeast strains. It did not cluster closely with its reference strains *D. hansenii* Y0219 and *D. hansenii* Y0610 or any of the yeast strains on the dendrogram. Instead, it was separated from the rest of the yeast strains by a bootstrap value of 100. *Candida famata* LD7 was 53 % and 49 % genetically similar to its reference strains *D. hansenii* Y0219 and *D. hansenii* Y0610, respectively. The similarity level between *Candida famata* LD7 and both of its reference strains indicated no relatedness. The similarity of *Candida famata* LD7 with *D. hansenii* Y0219, *C. diddensiae* Y0774 and *C. guilliermondii* HBD6.2 was found to be the highest at 53 % when compared to the similarity level with the other yeast strains tested. The yeast strains *D. hansenii* Y0219 and *D. hansenii* Y0610 appeared to be close with each other on the dendrogram as depicted by the similarity analysis with the DICE coefficient.

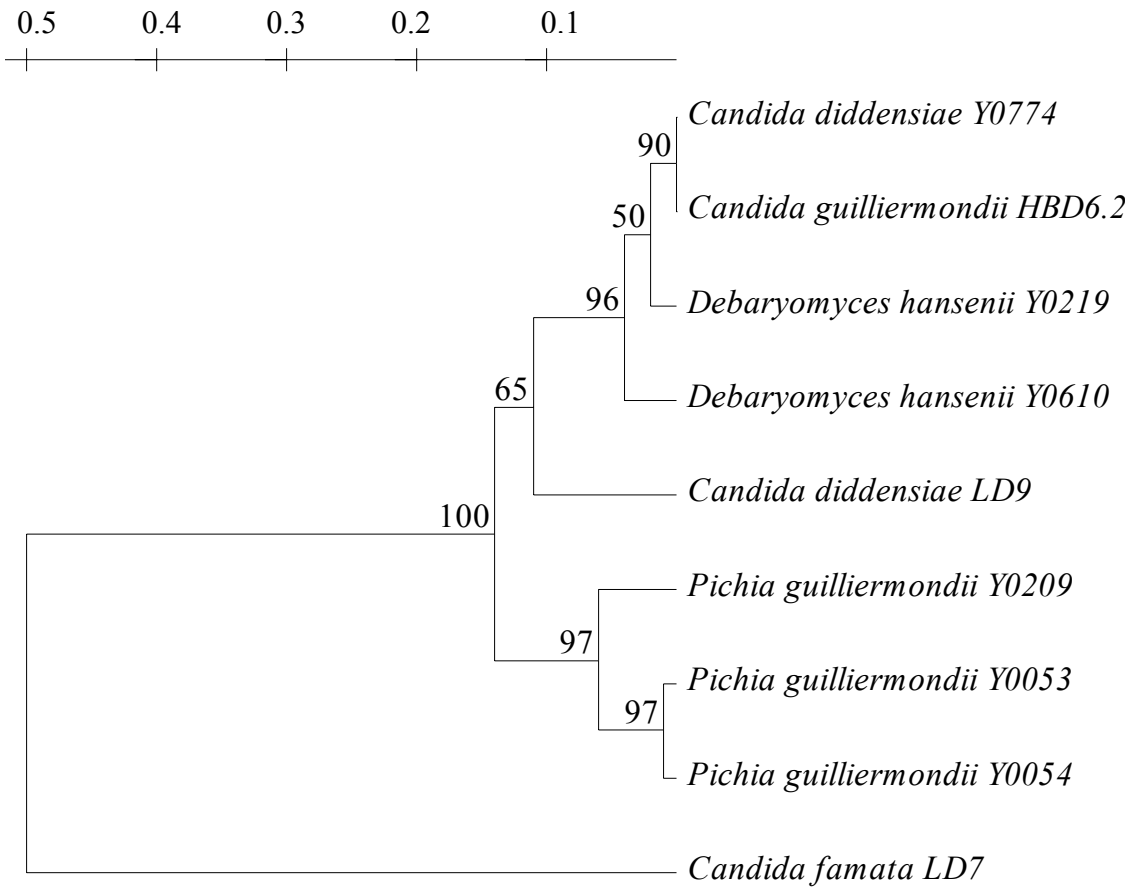

Fig. 3.17. UPGMA dendrogram of nine yeast strains based on distance coefficient of Nei and Li (1979).

3.4. Growth curves, enzyme activities and the stability profiles of HBD6.2

The growth profiles for HBD6.2 at different temperature and pH's are indicated in Fig 3.18 to Fig 3.20. The lag phase was between 0 to 15 hrs for the different pH's and temperatures. Linear increase in growth under all pH's at 25º C (Fig. 3.18) and 35º C (Fig. 3.20) occurred after the lag phase. It was only at 30º C, (Fig. 3.19) pH 5.5 and 6.0 that exponential growth was observed. This linear and exponential growth occurred between approximately 15 and 35 hrs. Maximal growth of approximately 0.035 g wet weight occurred at pH 5.5 with the lowest value at pH 5.0 when HBD6.2 was incubated at 25º C (Fig. 3.18). At 30º C maximal growth of approximately 0.054 g wet weight occured at pH 5.5 with the lowest value recorded at pH 4.0 (Fig. 3.19) and this was found to be the optimum growth condition for HBD6.2. At 35º C maximal growth of approximately 0.042 g wet weight was observed at pH 5.5 with the lowest value at pH 4.0 (Fig. 3.20).

At all three temperatures and pH's (Fig. 3.21 to Fig 3.23) enzyme activities in the first 35 hrs increased linearly with growth. However, after 35 hrs when the cells had gone into the stationary phase, enzyme activities were non-growth associated and maximum enzyme activities were produced at this stage. At 25º C, the highest enzyme activity of approximately 700 $U.ml^{-1}$ was observed at pH 5.5 with the lowest at pH 4.0 (Fig. 3.21). At 30º C and 35º C maximum phytase production of approximately 900 $U.ml^{-1}$ was observed after 65 hrs of incubation at a pH of between 5.0 and 6.0 with the lowest enzyme activity detected at pH 4.0 and pH 4.5 (Fig. 3.22 and Fig. 3.23).

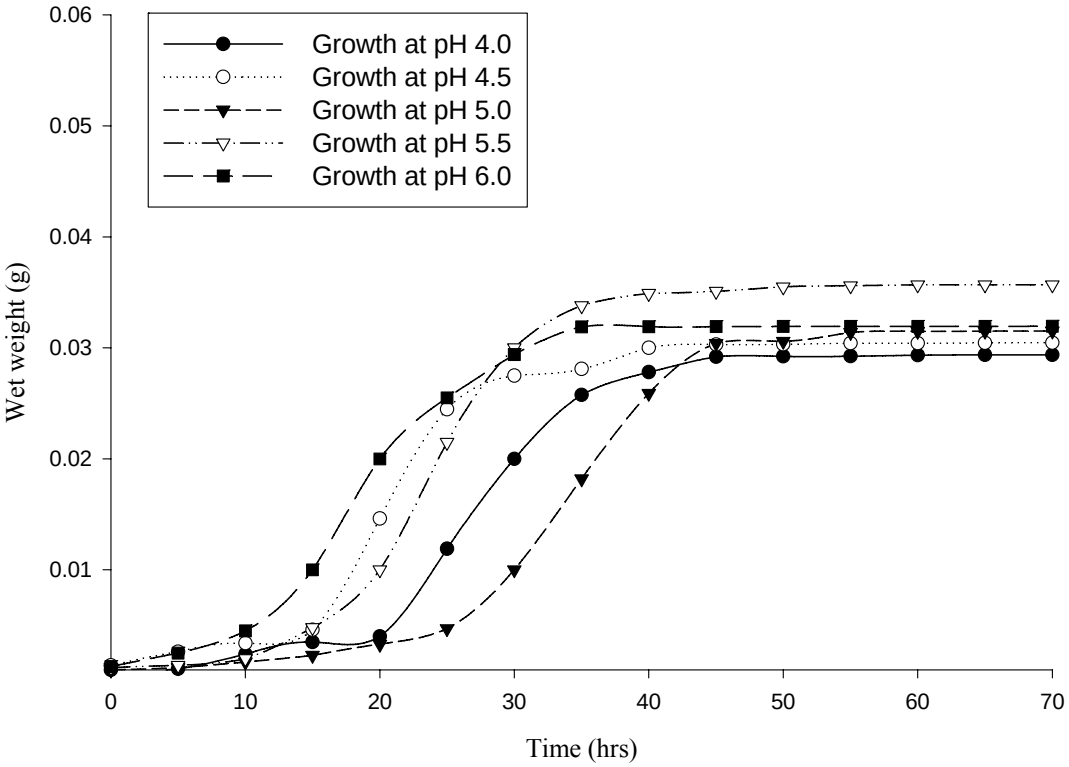

Fig. 3.18. Growth profiles of HBD6.2 at 25^{o} C.

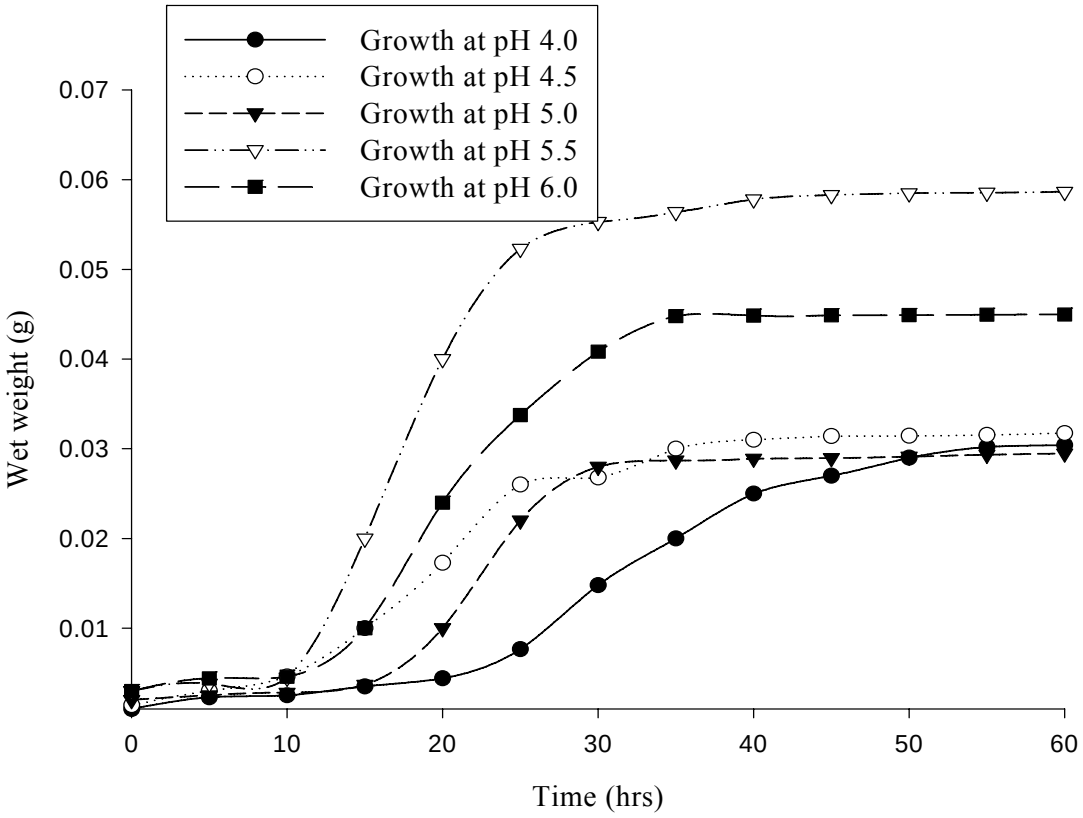

Fig. 3.19. Growth profiles of HBD6.2 at 30^{o} C.

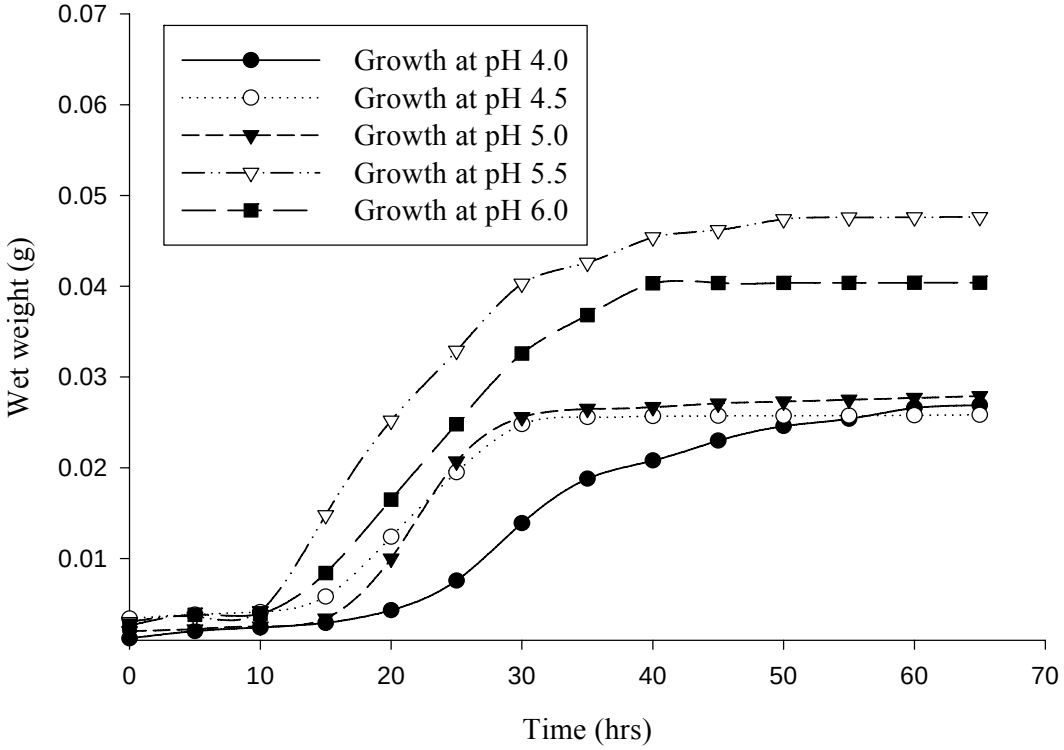

Fig. 3.20. Growth profiles of HBD6.2 at 35^{o} C.

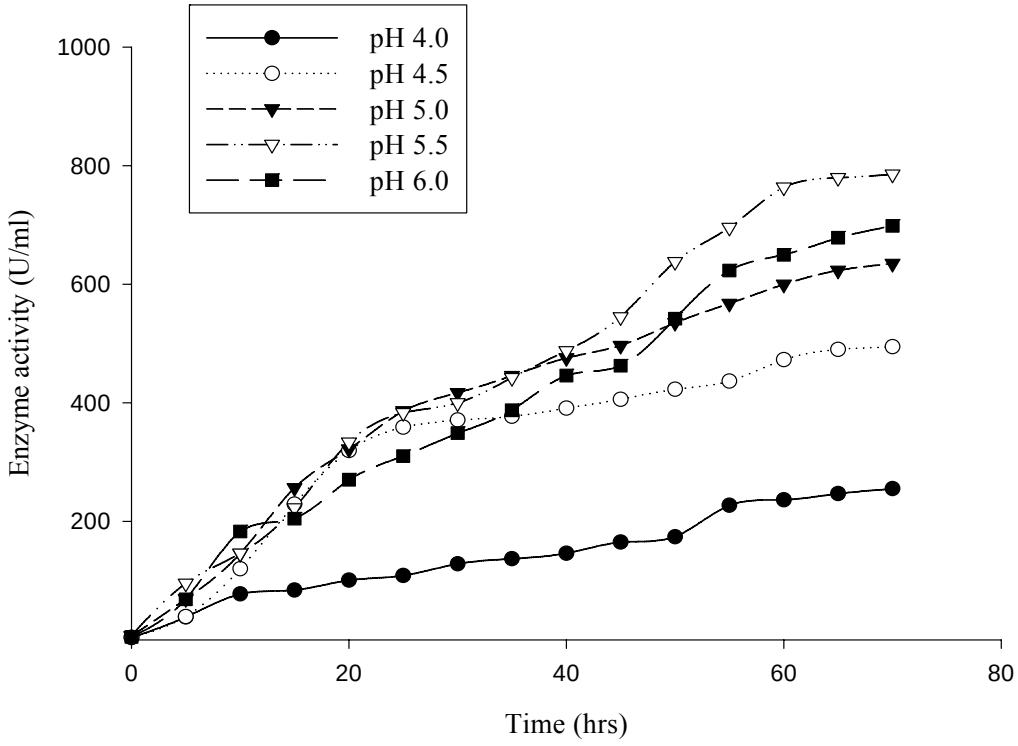

Fig. 3.21. Enzyme activities of HBD6.2 at 25^{o} C.

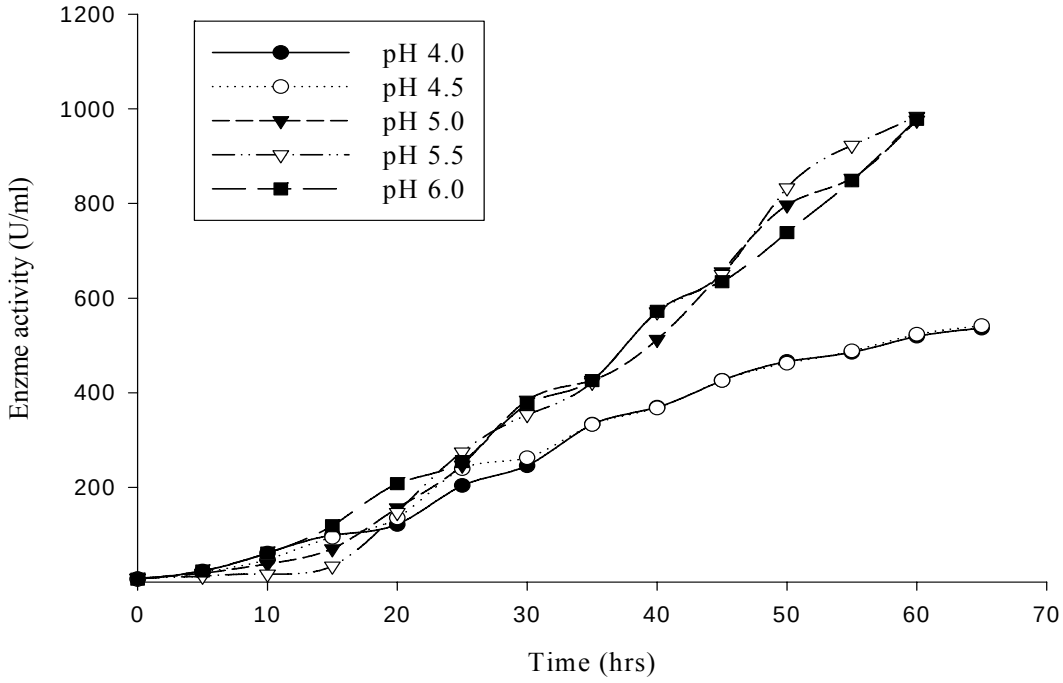

Fig. 3.22. Enzyme activities of HBD6.2 at 30^{o} C.

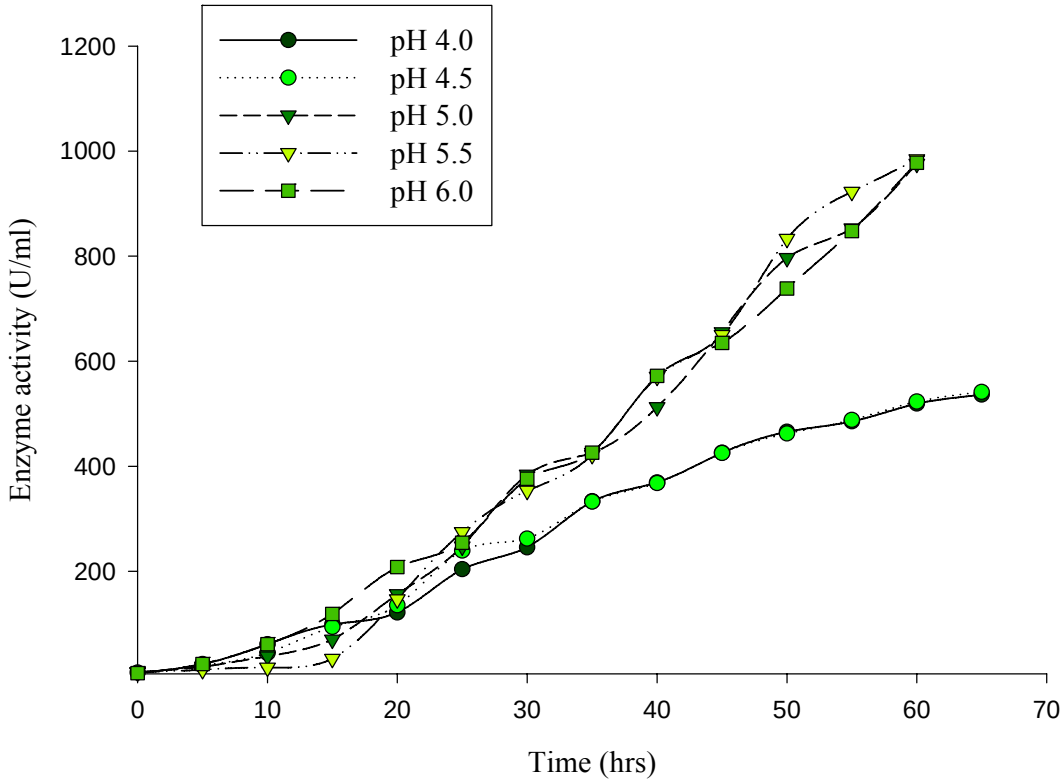

Fig. 3.23. Enzyme activities of HBD6.2 at 35^{o} C.

The relative percentage phytase activity obtained when the crude phytase from HBD6.2 was subjected to different temperature ranges is indicated in Fig 3.24. The highest relative phytase activity (100 % phytase activity) was observed at 35º C. The initial decrease from 35º C was sharp, becoming gradual at around 40º C to 50º C and then again sharply decreased from 50º C to 55º C. The relative enzyme activities were almost constant at 55º C to 65º C, thereafter dropped slowly again.

The relative percentage phytase activity obtained when the crude phytase from HBD6.2 was subjected to different pH values at a constant temperature of 35º C is indicated in Fig 3.25. The highest phytase activity (100 % phytase activity) was observed at a pH value of 5.5. As the pH increased from pH 2 to approximately 5.5, there was a gradual increase in relative enzyme activities. After the optimal activity at pH 5.5 the relative enzyme activity sharply declined reaching its lowest level at a pH of approximately 7.8.

Maximum activity was reached at 35º C (Fig 3.24) with an optimal activity at pH 5.5 (Fig 3.25). The next step was to determine the stability of the crude enzyme under these optimal conditions 35º C and pH 5.5 (Fig. 3.26) the enzyme retained almost 80 % of its activity after 5 hrs of incubation and indicated a decrease at around 5 to ±10 hrs of incubation. After this period, there was a gradual linear decline in activity.

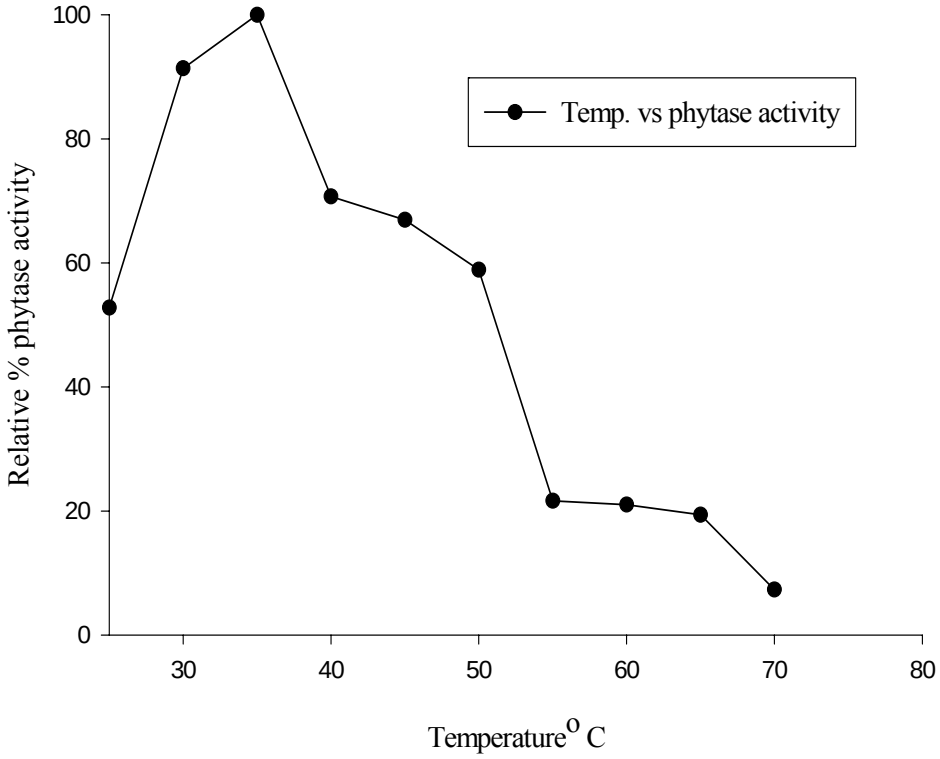

Fig. 3.24. Effect of temperature upon the activity of crude phytase from HBD6.2.

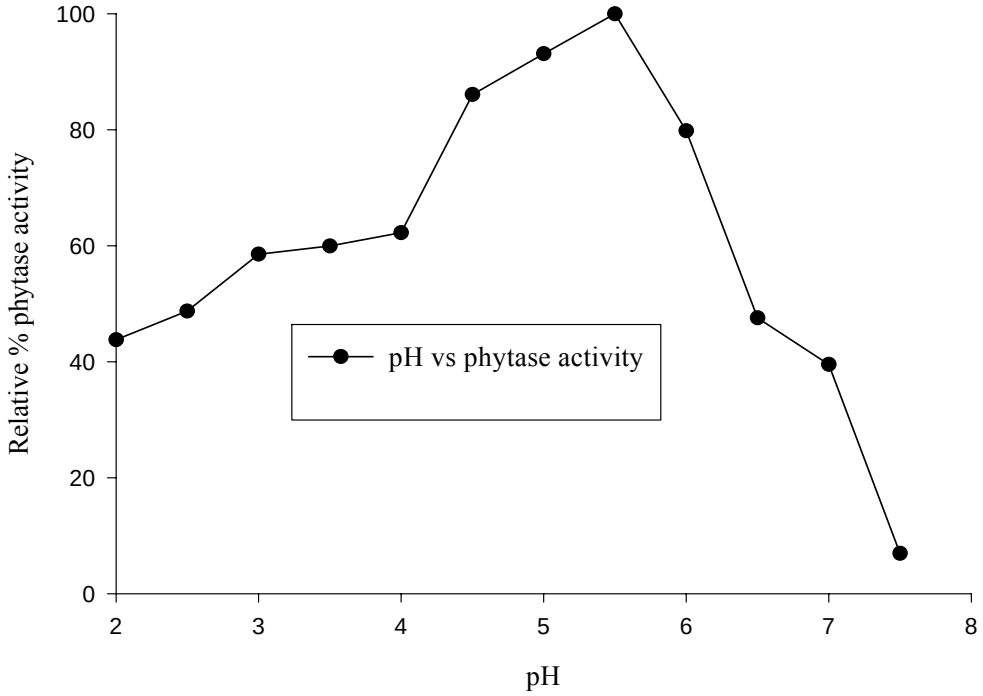

Fig. 3.25. Effect of pH on the activity of crude phytase from HBD6.2 at 35^{o} C.

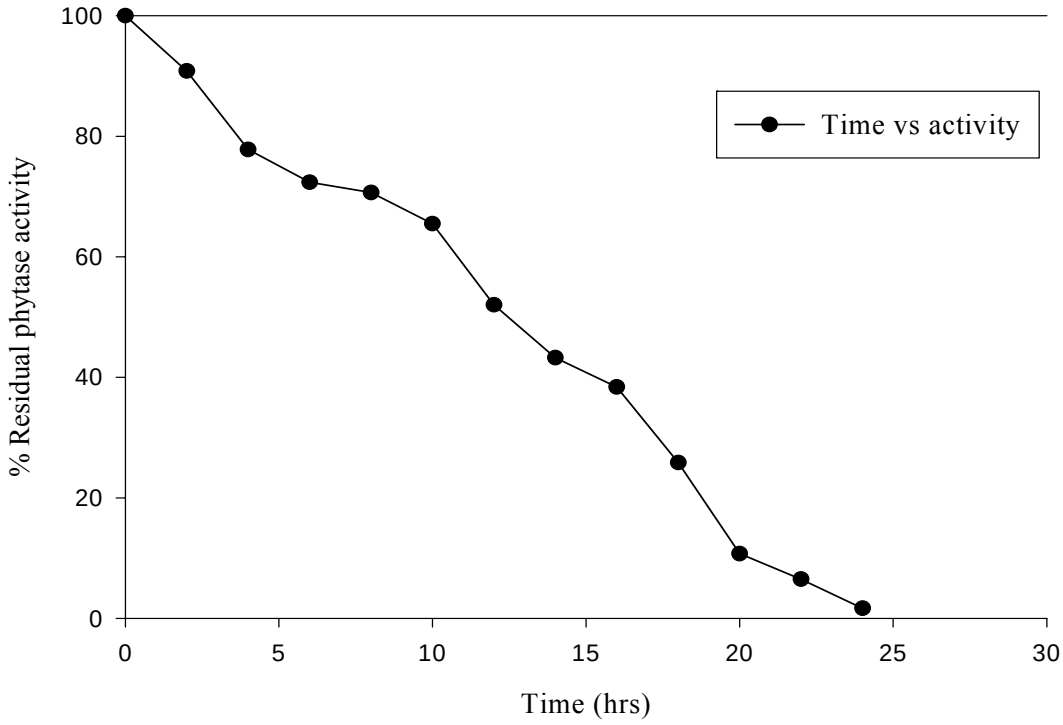

Fig. 3.26. Stability profile of crude enzyme from HBD6.2 (35^{o} C, pH 5.5).

3.5. Growth curves, enzyme activities and stability profiles of LD9

The lag phase for LD9 at 25º C and 35º C (Fig. 3.27 and Fig. 3.29) was between 0 to 5 hrs for the different pH values. A lag phase of between 0 to 10 hrs for all pH values tested was observed at 30º C except for pH 4.0, which was between 0 to 5 hrs (Fig. 3.28)**.** An-exponential increase in growth for all pHs at 25º C were observed (Fig. 3.27), whereas non-exponential growth was observed at 30º C and 35º C (Fig. 3.28 and Fig. 3.29) respectively. The exponential growth at 25º C occurred between 5 and 30 hrs (Fig. 3.27) The linear (non-exponential) growth were between 5 to 30 hrs at 35º C (Fig. 3.29**)** and 10 to 30 hrs at 30º C (Fig. 3.28). Maximal growth at 25º C of approximately 0.033 g wet weight was observed at pH 5.5 with the lowest value obtained at pH 4.0. At 30º C maximal growth (0.048 g wet weight) occured at pH 6.0 with the lowest value obtained at pH 4.0 and these values were found to be the optimum growth conditions for LD9. Maximal growth (0.041 g wet weight) occurred at pH between 5.0 and 6.0 at 35º C.

The enzyme activities increased linearly with growth in the fisrt 35 hrs at all temperatures and pH values (Fig. 3.30 to Fig. 3.32) for LD9. The highest enzyme activity of approximately 550 $U.ml^{-1}$ was observed at a pH between 5.5 and 6.0 after 65 hrs of incubation at 25º C with the lowest enzyme activity at pH 4.0 (Fig. 3.30). At a temperature of 30º C the highest enzyme activity of approximately 850 $U.m^{-1}$ was observed at a pH between 5.0 and 6.0 with the lowest at pH 4.0 (Fig. 3.31) and these were found to be the optimum conditions for the enzyme production for LD9. At 35º C the highest enzyme activity of approximately 820 $U.ml^{-1}$ was observed at a pH 5.0 to 6.0 with the lowest at pH 4.0 (Fig. 3.22).

The relative percentage phytase activity obtained when the crude phytase from LD9 was subjected to different temperature ranges are illustrated in Fig 3.33. The highest phytase activity (100 % phytase activity) was observed at a temperature of 35º C. The initial decrease from 35º C to 45º C was rapid, becoming gradual at around 50º C to 65º C, thereafter it dropped sharply again.

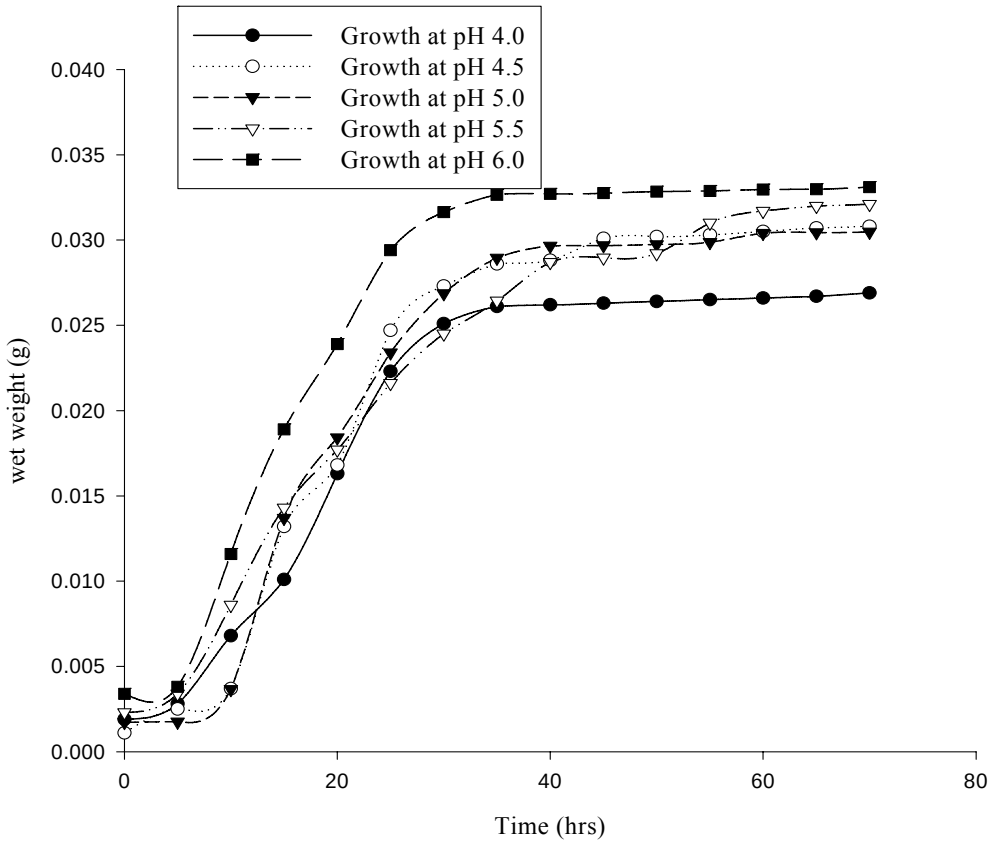

Fig. 3.27. Growth profiles of LD9 at 25^{o} C.

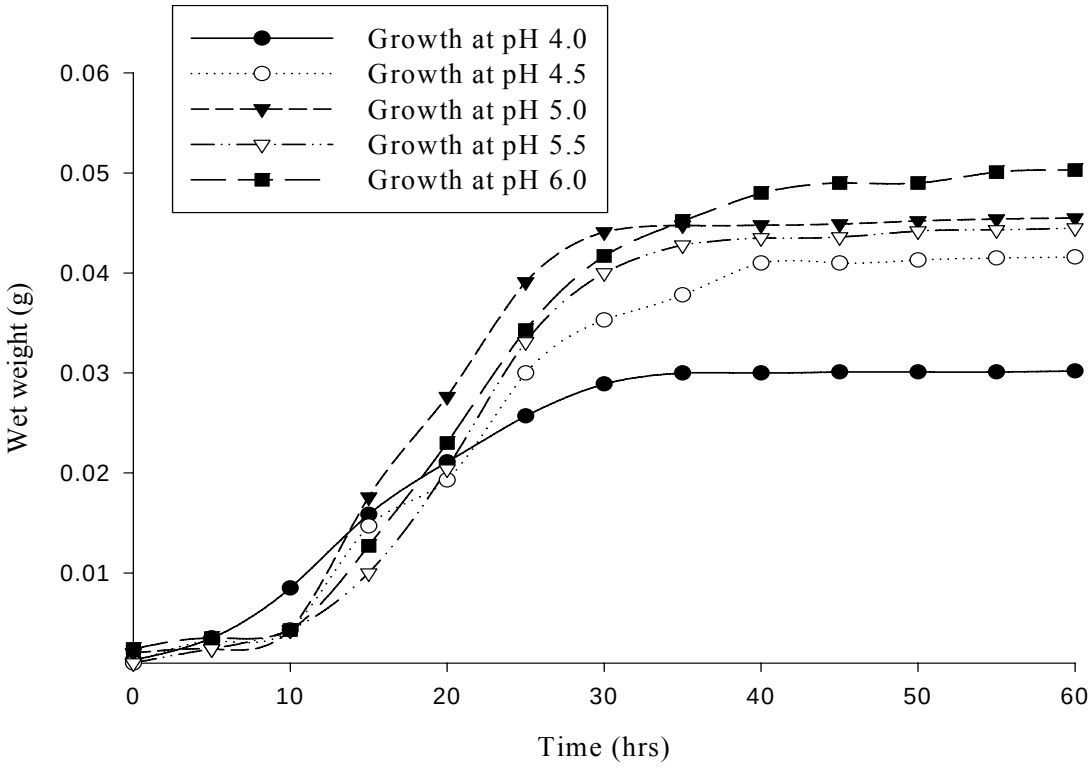

Fig. 3.28. Growth profiles of LD9 at 30^{o} C.

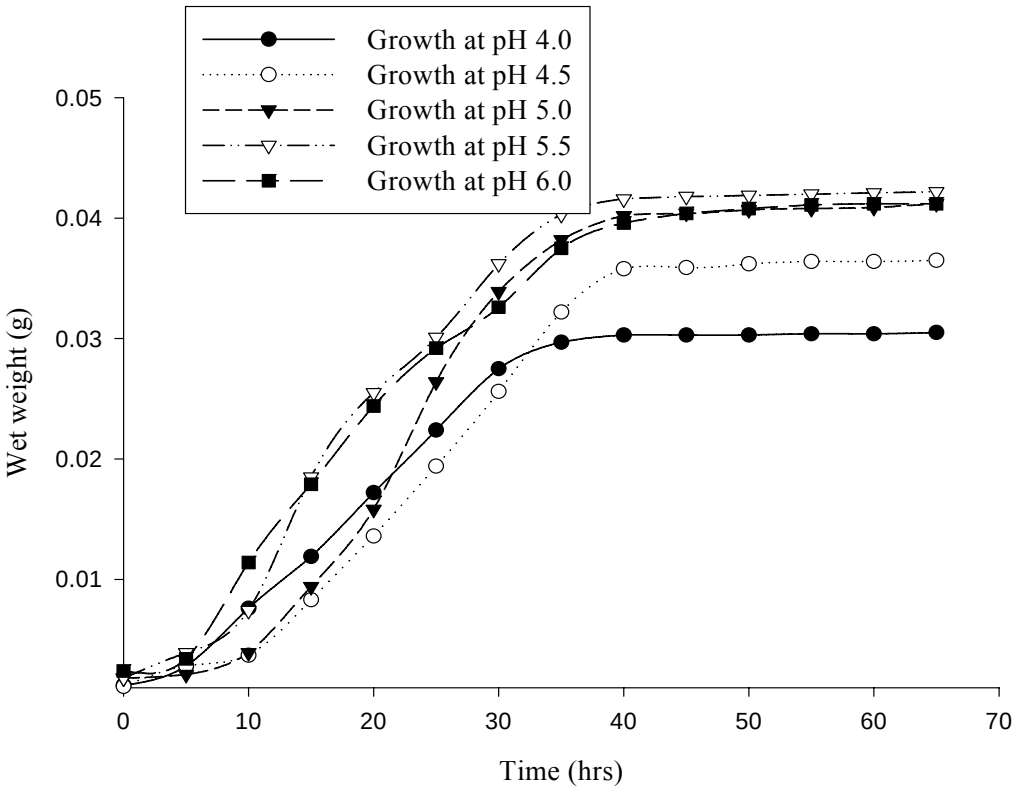

Fig. 3.29. Growth profiles of LD9 at 35^{o} C.

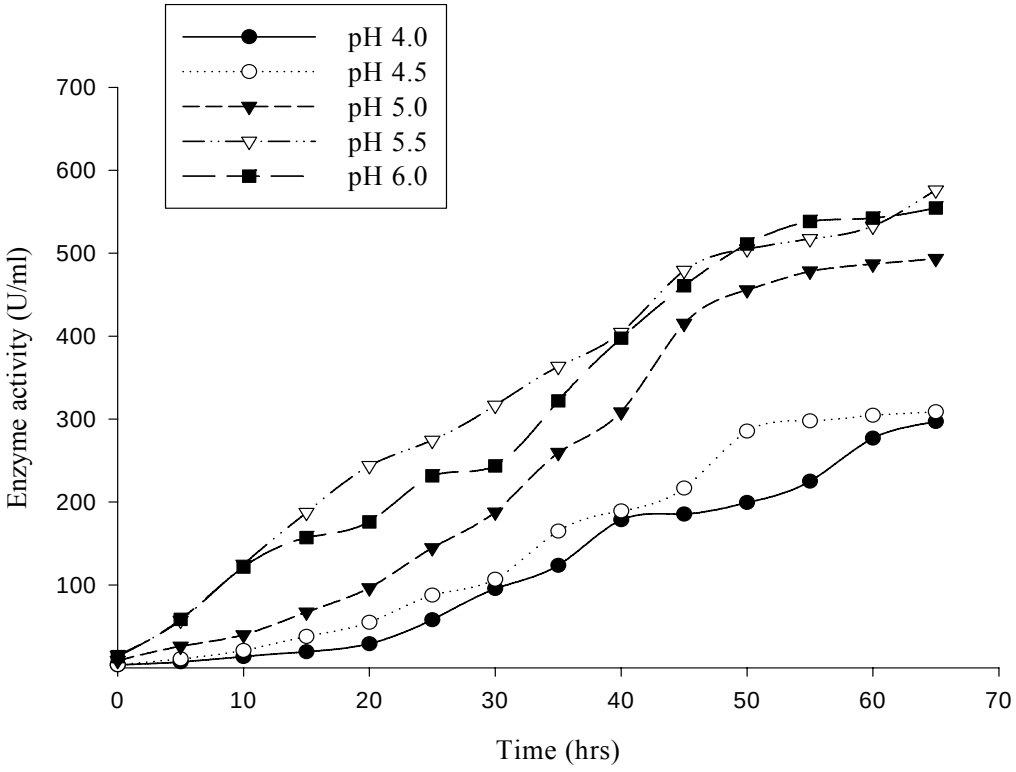

Fig. 3.30 Enzyme activities of LD9 at 25^{o} C.

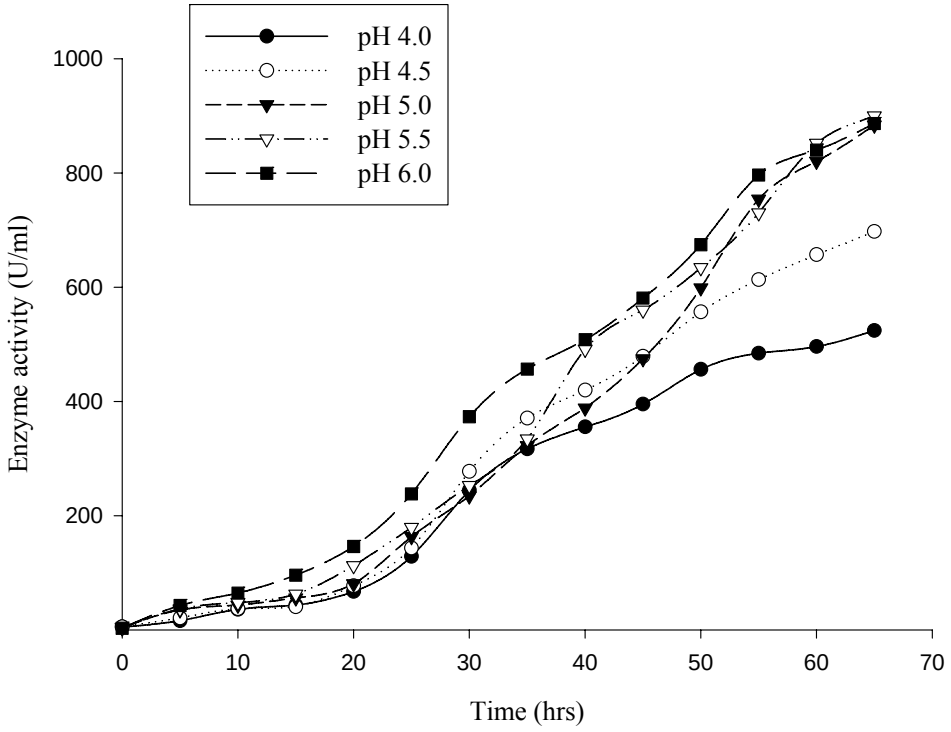

Fig. 3.31. Enzyme activities of LD9 at 30^{o} C.

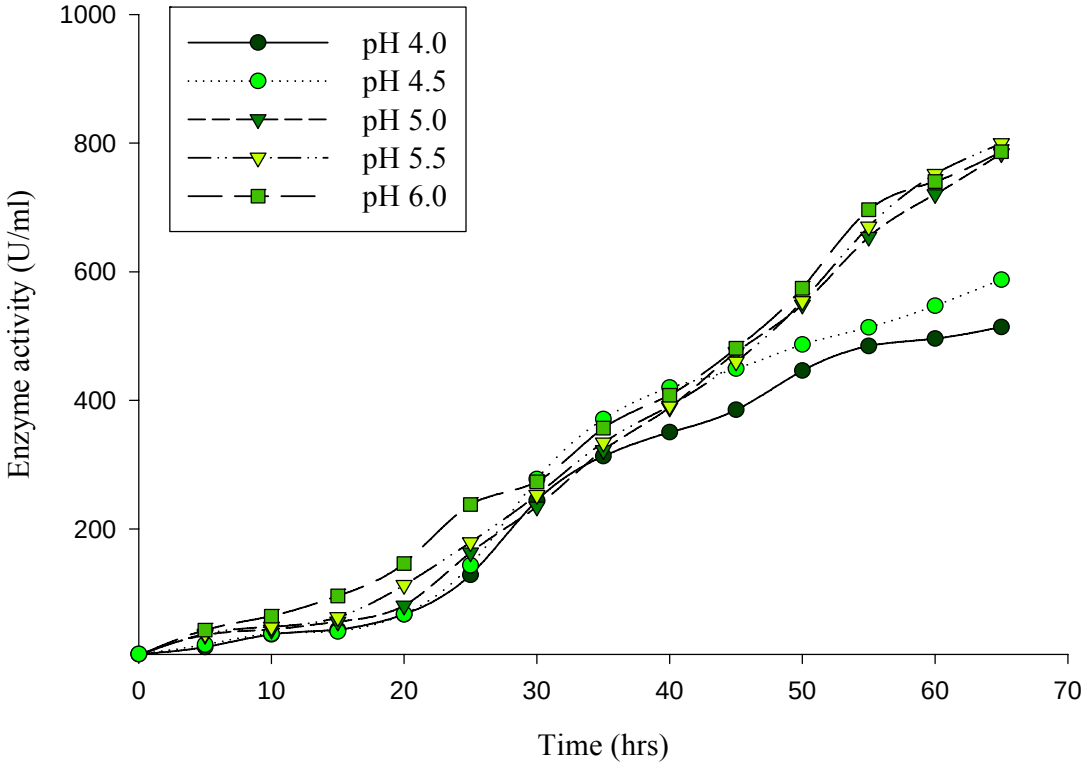

Fig. 3.32. Enzyme activities of LD9 at 35^{o} C.

The relative percentage phytase activity obtained when the crude phytase from LD9 was subjected to different pH values is indicated in Fig 3.34. There was a gradual increase in relative enzyme activity as the pH increased from pH 3 to pH 4.5. From pH 4.5 there was a sharp increase in relative enzyme activity to approximately 5.5. The optimal relative phytase activity (100 % phytase activity) was observed at pH 5.5. The relative enzyme activity sharply declined reaching its lowest level at pH 7.5.

Since maximum enzyme activity was reached at 35º C (Fig. 3.33) with an optimal activity at pH 5.5 (Fig. 3.34) the stability the crude enzyme was tested using these conditions. The enzyme retained about 85 % of its activity after 2.5 hrs of incubation and a gradual decrease in activity was noted thereafter (Fig. 3.35).

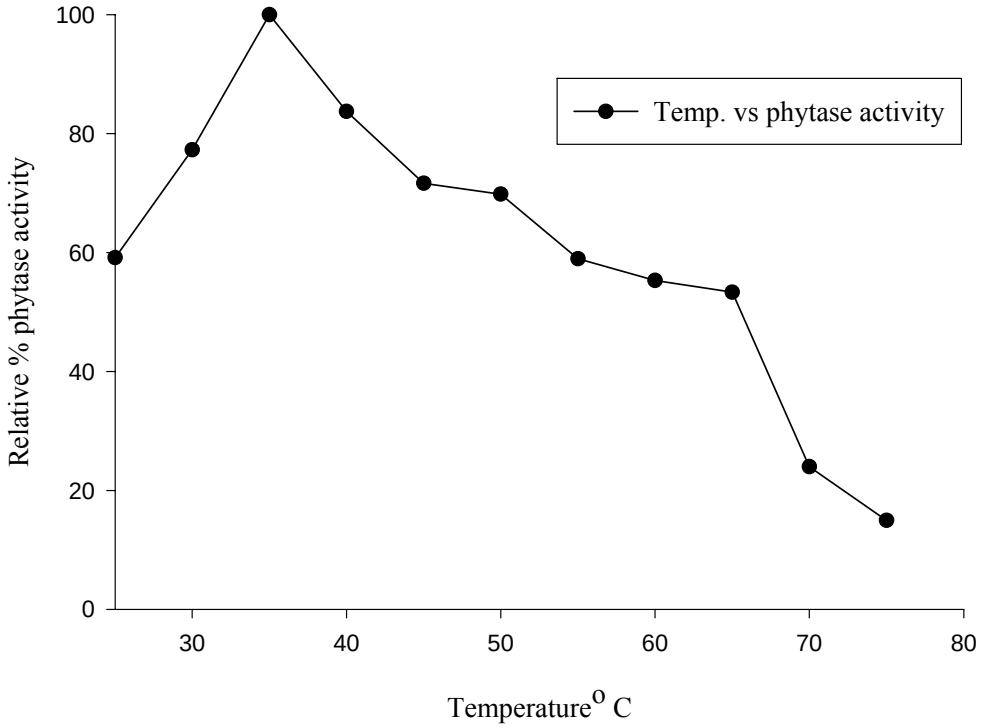

Fig. 3.33. Effect of temperature upon the activity of crude phytase from LD9.

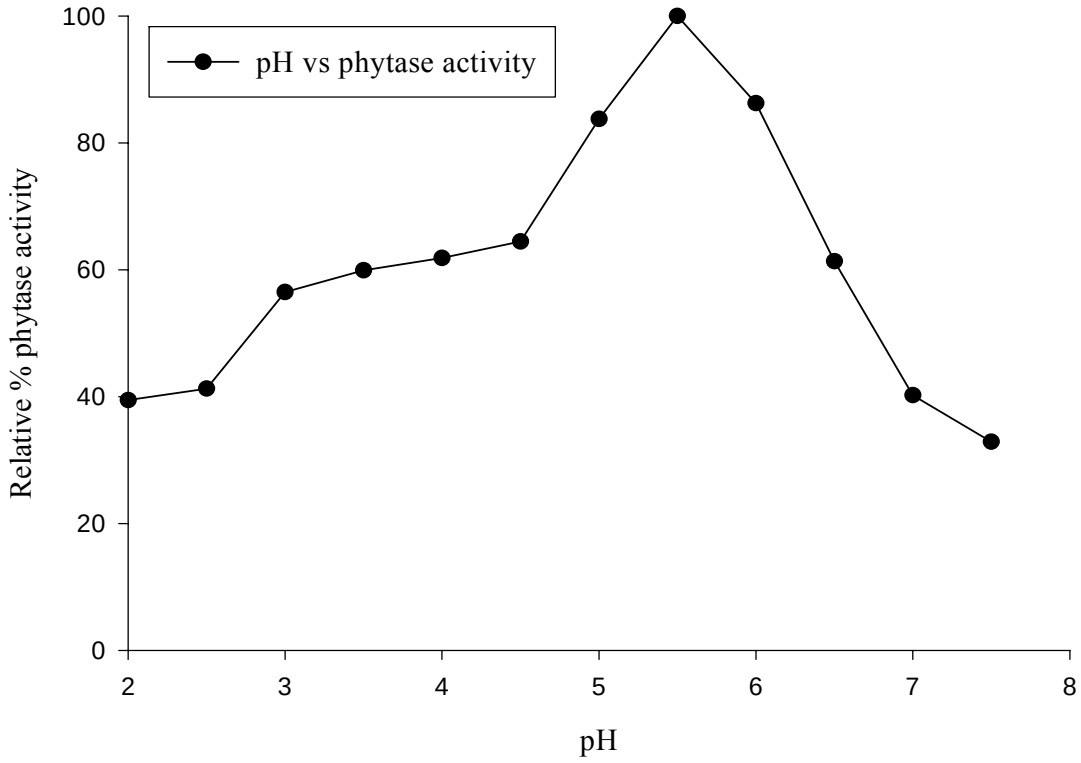

Fig. 3.34. Effect of pH on the activity of crude phytase from LD9.

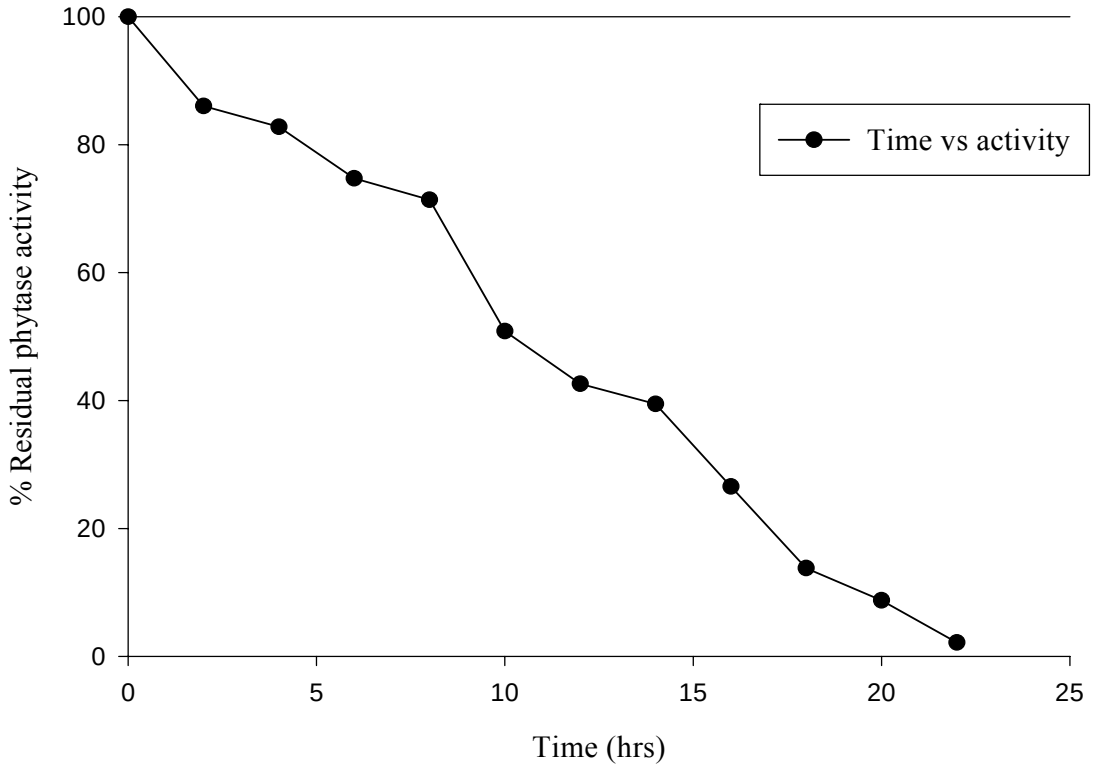

Fig. 3.35. Stability profile of crude phytase from LD9 (35^{O} C, pH 5.5).

3.6. Growth curves, enzyme activities and stability profiles of LD7

The growth curves for LD7, testing at different temperatures and pH values, are indicated in Fig. 3.36 to Fig. 3.38. The lag phase lasted from 0 to 15 hrs at all pH's tested at 25º C (Fig. 3.36) and 0 to 10 hrs at 30º C and 35º C (Fig. 3.37 and Fig. 3.38, respectively). A non-exponential increase in growth was noted at all temperatures and pH values. Linear growth occurred from 15 to 30 hrs at 25º C (Fig 3.36) and 10 to 30 hrs at 30º C and 35º C (Fig. 3.37 and Fig. 3.38, respectively). The best growth conditions for LD7 was found to be at 30º C with a pH value of 5.5 and 6.0 (0.068 g wet weight), followed by 35º C (0.035 g wet weight) and 25º C (0.03 g wet weight) at all pH values tested (Fig 3.36 to Fig 3.38).

The enzyme activity increased linearly with growth between 0 to 30 hrs at all temperatures and pH values tested (Fig. 3.39 to Fig. 3.41). However, after 30 hrs of incubation when the cells had gone into the stationary phase, the enzyme activities were non-growth associated and maximum enzyme activities were produced at this stage. At 25º C the highest enzyme activity of approximately 480 $U.ml^{-1}$ was observed after 65 hrs of incubation at pH's of 5.0, 5.5 and 6.0 respectively. At 30º C the highest enzyme activity of approximately 800 $U.ml^{-1}$ occurs at pH 5.5 and pH 6.0 with the lowest value obtained at pH 4.0 and pH 4.5. This was also found to be the optimal conditions for enzyme production. At 35º C the highest enzyme activity of approximately 700 $U.ml^{-1}$ occurs at pH 5.5 and pH 6.0 with the lowest values obtained at pH 4.0 and pH 4.5, respectively.

The relative percentage phytase activity obtained when the crude phytase from LD7 was subjected to different temperature ranges is indicated in Fig 3.42. The optimal phytase activity (100 % phytase activity) was observed at a temperature of 35º C. There was a sharp decline in phytase activity between 35º C and 40º C, followed by a gradual decrease for up to 70º C, thereafter it dropped sharply again.

The effect of pH (2.5 to 5.5) on the phytase activity of the crude enzyme is illustrated in Fig 3.43. The optimal enzyme activity was reached at pH 5.5

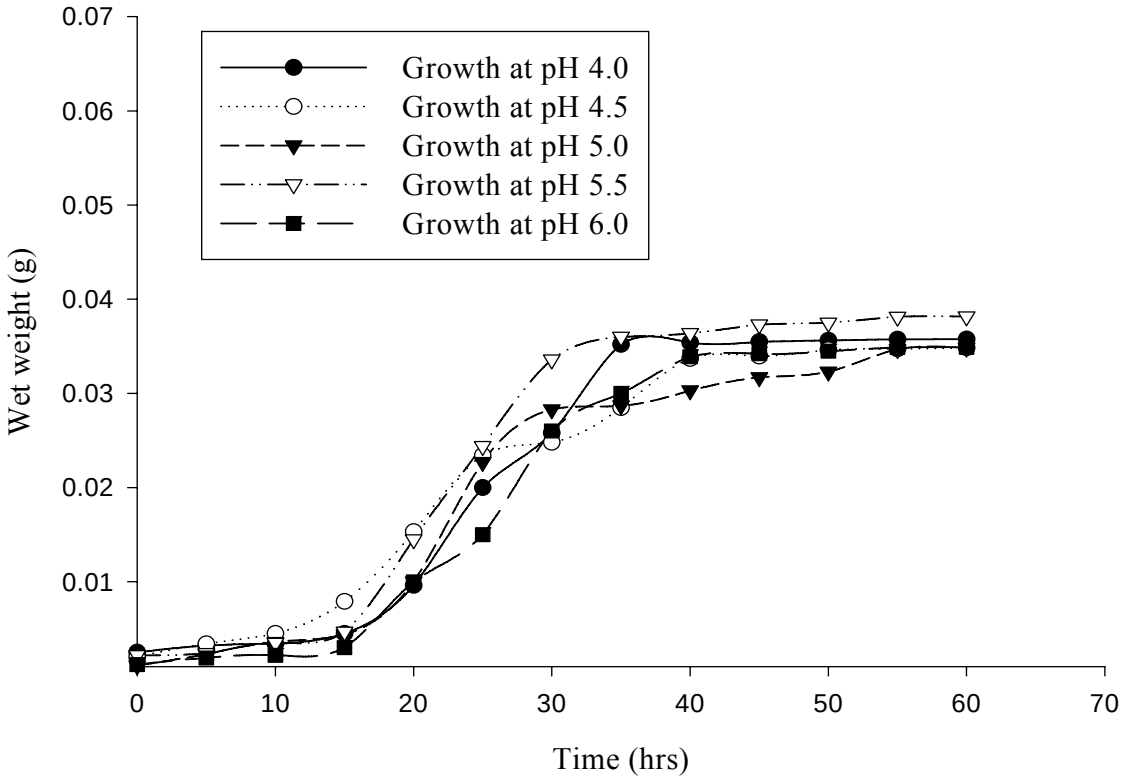

Fig. 3.36. Growth profiles of LD7 at 25^{o} C.

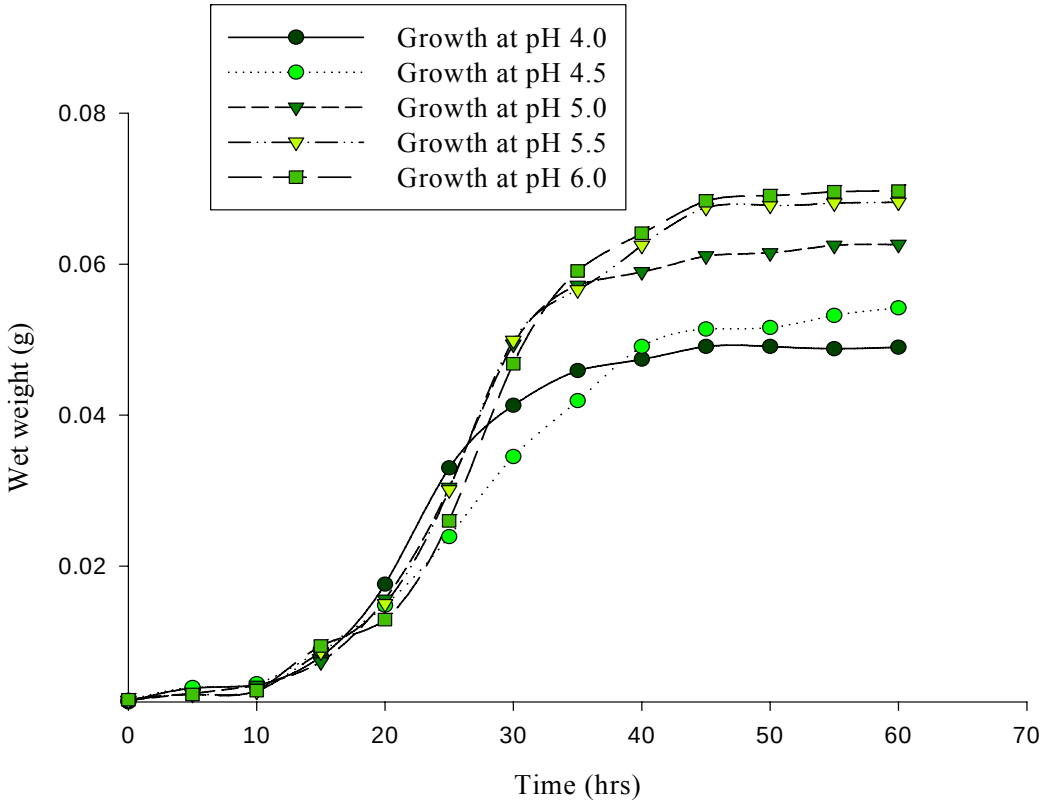

Fig. 3.37. Growth profiles of LD7 at 30^{o} C.

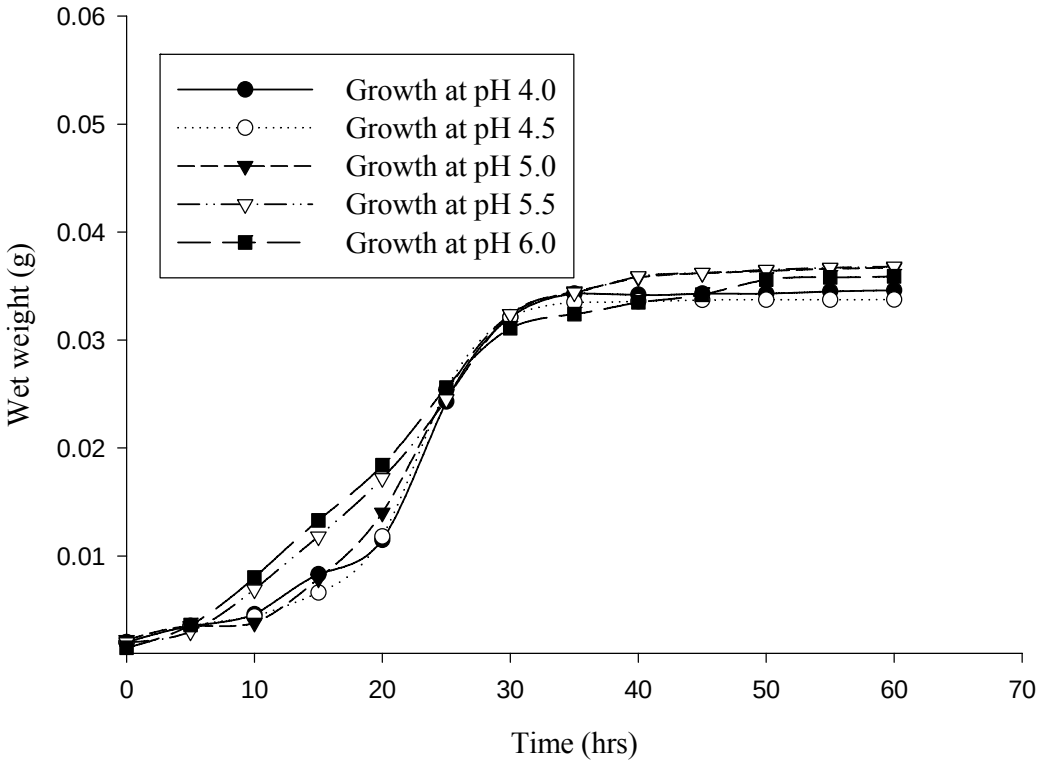

Fig. 3.38. Growth profiles of LD7 at 35^{o} C.

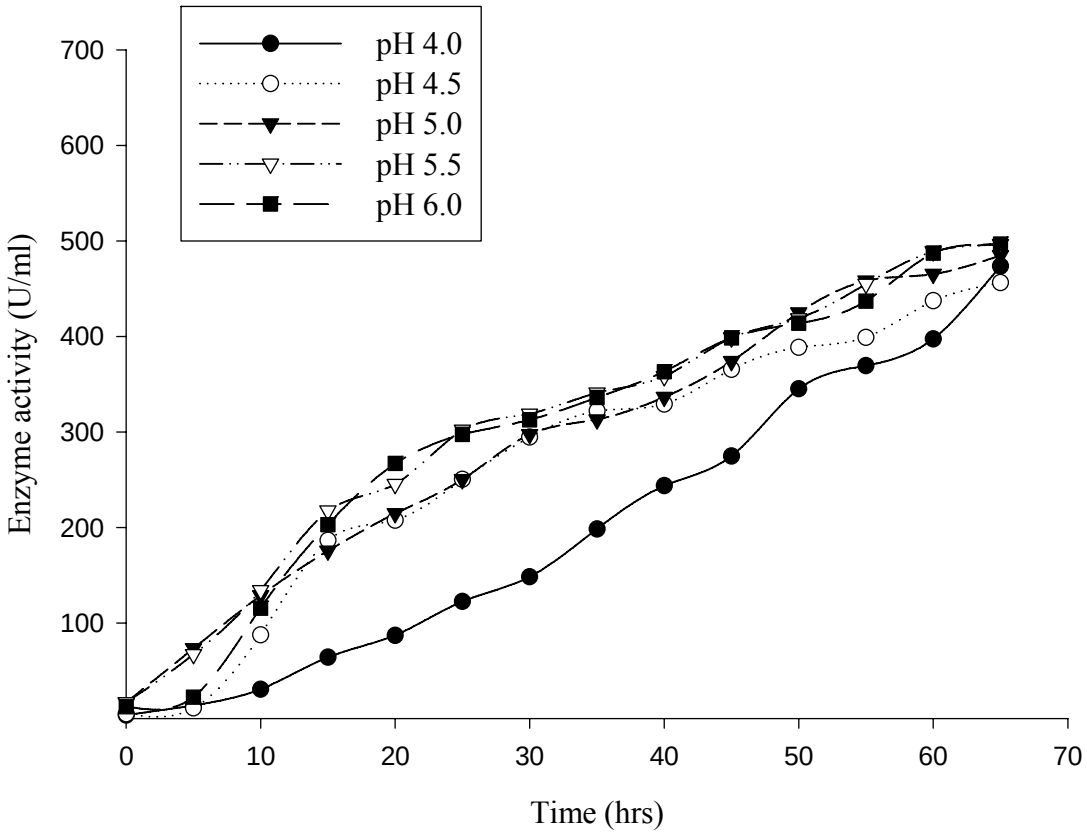

Fig. 3.39. Enzyme activities of LD7 at 25^{o} C.

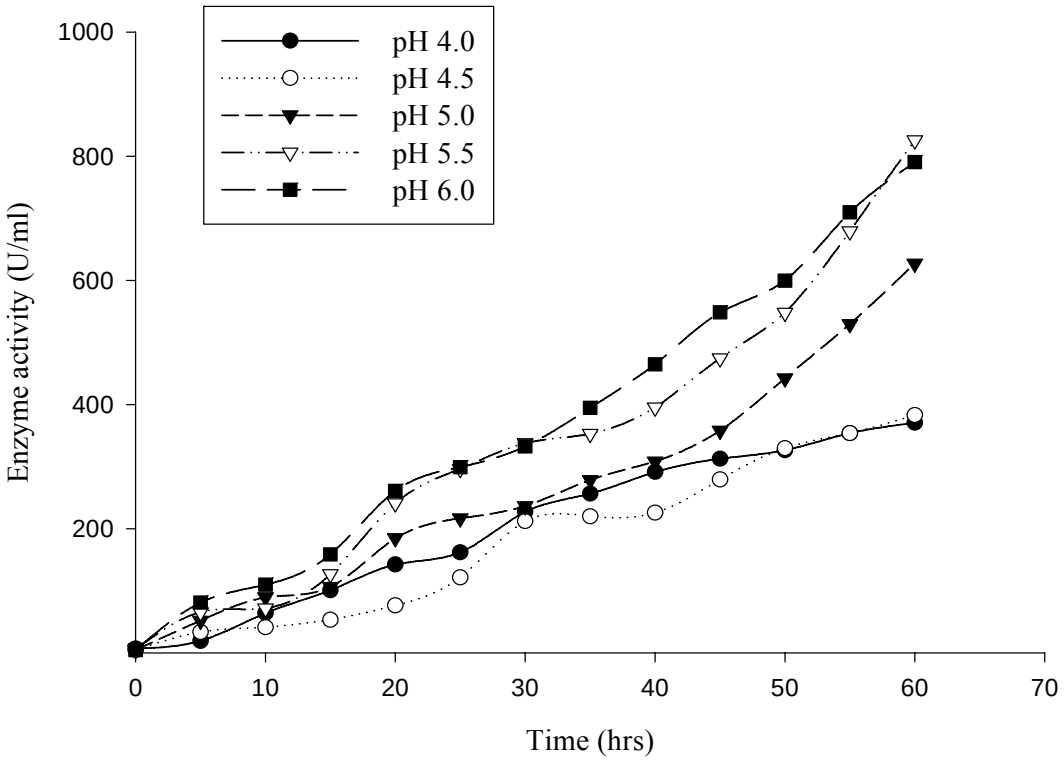

Fig. 3.40. Enzyme activities of LD7 at 30^{o} C.

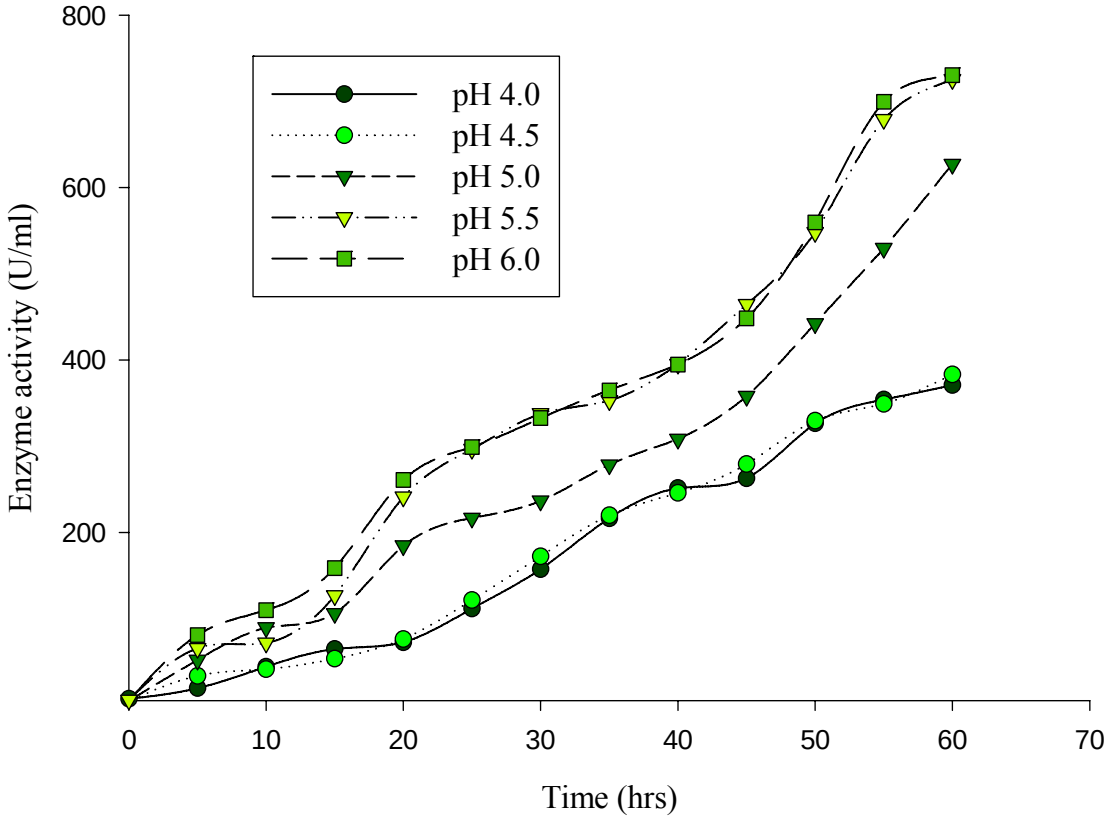

Fig. 3.41. Enzyme activities of LD7 at 35^{o} C.

after which the relative enzyme activity declined sharply reaching its lowest level at a pH of 7.5.

The maximum enzyme activity of LD7 was reached at 35º C (Fig. 3.42) with the optimal activity at pH 5.5 (Fig. 3.43). Consequently, these conditions were used to determine the stability of the crude enzyme. The enzyme retained almost 84 % of its activity after 2.5 hrs of incubation (Fig. 3.44). After this period, a gradual linear decrease in activity was noted.

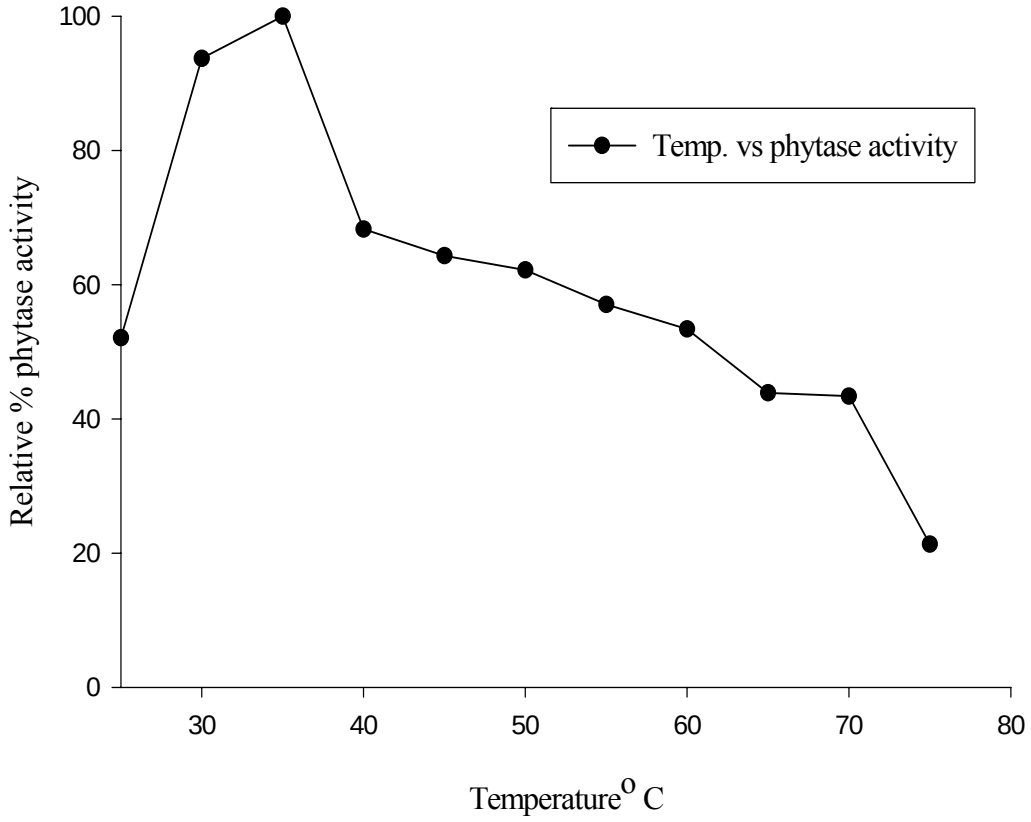

Fig. 3.42. Effect of temperature upon the activity of crude phytase from LD7.

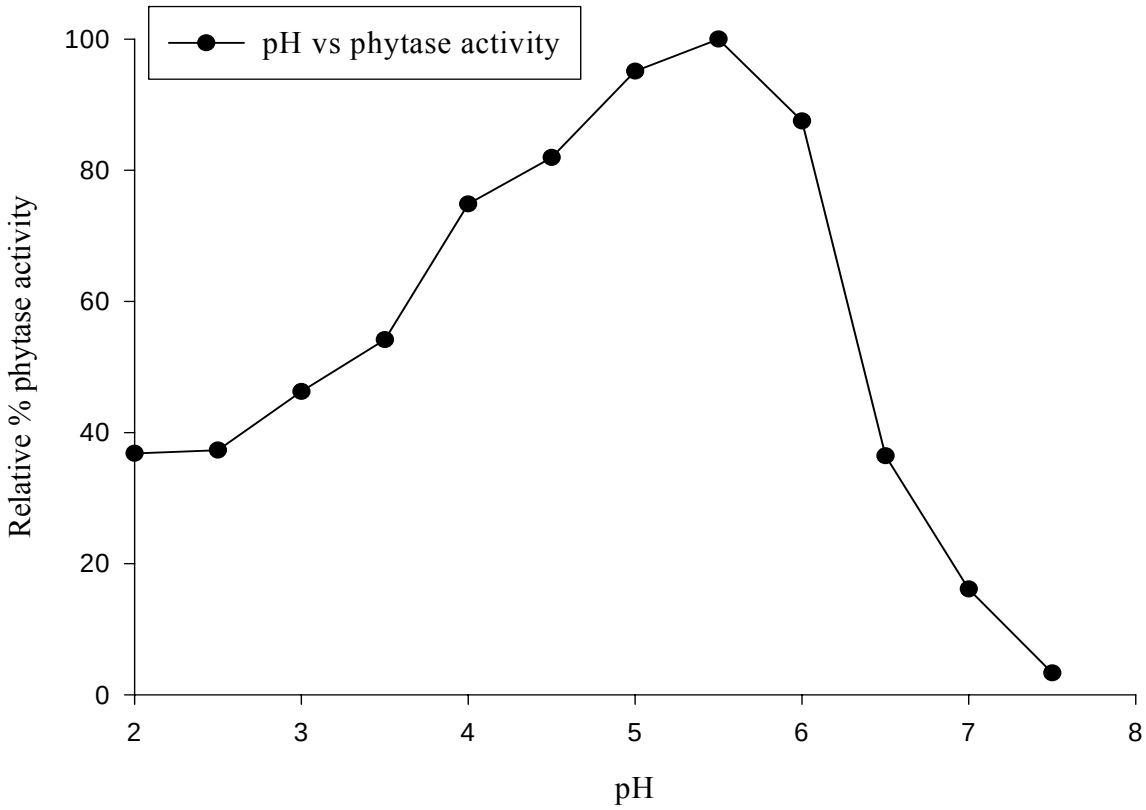

Fig. 3.43. Effect of pH on the activity of crude phytase from LD7.

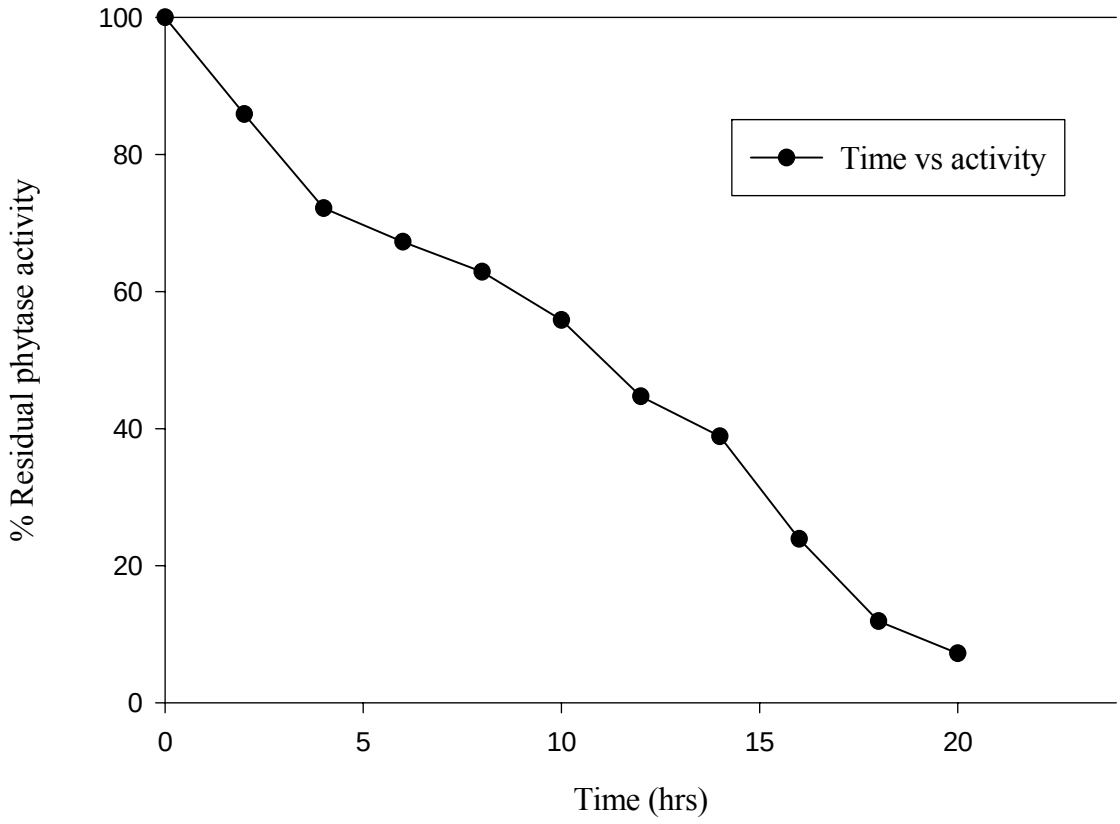

Fig. 3.44. Stability profile of crude phytase from LD7 (35^{o} C, pH 5.5).

CHAPTER FOUR

4. DISCUSSION

4.1. Screening of phytase producing yeasts

Twenty three phytase-producing yeasts isolated in the Limpopo Province were obtained from various soil samples on selective media (PSM agar plates). The phytase activities of these isolates were determined and the best three phytase producers were selected for further studies.

The phytase activity of yeasts was estimated at 20-1070 $U.ml^{-1}$, bacterial phytases at 200-388 $U.ml^{-1}$, fungal phytases at 600 $U.ml^{-1}$ and recombinant phytase at 6700-7600 $U.ml^{-1}$ (Quan *et al*., 2001). HBD6.2, LD9 and LD7 exhibited phytase activities of 676.0, 630.2 and 440.9 $U.ml^{-1}$, respectively (Table 3.1). These values are comparable to those just indicated above. Sano *et al*. (1998) obtained eighteen yeast strains from the Centraalbureau voor Schimmelcultures (CBS) and strains belonging to *Arxula adeninivorans* were the best assimilaters of phytate. Some strains of *Arxula adeninivorans* were secreting higher levels of phytase activity ranging between 17 and 257 $U.ml^{-1}$. Quan *et al*. (2001) isolated four yeast isolates that exhibited phytase activities of 260 to 284 $U.ml^{-1}$. Therefore the three strains (HBD6.2, LD9 and LD7) produced approximately three times more phytase than the yeast reported by Sano *et al*. (1998) and two of the strains HBD6.2 and LD9 produced phytase activity more or less similar to natural fungal phytases.

The three best phytase-producing yeast isolates (HBD6.2, LD9 and LD7) were identified using the methods of Yarrow (2000) and identification keys as outlined by Barnett *et al*. (2000) and Kurtzman and Fell (2000). None of the three yeast isolates could produce sexual spores, therefore all three yeast isolates were identified as anamorphic representatives of the yeast domain. The DBB test indicated that the yeast isolates belonged to the ascomycetous group of yeasts.

Yeast isolate HBD6.2 was identified as *Candida guilliermondii* based on its morphological and biochemical similarities, but differed from *Candida guilliermondii* in the assimilation of lactose and erythritol as the sole sources of carbon, the assimilation of ethylamine and cadaverine as the sources of nitrogen and tested positive for urease. LD9 was identified as *Candida diddensiae* but differed from *Candida diddensiae* in the assimilation of galactose and D-arabinose, sodium nitrite as a source of nitrogen and could not grow in the presence of 0.1 and 0.01 % cycloheximide. LD7 was clustered with the genus *Candida* due to its ascomycetous related properties. It related to *C. famata* but differed substantially in the colour of the colonies with *C. famata* producing white to cream coloured colonies and LD7 cream to pink coloured colonies.

4.2. Confirming the identified yeast isolates using RFLP-PCR

The PCR-RFLP technique was used to confirm the identification of the yeast isolates HBD6.2, LD9 and LD7 that were identified as *C. guilliermondii, C. diddensiae* and *Candida famata,* respectively, using conventional identification methods. In most cases teleomorphs of the anamorphic yeasts were used as benchmark organisms. Kurtzman and Blanz (2000) indicated that anamorphs had identical nuclear rDNA sequences to that of its teleomorphic counterparts. Therefore the use of teleomorphic yeasts to confirm the identity of anamorphic yeasts was valid.

According to the results on the UPGMA dendrogram (Fig. 3.17) *C. guilliermondii* HBD6.2 did not cluster with either of its reference strains, namely, *P. guilliermondii* Y0209, *P. guilliermondii* Y0053 and *P. guilliermondii* Y0054. However, it clustered tightly with *C. diddensiae* Y0774 and were 100 % genetically similar according to the analysis with the DICE coefficient (Table 3.18). The analysis of RFLP-PCR profiles indicated that all the bands were common to the two yeast strains (*C. guilliermondii* HBD6.2 and *C. diddensiae* Y0774). Based on the results of morphological and biochemical tests, *C. guilliermondii* HBD6.2 and *C. diddensiae* Y0774 differed only in the assimilation of melibiose, inulin, D-arabinose, and cadaverine and the fermentation of galactose.

The reference strains *P. guilliermondii* Y0209, *P. guilliermondii* Y0053 and *P. guilliermondii* Y0054, clustered together on the UPGMA dendrogram (Fig. 3.17), and that was the expected outcome since these yeast strains belong to the same species. This confers reliability of the clustering pattern on the dendrogram. In conclusion, HBD6.2 grouped with *C. diddensiae* Y0774 according to PCR-RFLP, because the identification was informed by the similarity in their DNA banding patterns, unlike with conventional classification where similarity analysis was based on the biochemical characteristics that could be influenced by factors such as mutation and environmental conditions.

C. diddensiae LD9 did not cluster closely with its reference strain *C. diddensiae* Y0774 based on the UPGMA dendrogram (Fig. 3.17). According to the analysis with the DICE coefficient (Table 3.18), *C. diddensiae* LD9 and *C. diddensiae* Y0774 were noted to be 87 % genetically similar, indicating that the two organisms may belong to the same genus. Chen *et al*. (2000) evaluated 401 clinical isolates with six reference strains and 27 type strains representing 34 species of yeasts. They suggested that related species could be distinguished by length polymorphism in their ITS2 region DNA. All the results obtained indicated that >85 % similarity in ITS2 region DNA existed among the clinical isolates of the same species and that intraspecific polymorphism occurred in this region for some clinical strains of *Candida* species and had 100 % sequence similarity compared with their type strains.

C. diddensiae LD9 also showed a higher level of similarity of 80 % to 91 % with all the yeast strains studied except for *Candida famata* LD7 which showed a 52 % genetic similarity. According to the banding profiles, most bands were common between *C. diddensiae* LD9 and *C. diddensiae* Y0774, even though *C. diddensiae* LD9 showed a number of polymorphic bands with *Alu*I (Fig. 3.6), *Hae*III (Fig. 3.9) and *Hpa*II (Fig. 3.10) enzymes that differed with the reference strain *C. diddensiae* Y0774. A clear identification of *C. diddensiae* was not possible, however, more strains especially from *Candida* need to be included for better comparison and possible identification.

Candida famata LD7 did not form a cluster with any of the yeasts tested. The polymorphic bands observed for *Candida famata* LD7 made its banding profile different from those of the other yeast strains. *D. hansenii* Y0209 and *D. hansenii* Y0610 are the reference strains for *Candida famata* LD7, however, the strains did not cluster together (Fig. 3.17). The analysis with the DICE coefficient (Table 3.18) indicated that *Candida famata* LD7 and *D. hansenii* Y0209 were 51 % genetically similar, while *Candida famata* LD7 and *D. hansenii* Y0610 were 48 % genetically similar. Genotypic data based on the banding pattern strongly suggested that *Candida famata* LD7 could be a different species from the other species tested. More studies need to be conducted to conclude if this strain (LD7) is a new *Candida* species or if it is related to other *Candida* species.

The results obtained showed that standard conventional methods were not reliable for defining and recognizing species as they rely on researchers trying to categorize physical features that can sometimes be unclear. Molecular techniques have been shown to be superior to phenotypic characteristics in assigning the genus or species name, e.g. PCR-based techniques are now being used due to their speed and accuracy since a huge database is available as a result of sequencing studies and this allows comparison for yeast strains identification **(**Bonaïti *et al*., 2005). Also the RFLP analysis of the internal transcribed spacer (ITS) region which flanks the conserved genes has also been found to be most useful since it allows species identification and typing of isolates (Andrighetto *et al*., 2000). The genotypic characteristics are true and reliable since they utilize the genetic code found in an organism's DNA. DNA sequence is stable and therefore, offers a reliable method to identify the unknown against known yeasts.

4.3. Effect of temperature and pH on enzyme activity

The effect of temperature and pH on the growth and the production of phytase by yeast isolates were studied in shake flasks at different temperatures (25, 30 and 35º C) and pH ranges (4.0, 4.5, 5.0, 5.5 and 6.0). The optimal growth temperature for all yeast isolates was 30º C (Fig. 3.19, Fig. 3.28 and Fig. 3.37) with HBD6.2 growing best at pH 5.5, LD9 at pH 6.0 and LD7 at pH 5.5 and 6.0. Enzyme activity started to increase from the beginning of growth and continued to increase up to 3 days of incubation. The optimum

temperature for phytase production by the three isolates was 30º C for LD9 and LD7; and 30º C or 35º C for HBD6.2 after 65 hrs of incubation. These outcomes coincide with the results found by Quan *et al*. (2001) where the optimum temperature for growth and phytase production of *Candida krusei* were found to be 30º C. However, these temperatures for phytase production were lower when compared to *Arxula adeninivorans* phytase activities reported at 44º C (Sano *et al*., 1999). Optimum pH's for phytase production for HBD6.2 were noted at pH 5.0 or 6.0. For LD9, optimum pH for phytase production was noted at pH 6.0 and LD7 at pH 5.5 or 6.0. These observations also coincide with the findings of Quan *et al*. (2001) who noted the optimum pH for growth and phytase production for *C. krusei* to be between 4.0 and 7.0, respectively. Phytase production was essentially non-growth associated, since maximum production of phytase occurred at the stationary phase.

The crude enzyme from HBD6.2, LD9 and LD7 displayed maximum activity at 35º C (Fig. 3.24, Fig. 3.33 and Fig. 3.42). Most fungal phytases characterized to date exhibited temperature optima in the 40º C to 60º C range (Casey and Walsh, 2004). Extracellular enzymes produced by mesophilic fungi generally display temperature optima below 60º C although a minority display a higher temperature optima (Casey and Walsh, 2004). Yeast phytases have an optimum temperature higher than 60º C, often around 75º C which is in contrast with the optimum temperature for phytase in strain *C. krusei* WZ-001 which was found to be 40º C (Quan *et al*., 2001).

The crude enzyme from the three yeast isolates studied displayed maximum activity at pH 5.5 (Fig. 3.25, Fig. 3.34, and Fig. 3.43). Phytases often have a low pH optimum range (pH 4.5 to 6.0) with yeasts having a pH range of between 4.0 to 5.0 (Quan *et al*., 2001). The fungal and bacterial (e.g. *E. coli*) phytases have pH optimum which varies from 2.2 to 8 and most microbial phytases, especially those of fungal origin, have been found to retain at least 80 % of the maximal activity at pH values between 4.0 and 7.3 (Hara *et al*., 1985). The cause for phytases to display such dual pH optima is likely due to (pH dependent) differences in charge distribution at the substrate-binding site thereby directly influencing substrate interaction (Casey and Walsh, 2004). This phenomenon

was however not observed with the isolated yeast strains (HBD6.2, LD9 and LD7). From a physiological view these enzymes (HBD6.2, LD9 and LD7) showed significant activity at a range necessary to facilitate phytate degradation in the salivary gland (pH 5.0 to 7.0), stomach (fed state pH 6.5, reducing to 4.0 to 5.5 upon stimulation of acid secretion) and upper duodenum (pH 4.0 to 6.0) (Casey and Walsh, 2004).

4.4. Thermal stability

The enzymes for the three yeast isolates HBD6.2, LD9 and LD7, were stable at 35º C, pH 5.5 for an average of 3 hrs (Fig. 3.26, 3.35 and 3.44) retaining almost 80 % of residual activity. These results differed from results obtained by Quan *et al*. (2001) for *C. krusei,* where they found that between 0º C and 50º C of incubation only a small change in the enzyme activity was observed, but the enzyme retained 50 % activity when incubated at 70º C.

4.5. Crude protein and SDS-PAGE analysis

The protein concentrations for HBD6.2, LD9 and LD7 were 0.501 $\mu g.ml^{-1}$, 0.432 $\mu g.ml^{-1}$ and 0.376 $\mu g.ml^{-1}$, respectively. Concentrated crude enzymes were run on the SDS-PAGE electrophoretic gel. No bands were observed on non-denaturing electrophoretic gels and the phytase enzymes could not be identified by zymogram analysis.

4.6. Conclusion and recommendation

In this study, three isolated yeasts *Candida guilliermondii* HBD6.2, *Candida diddensiae* LD9 and *Candida famata* LD7 indicated enzyme activities of 676.02, 630.21 and 440.94 $U.ml^{-1}$, respectively. The optimum growth temperature for the three yeast isolates was 30º C with HBD6.2 growing best at pH 5.5, LD9 at pH 6.0 and LD7 at pH 5.5 or 6.0. The optimum temperature for phytase production was also at 30º C for LD9 and LD7, and 30º C or 35º C for HBD6.2. The crude enzymes for the three yeasts were stable at 35º C for over 3 hrs of incubation and also, the crude enzymes showed optimal activity at pH 5.5. Almost all of the objectives set were achieved, except for the SDS-PAGE analysis which was inconclusive. More studies need to be conducted in order to confirm the identity of the yeasts isolated. LD9 and LD7 need to be further identified since they

did not cluster with any of the yeasts tested on the dendrogram. Other PCR-based techniques such as sequencing studies need to be employed together with more yeast strains especially *Candida* species for better comparison and possible identification of these yeast isolates. Secondly, the enzymes from three isolates could be purified and further characterized, for example in terms of enzyme characteristics. Future studies in phytase enzyme technology need to focus on more thermo-tolerant enzyme preparation, greater enzyme activity and enzymes which function optimally at low gastric pH values. Under these conditions, phytase will be used widely in animal diets to improve phytate-phosphorus bioavailability and reduce phosphorus excretion. In general, this work is an important milestone towards producing novel thermostable phytase enzymes that might be of use in biotechnological applications such as the animal feed, human health, pulp and paper industries. The enzymatic degradation of phytic acid will not produce mutagenic and highly toxic by-products, the exploitation of enzymes in the industrial process would be environmentally friendly and would assist in the development of novel cleaner technologies.

CHAPTER FIVE

5. REFFERENCES

Ahmad, T., Rasool, S., Sarwar, M., Haq, A., and Hasan, Z. 2000. Effect of microbial phytase produced from a fungus *Aspergillus niger* on bioavailability of phosphorus and calcium in broiler chickens. Anim. Feed. Sci. Tech. 83: 103-114.

Alasheh, S., and Duvnjak, Z. 1994. Effect of glucose concentration on biomass and phytase production and reduction of phytic acid content in canola meal by *Aspergillus carbonarius* during solid state fermentation process. Biotech. Prog. 10: 353-359.

Alasheh, S., and Duvnjak, Z. 1995. Phytase production and decrease of phytic acid content in canola meal by *Aspergillus carbonarius* in solid state fermentation process. World J. Microbiol. Biotech. 11: 228-231.

Andrighetto, C., Psomas, E., Tzanetakis, N., Suzzi, G., and Lombardi, A. 2000. Randomly amplified polymorphic DNA (RAPD) PCR for the identification of yeasts isolates from dairy products. Lett. Appl. Microbiol. 30: 5-9.

Ashyma, V., and Satyanarayana, T. 2001. Statistical optimization of the medium components by response surface methodology to enhance phytase production by *Pichia anomala*. Process Biochem. 37: 999-1004.

Barnett, J.A., Payne, R.W., and Yarrow, D. 2000. Characteristics and identification. 3rd Edition. Cmbridge University Press. UK. 1-4.

Bonaïti, C., Parayre, S., and Irlinger, F. 2005. Novel extraction strategy of ribosomal RNA and genomic DNA from cheese for PCR-based investigations. Int. J. food. Microbiol. 107(2): 171-179.

Brinch-Pedersen, H., Dahl-Sørensen, L., and Holm, P.B. 2002. Engineering crop plants: getting a handle on phosphate. Plant. Sci. 7(3): 118-120.

Campbell, I., and Duffus, J.H. 1988. In Yeast: A practical approach. IRL press. Washington DC. 141-146.

Cappa, F., and Cocconcelli, P.S. 2001. Identification of fungi from dairy products by means of 18S rRNA analysis. Inter. J. Food Microbiol. 69: 157-60.

Casey, A., and Walsh, G. 2004. Identification and characterization of a phytase of potential commercial interest. J. Biotech. 110: 313-322.

Chen, J., Oliveri, P., Li, C., Zhou, G., Gao, F., Hagadorn, J. W., Peterson, K. J., and Davidson, E. H. 2000. Precambrian Animal Diversity: Putative Phosphatized Embryos from the Doushantuo Formation of China. Proceed. National Acad. Sci. USA. 97: 4457-4462.

Cromwell, G. L., Stahly, T. S., Coffey, R. D., Monegue, H. J., and Randolph, J. H. 1993. Efficacy of phytase in improving the bioavailability of phosphorus in soybean meal and corn-soybean meal diets for pigs. J. Anim. Sci. 71: 1831-1840.

Davies, N. T. 1982. Effects of phytic acid on mineral availability. In Dietary Fiber in Health and Disease. Vahoung, G. V., and Kritchevsky, D. Eds., Plenum Press, New York.

D′Silva, C.G., Bae, H.D., Yanke, L.J., Cheng, K.-J., and Selinger, L.B. 2000. Localization of phytase in *Selenomonas ruminatium* and *Mitsuokella multiacidas* by transmission electron microscopy. Can. J. Microbiol. 46: 391-395.

Dvorakova, J., Volfova, O., and Kopecky, J. 1997. Characterization of phytase produced by *Aspergillus niger.* Folia Microbiol. 42: 349-352.

Ebune, A., Alasheh, S., and Duvnjak, Z. 1995. Production of phytase during solid state fermentation using *Aspergillus ficuum* NRRL-3135 in canola meal. Biores. Tech. 53 (1):7-12.Freund, W. D., Mayr, G. W., Tietz, C., and Schultz, J. E. 1992. Metabolism of inositol phosphates in the protozoan Paramecium. Eur. J. Biochem. 207: 359-367.

Fretzdorff, B., Brummer, J. M., Rochen, W., Greiner, R., Konietzny, U., and Jany, K. D. 1995. Reduktion des phytinsaure-gehaites bei der-herstellung von backwaren und getreidenahrmitteln. AID-verhraucherdienst 40: 12-20.

Freund, W. D., Mayr, G. W., Tietz, C., and Schultz, J. E. 1992. Metabolism of inositol phosphates in the protozoan Paramecium. Eur. J. Biochem. 207: 359-367.

Garrett, J.B., Keith, A.K., Eileen, O., Kerovuo J., Kim, W., Barton, N.R., Hazlewood, G.P., Short, J. M., Robetson, D.E., and Gray, K.A. 2004. Enhancing the thermal tolerance and gastric performance of a microbial phytase for use as a phosphate-mobilizing monogastric-feed supplement. Appl. Environ. Microbiol. 7(3): 118-125.

Greiner, R., Konietzny, U., and Jany, K.D. 1993. Purification and characterization of two phytases from *Escherichia coli*. Arch. Biochem. Biophys. 303: 107-113.

Greiner, R., Haller, E., Konietzny, U., and Jany, K. D. 1997. Purification and characterization of a phytase from *Klebsiella terrigena*. Arch. Biochem. Biophys. 341: 201-206.

Ha, N. C., Oh, B. C., Shin, S., Kim, H. J., Oh, T. K., Kim, Y. O., Choi, K. Y., and Oh, B. H. 2000. Crystal structures of a novel, thermostable phytase in partially and fully calcium loaded states. Nat. Struct. Biol. **7:** 147-153.

Han, Y. and Lei, X. G. 1999. Role of glycosylation in the functional expression of an *Aspergillus niger* phytase (phyA) in *Pichia pastoris*. Arch. Biochim. Biophys. 364: 83-90.

Hara, A., Ebina, S., Kondo, A., and Funaguma, T. 1985. A new type of phytase from pollen of *Typha latifolia* L. Agric. Biol. Chem. 49: 3539-3544.

Harland, B.F., and Harland, J. 1980. Fermentative reduction of phytate in Rye, White, and Whole Wheat Bread. The American Association of Cereal Chemists, Inc., Vol 57(3): 226-229.

Haros, M., Bielicka, M., and Sanz, Y. 2005. Phytase activity as a novel metabolic feature in *Bifidiobacterium*. Lett. Microbiol. 247: 231-239.

Hegeman, C.E., and Grabau, E.A. 2001. A novel phytase with sequence similarity to purple acid phosphatases is expressed in cotyledons of germinating soybean seedlings. Plant Physiol. 126: 1598-1608.

Kerovuo, J., Lauraeus, M., Nurminen, P., Kalkinnen, N., and Apajalahti, J. 1998. Characterization, molecular gene cloning and sequencing of a novel phytase from *Bacillus subtilis*. Appl. Environ. Microbiol. 64: 2079-2085.

Kerovuo, J., and Tynkkynen, S. 2000. Expression of *Bacillus subtilis* phytase in Lactobacillus plantarum 755. Lett. Appl. Microbiol. 30: 325-329.

Kim, Y.O., Kim, H.K., Bae, K.S., Yu, J.H., and Oh, T.K. 1998. Purification and properties of a thermostable phytase from *Bacillus spp.* DS11. Enzyme Microbiol. Technol. 22: 2-7.

Kim, Y.O., Ha, N.C., Oh, T.K., and Oh, B.H. 1999. Preliminary X-ray crystallographic analysis of a novel phytase from a *Bacillus amyloliquefaciens* strain. Acta Crystallographica, section D-Biol. Cryst. 55: 691-693.

Konietzny, U., and Greiner, R. 2004. Bacterial phytase: potential application, in vivo function and regulation of its synthesis. Braz. J. Microbiol. 35(1-2): 1-13.

Kostrewa, D., Grueninger-Leitch, F., D'Arcy, A., Broger, C., Mitchell, D., and van Loon, A.P.G.M. 1997. Crystal structures of phytases from *Aspergillus ficuum* at 2.5 A resolution. Nat. Struct. Biol. 4: 185-190.

Kostrewa, D., Wyss, M., DÁrcy, A., and van Loon, A.P. 1999. Crystal structure of Aspergillus niger pH 2.5 acid phosphatase at 2.4 Å resolution. J. Mol. Biol. 288: 965-974.

Kurtzman, C.P. 1998. Discussion of teleomorphic and anamorphic ascomycetous yeasts and a key to genera. In the Yeasts: A taxonomic study. 4th ed. In Kurtzman, C.P., and Fell, J.W (ed.). Elsevier Sci. Amsterdam. 111-121.

Kurtzman, C.P., and Fell, J.W. 1998. Definition, classification and nomenclature of the yeasts. In the Yeasts: A taxonomic study. 4th ed. In Kurtzman, C.P., and Fell, J.W (ed.). Elsevier Sci. Amsterdam. 1-26.

Kurtzman, C.P., and Blanz, P.A. 2000. Ribosomal RNA/DNA sequence comparison for assessing phlyogenetic relationships. In the yeasts. A taxonomic study. 4th ed. In Kurtzman, C.P., and Fell, J.W (ed.). Elsevier Sci. Amsterdam. 69-75.

Kurtzman, C.P., and Fell, J.W. 2000. The yeasts: A taxonomic study. Fourth revised and enlarged edition. Elsevier sci. B.V. New York.

Laboure, A. M., Gagnon, J., and Lescure, A. M. 1993. Purification and characterization of a phytase (myo-inositol hexakisphosphate phosphohydrolase) accumulated in maize (Zea mays) seedlings during germination. J. Biochem. 29: 413-419.

Lim, D., Golovan, S., Forsberg, C.W., and Jia, Z. 2000. Crystal structures of Escherichia coli phytase and its complex with phytate. Nat. Struct. Biol. 7: 108-113.

Liu, B.L., Rafiq, A, Tzeng Y., and Rob, A. 1998. Induction and characterization of phytase and beyond. Enzy. Microbiol. Technol. 22: 415-424.

Loewus, F.A., and Murthy, P.P.N. 2000. Myo-inositol metabolism in plants. Plant Sci. 150: 1-19.

Mayer, A. F., Hellmuth, K., Schlieker, H., Lopez-Ulibarri, R., Oertel, S., Dahlems, U., Strasser, A. W. M., and van Loon, A. P. G. M. 1999. An expression system matures: a

highly efficient and cost-effective process for phytase production by recombinant strains of *Hansenula polymorpha*. Biotechnol. Bioeng. 63: 373-81.

Merz, W.G. 1990. *Candida albicans* strain delineation. Clin. Microbiol. Rev. 3:321-334.

Miksch, G., Kleist, S., Friehs, K., and Flaschel, E. 2002. Overexpression of the phytase from Escherichia coli and its extracellular production in bioreactors. Appl. Microbiol. Biotech. 59: 685-694.

Mroz, Z., Jongbloed, A.W., and Kemme, P.A. 1994. Apparent digestibility and retention of nutrients bound to phytate complexes as influenced by microbial phytase and feeding regimen in pigs. J. Anim. Sci.72:126-132.

Mullaney, E.J., Daly, C.B., Kim, T., Porres, X.G., Lei, K.S., and Ullay, A.H.J. 2002. Site-directed mutagenesis of *Aspergillus niger* NRRL 3135 phytase at residue 300 to enhance catalysis at pH 4.0. Biochem. Biophys. Res. Commun. 279: 1016-1020.

Mullaney, E.J., and Ullah, A.H.J. 2003. The term phytase comprises several different classes of enzymes. Biochem. Biophys. Res. Comm. 412(1): 179-184.

Musters, W., Boon, K., van der Sande, C.A., van Heerikhuizen, H and Planta, R.J. 1990. Fuctional analysis of transcribed spacers of yeast ribosomal DNA. EMBO. J. 9: 3989-3996.

Nei, M., and Li, W. 1979. Mathematical model for studying genetic variation in terms of restriction endonucleases. Proc. Nat. Sci. 79: 5269-5273.

Norris, F.A., Wilson, M.P., Wallis, T.S., and Galyov, E.E. 1998. SopB, a protein required for virulence of Salmonella Dublin, is an inositol phosphate phosphatase. Process Nat. Sci. 95: 14057-14059.

O'Quinn, P. R., Knabe, D. A., and Gregg, E. J. 1997. Efficacy of Natuphos in sorghumbased diets of finishing swine. J. Anim. Sci. 75: 1299-1307.

Palacios, M.C., Haros, M., Rosell, C.M., and Sanz, Y. 2005. Characterization of acid phosphatase from *Lactobacillus pentosis*: regulation and biochemical properties. J. Appl. Micobiol. 98: 229-237.

Pallauf, J., and Rimbach, G. 1996. Nutritional significance of phytic acid and phytase. Arch. Anim. Nut. 50: 301-319.

Pandey, A., Szakacs, G., Soccol, C. R., Rodriguez-Leon, J. A., and Soccol, V. T. 2001. Production, purification and properties of microbial phytases. Biores. Tech. 77(3): 203-214.

Pasamontes, L., Haiker, M., Henriquez-Huecas, M., Mitchell, D. B., and van Loon, A. P.G.M. 1997. Cloning of the phytases from *Emericella nidulans* and the thermophilic pollen of *Typha latifolia L*. Agric. Biol. Chem. 49: 3539-44.

Quan, C., Zhang, L., Wang, Y., and Ohta, Y. 2001. Production of phytase in low phosphate medium by a novel yeast *Candida krusei*. J. Biosc. Bioeng. 92: 154-160.

Reddy, N. R., Pierson, M. D., Sathe, S. K., and Salunkhe, D. K. 1989. Phytates is cereals and legumes. CRC Press, Inc., Boca Raton, Fla. 345-349.

Rimbach, G., and Pallauf, J. 1992. The effect of a supplement of microbial phytase on zinc availability. Z. Ernahrungswiss. 31: 269-277.

Rohlf, F.J. 1998. NTSYSpc version 2.02i. Numerical taxonomy and multivariate analysis system. Exeter software. Setauket, NY.

Rose, M.D., Winston, F., and Hieter, P. 1990. Methods in yeast genetics: a laboratory course manual. Cold spring harbour laboratory press. NY. In press.

Sandberg, A.S., and Andlid, T. 2002. Phytogenic and microbial phytases in human nutrition. Int. J. Food Sci. Technol. 37: 823-833.

Sandberg, A. S., Hulthen, L. R., and Turk, M. 1996. Dietary *Aspergillus niger* phytase increases iron absorption in humans. J. Nut. 126: 476-480.

Sano, K., Fukuhara, H., and Nakamura, Y. 1998. Phytase of the yeast *Arxula adeninivorans*. Lett. Biotech. 21: 33-38.

Scott, J. J. 1991. Alkaline phytase activity in nonionic detergent extracts of legume seeds. Plant Physiol. 95:1298-1301.

Shamsuddin, A.M. 2002. Anti-cancer function of phytic acid. Int. J. Food Sci. Technol. 37:769-782.

Shimizu, M. 1992. Purification and characterization of phytase from *Bacillus subtilis* (natto) N-77. Biosci. Biotech. Biochem. 56: 1266-1269.

Shin, S., Ha, N.C., Oh, B.C., Oh, T.K., and Oh, B.H. 2001. Enzyme mechanism and catalytic property of β propeller phytase, structure 9: 851-858.

Sreeramulu, G., Srinivasa, D.S., Nnd, K., and Joseph, R. 1996. *Lactobacillus amylovorus* as a phytase producer in submerged culture. Lett. Appl. Micb. 23(6): 385-388.

Sunitha, K., Jung-Kee, L., and Tae-Kwang, O. 1999. Optimization of medium components for phytase production by *E. coli* using response surface methodology. Process Biochem. Bioeng. 21(6): 1-6.

Tambe, S.M., Kaklij, G.S., Kelkar, S.M., and Parekh, L.J. 1994. Two distinct molecular forms of phytase from Klebsiella aerogenes: evidence for unusually small active enzyme peptide. J. Ferment. Bioeng. 77: 23-27.

Urbano, G., Lopez-Jurado, M., Aranda, C., Vidal, V., Tenorio, E., and Porre, J. 2000. The role of phytic acid in legumes: antinutrient or beneficial function. Physiol. Biochem. 56: 283-294.

Van der Peer, Y., and De Wachter, R. 1994. TREECON for windows version 1.3b: a software package for the construction and drawing of evolutionary tree for the Microsoft windows environment. Comput. Appl. Biosci. 10: 569-570.

Vasdinyei, R., and Deák, T. 2003. Characterization of yeast isolates originating from Hungarian dairy products using traditional and molecular identification techniques. Inter. J. Food Microbiol. 86: 123-130.

Vats, P., and Banerjee, U.C. 2002. Studies on the production of phytase by a newly isolated strain of *Aspergillus niger* var teigham obtained from rotten wood-logs. Process Biochem. 38: 211-217.

Vats, P., and Banerjee, U.C. 2004. Production studies and catalytic properties of phytases (myo-inositolhexakisphosphate phosphohydrolases): an overview. Enzy. Microbiol. Tech. 35: 3-14.

Vohra, A., and Satyanarayana, T. 2003. Phytases: microbial sources, production, purification and potential biotechnological applications. Crit. Rev. Biotech. 23(1): 29-60.

Wodzinski, R.J., and Ullah, A.H.J. 1996. Phytase. Adv. Appl. Microbiol. 42: 263-303.

Wyss, M., Pasamontes, L., Remy, R., Kohler, J., Kusznir, E., Gadient, M., Muller, F., and van Loon, A. P. G. M. 1998. Comparison of the thermostability properties of three acid phosphatases from molds: *Aspergillus fumigatus* phytase, *A. niger* phytase, and *A. niger* pH 2.5 acid phosphatase. Appl. Environ. Microbiol. 64: 4446-4451.

Wyss, M., Pasamontes, L., Friedlein, A., Remy, R., Tessier, M., Kronenberger, A., Middendorf, A., Lehmann, M., Schnoebelen, L., Röthlisberger, U., Kusznir, E., Wahl, G., Muller, F., Lahm, H. W., Vogel, K., and van Loon, A. P. G. M. 1999a. Biophysical characterization of fungal phytases (myo-inositol hexakisphosphate phosphohydrolases): molecular size, glycosylation pattern, and engineering of proteolytic resistance. Appl. Environ. Microbiol. 65: 359-366.

Wyss, M., Brugger, R., Kronenberger, A., Remy, R., Fimbel, R., Oesterhelt, G., Lehmann, M. and van Loon, A. P. G. M. 1999b. Biochemical characterization of fungal phytases (myo-inositol hexakisphosphate phosphohydrolases): catalytic properties. Appl. Environ. Microbiol. 65: 367-373.

Yang, W.J., Matsuda, Y. Sano, S., Masutani, H., and Nakagawa, A. 1991. Purification and characterization of phytase from rat intestinal mucosa. Biochim. Biophys. Acta 1075: 75-82.

Yarrow, D. 2000. Methods for the isolation, maintenance and identification of yeast. The Yeasts: A taxonomic study. 4th ed. In Kurtzman, C.P., and Fell, J.W 2000. Elsevier Sci. New York. 77-97.

Yoon, S.J., Choi, Y.J., Min, H.K., Cho, K.K., Kim, J.W., Lee, S.C., and Jung, Y.H. 1996. Isolation and identification of phytase producing bacterium, *Enterobacterspz* 4 and enzymatic properties of phytase enzyme. Enzy. Microbiol. Tech. 18(6): 449-454.

Zamudio, M., González, A., and Bastarrachea, F. 2002. Regulation of *Raoultella terrigena* comb. Nov. phytase expression. Can. J. Microbiol. 48: 71-81.

Zhang, L., Lijia, A., Xiaorong, G., and Wang, Y. 2004. Properties of *A. Ficuum* AS3.324 phytase expressed in tobacco. Process Biochem. 40: 213-216.